ACTIVATION OF SURVIVAL PATHWAYS IN NUTRIENT RESTRICTED COLORECTAL CANCER CELLS

A THESIS SUBMITTED TO
THE GRADUATE SCHOOL OF NATURAL AND APPLIED SCIENCES
OF
MIDDLE EAST TECHNICAL UNIVERSITY

BY

GÖKSU ORAL

IN PARTIAL FULFILLMENT OF THE REQUIREMENTS
FOR
THE DEGREE OF MASTER OF SCIENCE
IN
BIOLOGY

JANUARY 2023

Approval of the thesis:

ACTIVATION OF SURVIVAL PATHWAYS IN NUTRIENT RESTRICTED COLORECTAL CANCER CELLS

submitted by **GÖKSU ORAL** in partial fulfillment of the requirements for the degree of **Master of Science** i**n Biology, Middle East Technical University** by,

Prof. Dr. Halil Kalıpçılar
Dean, Graduate School of **Natural and Applied Sciences** _____

Prof. Dr. Ayşegül Gözen
Head of the Department, **Biological Sciences** _____

Prof. Dr. Sreeparna Banerjee
Supervisor, **Biological Sciences, METU** _____

Examining Committee Members:

Prof. Dr. Nülüfer Tülün Güray
Biological Sciences, METU _____

Prof. Dr. Sreeparna Banerjee
Biological Sciences, METU _____

Assoc. Prof. Dr. Işık Yuluğ
Molecular Biology and Genetics, Bilkent University _____

Date: 09.01.2023

I hereby declare that all information in this document has been obtained and presented in accordance with academic rules and ethical conduct. I also declare that, as required by these rules and conduct, I have fully cited and referenced all material and results that are not original to this work.

Name Last name : Göksu Oral

Signature :

ABSTRACT

ACTIVATION OF SURVIVAL PATHWAYS IN NUTRIENT RESTRICTED COLORECTAL CANCER CELLS

Oral, Göksu
Master of Science, Biology
Supervisor : Prof. Dr. Sreeparna Banerjee

January 2023, 129 pages

Limited nutrient availability in the tumor microenvironment can cause metabolic rewiring of cancer cells, resulting in the activation of various stress response pathways such as autophagy for survival. Our study showed for the first time that incubation of LoVo cells with a nutrient restriction medium containing low glucose, glutamine, and serum for 48 h resulted in the concurrent activation of two antagonistic proteins: the AMP Kinase pathway (AMPK) which is phosphorylated in response to low energy and activates catabolism and Ribosomal protein S6 (RPS6), which is activated in response to anabolic signaling, leading to protein synthesis and cell growth. The activation of AMPK was attributed to the low energy generation in the nutrient-restricted cells, leading to the induction of autophagy, as expected. The surprising observation of phosphorylation of RPS6 in the nutrient-restricted cells was attributed to the partial activation of mTORC1 and a robust activation of the MAPK pathway. The latter pathway could also be implicated in the high cell viability observed even after prolonged starvation since treatment of starved cells with a MAPK inhibitor led to a remarkable increase in cell death. Analysis of publicly available reverse phase protein array (RPPA) data from colorectal tumors with high phosphorylation of both RPS6 and AMPK revealed enrichment of

oncogenic growth and transcription factors. Overall, our data suggest that low availability of nutrients may lead to the co-activation of AMPK and RPS6 as a survival mechanism in colorectal cancer cells.

Keywords: Colorectal Cancer, Nutrient Restriction, Autophagy, mTOR pathway, MAPK pathway

ÖZ

BESİN AÇLIĞINA MARUZ BIRAKILAN KOLOREKTAL KANSER HÜCRELERİNDE HAYATTA KALMA YOLAKLARININ AKTİVASYONU

Oral, Göksu
Yüksek Lisans, Biyoloji
Tez Yöneticisi: Prof. Dr. Sreeparna Banerjee

Ocak 2023, 129 sayfa

Tümör mikro-çevresindeki kısıtlı besin varlığı, kanser hücrelerinin hayatta kalmak için otofaji gibi yolakların aktivasyonu ile metabolik olarak kendilerini yeniden düzenlemesine neden olmaktadır. Çalışmamız LoVo hücrelerinin düşük konsantrasyonda glikoz, glutamin ve serum içeren besiyeri ile 48 saat inkübasyonunun, düşük enerjiye bağlı olarak fosforile olan ve katabolizmanın aktivasyonundan sorumlu AMP Kinaz yolağı ile anabolik sinyal yolaklarına bağımlı olarak protein sentezinden ve hücre büyümesinden sorumlu Ribozomal protein S6'nın eşzamanlı aktivasyonu ile sonuçlandığını göstermiştir. AMPK yolağının aktivasyonu, beklenildiği gibi, besin kısıtlı hücrelerde düşük enerji üretimine bağlı olarak otofajinin tetiklenmesiyle açıklanabilir. Beklenilenin aksine kısıtlı besin varlığına maruz kalan hücrelerde RPS6'nın fosforilasyonu ise, mTORC1 yolağının kısmi aktivasyonuna ve aktif MAPK yolaklarına bağlanmıştır. MAPK yolağının aktivasyonunun hücre canlılığı üzerine pozitif etkisi, besin kısıtlı hücrelerin MAPK inhibitörü ile tedavisi sonrasında hücre ölümünde dikkate değer bir artış ile gözlemlenmiştir.

Hem RPS6 hem de AMPK yolağının aktivasyonuna sahip kolorektal tümörlerin halka açık ters faz protein dizisi (RPPA) verilerinin analizi, onkojenik büyüme ve transkripsiyon faktörlerinin zenginleştiğini ortaya çıkarmıştır, ki bu da aksi halde oldukça farklı olan bu yolakların birlikte aktivasyonunun hayatta kalma mekanizması olarak kullanıldığını düşündürmektedir.

Genel olarak, verilerimiz, kısıtlı besin ortamının, kolorektal kanser hücrelerinde hayatta kalma mekanizması olarak AMPK ve RPS6'nın birlikte aktivasyonuna yol açabileceğini göstermektedir.

Anahtar Kelimeler: Kolon Kanseri, Besin Açlığı, Otofaji, mTOR sinyal yolağı, MAPK sinyal yolağı

To my family and love

For always being by my side and believing in me...

ACKNOWLEDGMENTS

First and foremost, I would like to express my heartfelt gratitude to my supervisor, Prof. Dr. Sreeparna Banerjee, for allowing me to complete my master's degree in her lab. I am most grateful to her for providing highly valuable scientific input, for her unending support and patience, wisdom, guidance, and immense knowledge. Her perspective and advice helped me to become a better researcher.

I would like to thank my jury members Prof. Dr. Tülün Nülüfer Güray and Assoc. Prof. Işık Yuluğ for their suggestions and contributions.

A great debt of gratitude is also owed to my lab mates. First of all, I would like to thank especially my miRNA team family who are very valuable to me. I would like to thank Aliye Ezgi Güleç and Hepşen Hazal Hüsnügil for welcoming me in the best way since the first day, guiding me along the way, and providing me with endless support and encouragement. They taught me so much about scientific research and gave me invaluable perspectives during the interpretation of my data and they truly helped me grow as a woman in science. I'd like to thank Nazlı Şevval Menemenli for always listening and understanding me when I'm down, for giving me security and assurance I can always rely on, for being so kind and considerate, and for always being there for me when I need help without hesitation. I'll never forget the miRNA team coffee sessions, which increased my motivation and made me feel understood.

I would like to thank Aydan Torun for always being in the lab early in the morning, making sure everything runs smoothly, and putting her own work aside to listen to me when I needed someone to talk to. She was also the one who first taught me several lab techniques, for which I am truly thankful. I will always miss our enjoyable discussions about literature, and media in which her taste is so good that I always look forward to watching and reading what she recommends. I would like to thank Hoşnaz Tuğral for always making me feel happy and relaxed whenever we talked. She is the sweetest soul I have ever met, and I consider myself privileged to

be her friend. Many thanks to Esin Gülce Seza for helping me relentlessly whenever I asked, Çağdaş Ermiş for his encouragement and support not only during my Master's but also during my Chemistry journey, İsmail Güderer for his friendship and technological expertise and support 24 hours a day and Nisan Korkmaz for the joy she brings to our lab. Your support has been invaluable and I am so grateful to have had you as lab mates and friends. Thank you.

I would also like to thank my best friend Çağlar Kaygalak for being there for me through both good and bad times, her presence has been a constant source of comfort and strength. She has helped me to love, believe, and accept myself as I am, and her friendship is invaluable to me and I am truly blessed to have her in my life.

I would like to thank my family for raising me to be the person I am today. They have always been my rock, and their unwavering love and support have been a constant source of strength and comfort. They have always made me feel that I am not alone and that they have my back no matter what. Their sacrifices, guidance, and encouragement have been the foundation of my life. I am truly grateful for everything they have done for me, and I would not be where I am today without them.

I would also like to thank my sole and only love, Emrehan Tüzün, for his endless love and support which is the constant source of strength and happiness in my life. He supported me at every step of my journey and encouraged me to pursue my dreams. His unwavering love and support have made everything possible. I am blessed to have him in my life and couldn't have done it without him. I was in heaven with you for three years and can't wait to be more for the rest of my life…

Special thanks to TÜBİTAK BİDEB for supporting me throughout my MSc program and for the partial funding of this work under the grant number TUBİTAK 118Z116 and 122Z320.

This study is partially funded by METU BAP Project GAP-108-2022-10893.

TABLE OF CONTENTS

LIST OF TABLES

TABLES

LIST OF FIGURES

FIGURES

LIST OF ABBREVIATIONS

ABBREVIATIONS

CRC	Colorectal Cancer
PAGE	Polyacrylamide Gel Electrophoresis
PBS	Phosphate-Buffered Saline
PVDF	Polyvinylidene Fluoride
ROS	Reactive Oxygen Species
SDS	Sodium Dodecyl Sulfate
TBS-T	Tris-buffered Saline and Tween-20
TCA	Tricarboxylic Acid
ETC	Electron Transport Chain
mTOR	Mechanistic Target of Rapamycin
α-KG	α-ketoglutarate
ISR	Integrated Stress Response
CMA	Chaperon Mediated Autophagy
CLEAR	Coordinated Lysosomal Expression and Regulation
GCN2	General Control Nonderepressible 2
ATF4	Activating Transcription Factor 4
RPS6	Ribosomal Protein S6
CAM	Chorioallantoic Membrane
Baf	Bafilomycin

TFEB	Transcription Factor EB
MAPK	Mitogen-Activated Protein Kinase

CHAPTER 1

INTRODUCTION

1.1 Cancer Cell Metabolism

To sustain homeostasis, all cells require an energy source. Sustaining homeostasis involves energy-intensive processes like DNA repair, basal transcription and translation, cytoskeletal dynamics, and vesicle trafficking. In addition to sustaining homeostasis, proliferating cells require additional energy for growth and division. Rapidly proliferating cells also require energy for biomass production. As a result, these cells must obtain additional nutrients and turn them into biosynthetic building blocks required for new cell formation (Lunt & vander Heiden, 2011).

Cancer is associated with uncontrolled cell proliferation. Reprogramming of energy metabolism has recently been included as a hallmark of cancer (Hanahan & Weinberg, 2011).In the presence of nutrients, oncogenic signaling pathways direct enhanced nutrient acquisition and generate biomass necessary for rapid cell growth and proliferation(Boroughs & Deberardinis, 2015).

Cancer cells also differ in their nutrient dependence, with some having altered glucose metabolism, others having altered one-carbon metabolism, or having an increased reliance on amino acid metabolism (S. Bose et al., 2020). Nonetheless, most tumors can be exposed to a low-nutrient environment, particularly during the early stages when the vasculature is immature, or during later stages when the tumor is in the process of metastasizing. To accurately reflect the low nutrient availability in a tumor microenvironment, numerous nutrient deprivation techniques have been used. The majority of such protocols in the literature rely on either the short-term complete elimination or a longer term reduction of the three main carbon sources: glucose, non-essential amino acids like L-glutamine, and serum. It should be

remembered that the effect of nutrient deprivation on cell behavior may differ depending on the nutrients that are available and how long the starvation lasts. Different cell types may respond differently to nutrient deprivation in culture due to their unique nutrient requirement (Ahmadiankia, 2020).

1.1.1 Glucose Metabolism

Glucose is the primary source of carbons for energy generation as well as biomass generation. Quiescent cells tend to be more catabolic and convert glucose to pyruvate via glycolysis which can then be oxidatively converted to CO2 in the tricarboxylic acid (TCA) cycle and the electron transport chain (ETC) to generate large amounts of ATP (Pavlova & Thompson, 2016).

In the absence of oxygen, pyruvate can be reduced to lactic acid by fermentation, primarily to regenerate the electron carrier NAD+. This process is significantly less efficient in generating ATP than the TCA cycle combined with oxidative phosphorylation (OXPHOS). In 1924, Otto Warburg discovered that primary tumor cells display increased reliance on glucose for glycolysis and release lactic acid even in the presence of oxygen (Pavlova & Thompson, 2016). It is now widely acknowledged that the primary purpose of the flux of glucose through glycolysis and the pentose phosphate pathway is to produce metabolic intermediates that serve as the building blocks for the production of nucleic acids, amino acids, and fatty acids (Alfarouk et al., 2020).

Withdrawal of glucose from the culture medium is known to affect numerous aspects of cell behavior. Many different cell types, including colorectal cancer (CRC) cells, have shown cell cycle arrest, changes in survival, increased sensitivity to chemotherapy, or chemoresistance when glucose availability was restricted (Ahmadiankia, 2020).

1.1.2 Amino Acid Metabolism

A high-rate tumor of cell proliferation can change the requirements of cells for amino acids and have an impact on related metabolic pathways (S. Bose et al., 2020). Amino acids are used by cancer cells for protein synthesis as well as metabolic intermediates. Amino acids can contribute to the formation of intermediates in the TCA cycle by a process known as anaplerosis. Amino acids can be sensed by the promiscuous nutrient-sensing mechanistic Target of Rapamycin Complex 1 (mTORC1), which regulates cell survival and growth (please see Section 1.2 for more details on nutrient sensing pathways). Amino acid availability therefore can also have an effect on cell growth and proliferation (Kanarek et al., 2020).

Among the different non-essential amino acids that can be synthesized in cells, glutamine is metabolized more abundantly in cancer cells (Miyo et al., 2016). It is physiologically an important source of carbon and nitrogen for the proliferation of cancer cells. Glutamine can be converted to glutamate and then to α-ketoglutarate (α-KG), which can be fed into the TCA cycle and keep it functioning (de Berardinis & Chandel, 2016). Glutamine also serves as a nitrogen source for the synthesis of nitrogen-containing building blocks such as other non-essential amino acids, purines, pyrimidines, and glucosamine-6-phosphate. In addition, glutamine takes part in the process of the uptake of essential amino acids from the extracellular environment. For instance, the amino acid antiporter LAT1/SLC7A5 imports leucine through the plasma membrane in coupling with a glutamine efflux.

Due to increased metabolic activity, cancer cells are constantly exposed to oxidative stress during tumorigenesis. The cells' antioxidant capacity must be increased in order to maintain oxidative homeostasis. Glutamine has a significant role in cellular anti-oxidative mechanisms by contributing to the synthesis of the endogenous antioxidant glutathione. Glutamine oxidation can also help maintain redox homeostasis by donating a carbon to malic enzyme that generates NADPH which is used to reduce oxidized glutathione (GSSG) and prevent oxidative stress (Nguyen & Durán, 2018). Several cancers have been reported to have varying degrees of

glutamine dependency; high glutamine dependency is typically linked to a more aggressive phenotype and therapy resistance (DeBerardinis, 2013).

The oncogenic transcription factor c-Myc is the main regulator of glutamine uptake and is frequently upregulated in proliferating cells (Porporato et al., 2020). c-Myc promotes the expression of glutamine transporters like SLC1A5/ASCT2 and glutamine-catabolizing enzymes like glutaminase 1 (GLS1); the latter promotes glutamine uptake through the transporter by converting glutamine to glutamate (Ohshima & Morii, 2021).

1.1.3 Growth Factors and Cytokines (Serum)

Numerous cytokines and growth factors found in serum are necessary for the cells to perform their signaling functions. Serum starvation is a common technique used, particularly in studies of signal transduction and experiments involving cell cycle synchronization (Langan et al., 2016). Serum starvation or deprivation is associated with decreased basal activity and synchronizes the proliferating cell population by causing G0/G1 cell cycle arrest (Langan et al., 2016).

Growth factors are one of the inputs that regulate both mTORC1 and mTORC2 hence cell growth, proliferation, and survival. Numerous studies have been conducted on the molecular processes that control mTORC1 activation. As a result, a major mediator of growth factor-induced mTORC1 activation has been identified as the phosphatidylinositol-3 kinase (PI3K)/Akt signaling pathway. Upon growth factor stimulation, PI3K is activated and catalyzes the production of phosphoinositide-3,4,5-triphosphate (PIP3) which recruits and activates Akt at the plasma membrane. When AKT is activated, it inactivates TSC2, which in turn activates the small GTPase Rheb, which stimulates and activates mTORC1. Moreover, active Akt inhibits PRAS40 and prevents it from inhibiting mTORC1 (Dufour et al., 2011). Besides PI3K/Akt axis, growth factors also activate mTORC1 via the Mek/Erk signaling pathway. Raptor is phosphorylated by p90RSK and TSC2

is phosphorylated by Erk, both of which have been proposed as activators of mTORC1 via the Erk signaling pathway.

Apart from mTORC1 activation, the Ras/Raf/MEK/ERK signaling cascade is directly used by growth factors and mitogens to transmit signals in order to control gene expression and prevent apoptosis (Roberts & Der, 2007). Mutations or aberrantly expressed components of these pathways are associated with anti-apoptotic and drug-resistance phenotypes in human cancer (McCubrey et al., 2007).

It is reported that serum deprivation caused CRC to enter a dormant state characterized by no proliferation, death, and drug resistance (Zhang et al., 2022). It was found that serum deprivation caused the side population of cancer cells to proliferate, which has been shown to be enriched in cancer stem cells, a property thought to contribute to drug resistance (de Marval et al., 2013). Another study with prostate cancer found that serum deprivation triggers an adaptive mechanism to tolerate oxidative stress and survival by inducing reactive oxygen species, which provides an early oxidative stress environment (White et al., 2020). It is worth noting that different cell types may behave differently in response to serum deprivation many studies have shown that nutrient deprivation reduces cell basal activity; however, there are also studies that show starvation in cancer cells may specifically induce stress, and that cancer cells are capable of enhancing their resistance to unfavorable microenvironment to facilitate cell survival and metastasis (Ahmadiankia, 2020).

1.2 Energy Sensing Pathways in Cells

Nutrient sensing is one of the most fundamental biological processes involved in cell division, growth, differentiation, and death. Cells require a rapid and accurate perception of the dynamic changes in intracellular and extracellular metabolites in order to interact with the environment and coordinate the biological network within (Wang & Lei, 2018). Nutrient sensors that can activate signaling pathways for

catabolic or anabolic reactions are especially crucial in cancer cells since these pathways are crucial for the production of biomass and energy. AMPK and mTOR signaling pathways are among the best-studied nutrient-sensing signaling pathways.

1.2.1 AMPK Pathway

Adenosine 5′-monophosphate-activated protein kinase (AMPK) becomes activated when the AMP/ATP ratio is high, as it is in cells under energy stress like starvation, oxidative stress, or hypoxia (Robles-Flores et al., 2021). Generally, AMPK signaling activates catabolic pathways to produce ATP like glycolysis and autophagy while inactivating anabolic (biosynthetic) pathways, which inhibits cell growth while preserving ATP (Inoki et al., 2012).

Energy stress caused by starvation or hypoxia activates the upstream kinase Liver Kinase B1 (LKB1), which phosphorylates AMPK at Thr -172, a negatively charged phosphate group that stabilizes the activation loop and positions key residues involved in substrate binding and catalysis, resulting in a 100-fold increase in activity (Shackelford & Shaw, 2009). Alternatively, calmodulin-dependent protein kinase kinase 2 (CAMKK2) can activate AMPK in a cytosolic Ca^{2+} concentration-dependent manner, which can prepare the cell for energy utilization (Carling et al., 2008). Although AMPK is thought to be a tumor suppressor since it is an essential mediator of the tumor suppressor LKB1, recent data suggest that it plays a role in tumor cell adaptation to low nutrient availability, and thus in cell survival (K. Bose et al., 2019). Signaling via AMPK may increase survival and proliferation by cooperating with oncogenes such as c-Myc (Robles-Flores et al., 2021) suggesting AMPK to be a potential therapeutic target in metabolic syndrome and cancer (Kim et al., 2016).

1.2.2 The mTOR Pathway

mTOR is a nutrient-sensing protein that serves as a key regulator of cellular growth and metabolism. Glucose, insulin, and amino acids are known to activate mTOR, which favors anabolism and cell growth (Simcox & Lamming, 2022). The mTOR protein acts via two separate multi-protein complexes, mTOR complex 1 (mTORC1) and mTOR complex 2 (mTORC2). Besides several shared components, the mTORC1 complex consists of the negative regulator PRAS40 and the regulatory-associated protein of mTOR (Raptor) (Robles-Flores et al., 2021).To promote protein translation and general anabolic metabolism, Raptor recruits mTORC1 to the lysosome and leads to the activation of ribosomal S6 kinase (S6K) and eukaryotic translation initiation factor 4E-binding protein 1 (4E-BP1) which are best characterized as downstream effectors of the mTORC1 complex (Chauvin et al., 2014).

4E-BP1 is a negative regulator of translation and is phosphorylated and inactivated by mTORC1. Inactivated 4E-BP1 dissociates to start cap-dependent translation so that several proteins involved in cell growth, proliferation, and cell cycle regulation can be translated by eIF-4E. (Qin et al., 2016). The 40S ribosomal protein (RP) S6 can be activated by phosphorylation of S6K1 via mTORC1, S6K1 in turn phosphorylates RPS6 at S235/236 and S240/244. Activated RPS6 responds to anabolic signals by enhancing the translation efficiency of 5’ terminal oligopyrimidine tracts (TOPs) type of RNAs that encode numerous components necessary for protein translation, including ribosomal proteins, pro-elongation factors, and polyA-binding proteins (Chauvin et al., 2014).

It is well understood that mTORC1 must be localized to lysosomes in order to detect and respond to changes in amino acid levels. Upon increase in cellular amino acid levels, mTORC1 is recruited to the lysosomal surface where it is activated by the small GTPase Rheb (Ras homolog enriched in the brain) in its GTP-loaded form. The activity of Rheb is controlled by a complex that includes tuberous sclerosis complex 1 (TSC1), TSC2, and TBC1 domain family member 7. (TBC1D7) which is

also localized to lysosomes and acts as a GTPase-activating protein (GAP) that inhibits Rheb activity In the presence of growth factors or insulin TSC releases its inhibitory activity on Rheb so that mTORC1 to be activated. Meanwhile, active Rag GTPases and a Ragulator that anchors Rag GTPases to lysosomes are required for the amino acid-dependent translocation of mTOR to the lysosome. It has been proposed that amino acids cause RagA/B proteins to load GTP, promoting raptor binding and the formation of an activated mTORC1 complex (Napolitano et al., 2022). Moreover, recent studies revealed that mTORC1 regulates lysosomal function and requirement in response to energetic and degradative needs by activating transcription factor EB (TFEB), a master regulator of lysosomal biogenesis that promotes the expression of several lysosomal proteins (Puertollano, 2014).

Multiple upstream signals are integrated with mTORC1 activation and inhibition. For example, the PI3K-Akt and MAPK/Ras pathways in response to growth factors and insulin increase mTORC1 activity. Signaling via AMPK can inhibit mTORC1 activity in response to energy stress by phosphorylating TSC2 and increasing its GAP activity, or by phosphorylating Raptor and dissociating from mTOR so that the biosynthesis process becomes inactive (Robles-Flores et al., 2021).

Hypoxia and nutrient depletion are two conditions that frequently affect rapidly proliferating cancer cells primarily due to poor vasculature. These circumstances force them to adapt in order to survive, along with other stressors like hyperactive metabolism, mitochondrial dysfunction, etc. Autophagy involves the formation of double-membraned vesicles called autophagosomes around cargo, which then fuse with lysosomes to produce autophagolysosomes for cargo degradation (Levy et al., 2017). The activation of autophagy during nutrient depletion in cancer cells can maintain cellular homeostasis, while also providing metabolites and energy. On the other hand, cancer cell growth depends on energy-consuming anabolic processes that are likely to benefit from mTORC1 activation, which promotes the production of biosynthesis-related building blocks and thus promotes abnormal proliferation. mTORC1 activation is generally associated with the inhibition of autophagy since anabolic and catabolic pathways generally do not co-exist in cells. To benefit from

both, however, cancer cells must maintain a fine balance between mTORC1 activity and autophagy (Robles-Flores et al., 2021). Furthermore, cancer cells may carry out a paradoxical co-activation of mTORC1 and autophagy in order to ensure cell survival. In this, amino acids released from the breakdown of proteins by autophagy can activate the mTORC1 pathway, ensuring cell growth and survival (Condon & Sabatini, 2019).

1.3 Stress Response Pathways Activated in Response to Nutrient Restriction

Survival of tumor cells under hypoxia and poor nutrient availability is dependent on the activation of various stress response pathways such as autophagy and the integrated stress response (ISR) pathway.

1.3.1 Autophagy

Autophagy is a catabolic mechanism that is conserved throughout evolution and is crucial for recycling biomolecules by disposing of aggregated, misfolded, and long-lived proteins or damaged organelles (Ravanan et al., 2017). Autophagy primarily serves as a tumor suppressor at the beginning of tumorigenesis by limiting cytoplasmic damage and inflammation. On the other hand, when activated at the later stages of tumorigenesis, autophagy can help stressed cancer cells survive by supplying them with energy and biomolecules (Liu & Ryan, n.d.). The type of stress, the timing of the stress, the genetic makeup of the cells, and the nature of the microenvironment are all factors that affect the autophagic response.

There are three types of autophagy: microautophagy, chaperon-mediated autophagy (CMA), and macroautophagy which are further divided into bulk and selective autophagy based on cargo type (Kocaturk et al., 2019). Bulk autophagy is thought to be non-selective toward the cargo and serves to recycle macromolecules to compensate for required nutrients (Zaffagnini & Martens, 2016). Selective autophagy, on the other hand, brings specific cytoplasmic constituents such as

mitochondria, lysosomes, endoplasmic reticulum (ER), and ribosomes into the autophagosome (Levine & Kroemer, 2019).

The main proteins linked to the induction of autophagy are Beclin-1 and uncoordinated (UNC) 51-like kinase 1/2 (ULK1/2), whereas LC3 (microtubule-associated protein 1 light chain 3) and p62 are involved in the flux of macromolecules from the autophagosomes to the lysosomes during autophagy. Autophagy is initiated by the ULK1/2 complex which phosphorylates Beclin-1 to activate the lipid kinase activity of Vps34 (a class III PI3K), to initiate nucleation of the autophagosome membrane. Vps34 promotes the formation of phosphatidylinositol 3-phosphate (PtdIns3P), which serves as a platform for PI3P-binding domain-containing autophagy proteins to successfully initiate the formation of a double membrane structure (Pattingre et al., 2005). The cytosolic soluble microtubule-associated protein 1A/1B-light chain 3 (LC3-I) is conjugated to phosphatidylethanolamine to form LC3-phosphatidylethanolamine conjugate (LC3-II), which is recruited to autophagosomal membranes. Western blot analysis of LC3 II expression is frequently used as a dependable indicator of the induction of autophagy (Klionsky et al., 2016). p62 is referred to as an adaptor ubiquitin-binding autophagic adaptor that mediates the engulfment of autophagic cargo, including mitochondria, intracellular pathogens, and a subset of cytosolic proteins (Palm & Thompson, 2017). There is consequently a correlation between successful autophagic degradation (autophagic flux) and a decline in p62 protein levels.

The autophagic process is highly regulated and depends on two primary nutrient-sensing complexes: the mammalian target of rapamycin (mTOR) and AMP Kinase (AMPK) (González et al., 2020). Amino acid transporters at the plasma membrane supply cytosolic amino acids that can activate mTORC1 signaling. However, when cytosolic amino acids are depleted, mTORC1 signaling is inhibited and autophagy is activated to replenish amino acid pools via lysosomal protein degradation. mTORC1 acutely and negatively regulates autophagic flux through the direct phosphorylation of ULK 1, ULK2, and ATG13 (Condon & Sabatini, 2019).

AMPK is another major energy sensor in cells that is activated when there is a lack of energy (low ATP) as a result of either mitochondrial dysfunction or glucose withdrawal. Activated AMPK promotes autophagy by phosphorylating Beclin1, type III PI3K Vps34, and ULK1 along with the inhibition of mTORC1 (Hernandez & Perera, 2022) (Figure 1.1).

Upon prolonged starvation, regeneration of lysosomes becomes important. This is achieved through the transcriptional activity of TFEB, TFE3, and MITF, which can transcriptionally upregulate CLEAR (Coordinated Lysosomal Expression and Regulation) motif-containing genes lysosome genes (Napolitano et al., 2018). This increases lysosome numbers and function (autophagic flux) to enable the cell to metabolically adapt to environmental stress (Raben & Puertollano, 2016). The activity of these transcription factors can be regulated by phosphorylation by the mTORC1 complex in response to stress (Raben & Puertollano, 2016). Recently, it was shown that active mTOR complex sequesters TFEB near the lysosome and prevents it from translocating to the nucleus. However, when mTOR is inhibited TFEB is released to translocate to the nucleus and upregulate gene expression (Napolitano et al., 2018).

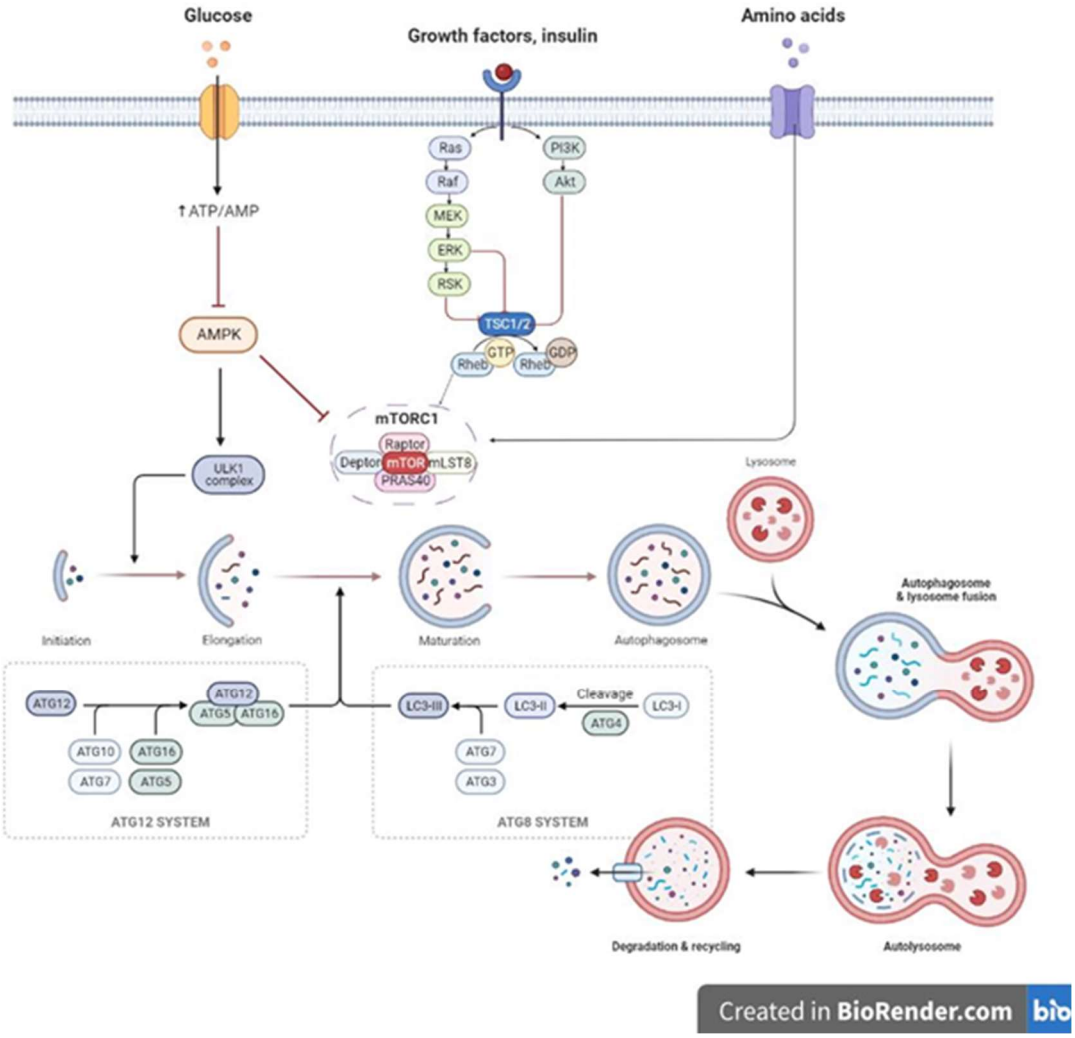

Figure 1.1 Autophagic Process

Autophagy occurs in a series of steps. When the ULK1 complex dissociates from the mTORC1 under nutrient-restricted conditions autophagy is initiated and the phagophore formation is driven by the activated ULK1 complex. The PI3K complex then induces nucleation. The Atg5-Atg 12-Atg16L and LC3II-PE conjugates mediate the maturation step. When phagophores mature into autophagosomes, autophagic cargo is enriched and encapsulated. After that, autophagosomes fuse with lysosomes to form autophagolysosomes. Lysosomal enzymes then degrade the cargo contained within the autophagolysosome. Created with BioRender.com.

1.3.2 Integrated Stress Response

The integrated stress response (ISR) is a complex signaling pathway that is activated in response to both extrinsic factors, such as hypoxia, starvation, and viral infection, and intrinsic factors, such as endoplasmic reticulum (ER) stress (Pakos-Zebrucka et al., 2016). The central event that converges all stress stimuli that activate ISR is the phosphorylation of eukaryotic translation initiation factor 2 alpha (eIF2α) on serine 51 by one of four eIF2α kinase members. Phosphorylation of eIF2a increases its affinity toward guanine nucleotide exchange factor eIF2B and the interaction prevents eIF2B from exchanging GDP for GTP. This reduces the available pool of free GTP-bound eIF2 and causes a global decrease in cap-dependent translation, lowering the consumption of macromolecules such as amino acids during times of scarcity (Chu et al., 2021).

The four different eIF2 kinases that can phosphorylate eIF2α respond to different cell states: PERK, which is located in the ER, is activated when a cell experiences ER stress due to the accumulation of unfolded protein, loss of calcium homeostasis, or changes in cellular energy. According to the traditional model for PERK activation by ER stress, when misfolded proteins accumulate in the ER lumen, the chaperone protein GRP78 becomes dissociated from PERK, resulting in its autophosphorylation and activation. PERK can be also activated by the direct binding of misfolded proteins (Korennykh & Walter, 2012). Additionally, PERK activation, in response to glucose deprivation has been reported in neuronal cells where it was demonstrated that ATP depletion leads to PERK activation via inhibition of the sarcoplasmic/ER Ca^{2+}-ATPase pump. Interestingly, oncogene activation in cancer cells causes increased proliferation and protein synthesis which can activate the ISR via PERK (Tian et al., 2021).

Among the other three kinases, PKR is activated in the presence of double-stranded RNA (dsRNA) during viral infections. Heme-regulated eIF2a kinase (HRI) is expressed mainly in erythroid cells and is activated in the absence of heme and protects the erythroid cells from the accumulation of toxic globin aggregates during

iron deficiency. General control nonderepressible 2 (GCN2) is activated during amino acid deficiency by binding to deacylated transfer RNAs and preventing global translation. Additionally, GCN2 activation was also reported in cancer cells upon long-term glucose starvation which is most likely in direct effect caused by the consumption and therefore depletion of amino acids as an alternative energy source in the absence of glucose (Pakos-Zebrucka et al., 2016).

Phosphorylation of eIF2a on serine 51 reduces global protein synthesis while allowing translation of only selected genes like activating transcription factor 4 (ATF4) which helps cells to survive and recover by increasing translation of stress-responsive genes. The downstream targets of ATF4 include amino acid biosynthesis pathways like asparagine synthetase and amino acid transporters to replenish nutrient levels and reestablish cellular homeostasis (Harisha Rajanala et al., 2019). Recent research has linked ATF4 and CHOP to autophagy induction in mammalian cells. It was shown that ATF4 or CHOP can bind to specific promoter elements in their target genes in response to amino acid starvation or ER stress, resulting in the induction of transcription of autophagy-related genes (B'Chir et al., 2013). Another target of ATF4 is Sestrin-2 which was reported as a direct inhibitor of mTORC1 under amino acid starvation in mouse embryonic fibroblasts (Ye et al., 2015). In contrast, a recent study has shown that activation of ISR inhibits global translation, which increases the availability of free amino acid, which in turn can activate mTORC1 (Torrence et al., 2021).

1.4 Nutrient Restriction and Cancer Cell Behavior

In response to poor nutrient availability and hypoxic stress, cancer cells have the ability to rewire their metabolism and signaling activities in order to survive and proliferate (Ding et al., 2015). Survival of tumor cells under such challenging circumstances can affect cell behavior such as cell cycle progression, proliferation, or response to drugs, and lead to the activation of numerous signaling pathways (Vaziri-Gohar et al., 2022).

1.4.1 Cell Cycle and Proliferation

Numerous studies in various cancer models, including colorectal cancer, have found that the effect of nutrient restriction on cancer cell survival and proliferation varies depending on the type of nutrient restriction, treatment duration, and cellular status. For instance, it was demonstrated that HT29 cells subjected to 48h serum starvation went into a reversible quiescent state accompanied by increased expression of Mirk-mediated destabilization of G1 cyclins (H. Shi et al., 2009). Supporting this, 6 h and 12 h treatment of HCT-116 cells with serum-free medium decreased their viability via a Smad4/PUMA-mediated mechanism (Lee et al., 2011).

However, there are also studies that have shown an increase in colorectal cell survival with nutrient restriction. For instance, amino acid starvation of several CRC cell lines including LoVo for 24 h activated protective autophagy (Sato et al., 2007). Similarly, DLD-1 cells that were starved of glucose, glutamine, or serum for 24, 48, or 96 hours were shown to evade apoptosis and thus survive via proteolytic cleavage of Myc (Conacci-Sorrell et al., 2014).

1.4.2 Sensitivity to Drugs

Drug resistance causes disease relapse and metastasis, complicates the improvement of clinical outcomes for cancer patients, and is the most significant barrier to successful cancer therapy. The mechanisms underlying chemoresistance include induction of expression of transporter pumps, oncogenes, loss of tumor suppressor genes, aberrant mitochondrial alterations, and DNA repair, along with the induction with autophagy, epithelial-mesenchymal transition (EMT), and cancer stemness. Nutrient restriction may play a dual role in cancer by activating pro-survival mechanisms which can decrease the cytotoxic effects of drugs. On the other hand, nutrient restriction can also activate mechanisms recognized as cell death pathways and sensitize cancer cells to drugs (Naveed et al., 2014).

Drug resistance requires the activation of and interaction between numerous factors. Oncogenic proteins such as EGFR, Akt, or NFκB, may modulate apoptosis-related gene expression and contribute to EMT, cell stemness, and autophagy (Zheng, 2017). Chemoresistance was found to be associated with increased protective autophagy and decreased apoptosis in bladder cancer cells treated with Gossypol (Ojha et al., 2015) and osteosarcoma cells treated with cisplatin (Mani et al., 2015). The use of the autophagy inhibitor chloroquine was shown to restore chemosensitivity and increase cancer cell death (Ojha et al., 2015). There are several mechanisms by which autophagy contributes to cancer cell drug resistance. One such mechanism is lysosomal drug sequestration in which lysosomes can trap hydrophobic weak-base chemotherapeutics and decrease their availability at the intracellular target site (Guo et al., 2016). Autophagy can also protect cancer cells by capturing damaged organelles caused by drug treatment that would otherwise induce apoptosis, thereby promoting survival (Hraběta et al., 2020). Increased stemness in response to nutrient restriction has been observed in serum-starved lung and breast cancer cells due to the upregulation of factors such as Sox2, MDR1, and Bcl-2 (Yakisich et al., 2017). Another study with CRC cells reported that glucose deprivation induced multi drug resistance via activation of the PERK/ATF4 pathway, resulting in an increase in multidrug resistance gene 1 (MDR1) expression by ATF4 (Hu et al., 2016).

The nutrient restriction has been shown in several studies to sensitize cancer cells to chemotherapeutic drugs (Y. Shi et al., 2012; Thomas et al., 2020). The primary mechanism, in this case, was increased ROS generation and oxidative stress caused by serum deprivation, which in turn increased chemotherapeutic sensitivity (Zhuge & Cederbaum, 2006). It is likely that such a mechanism would rely on the loss of endogenous antioxidants such as glutathione.

1.5 Nutrient Restriction and Translation

Ribosomal Protein S6 (RPS6) is one of the components of 40S small ribosomal subunit of the eukaryotic ribosomes that participates in the regulation of mRNA

translation, cell proliferation, growth, differentiation, DNA repair, apoptosis, and glucose metabolism in cells (Proud & Xie, 2021).

mRNA translation is tightly controlled by signaling pathways that sense environmental stress like UV radiation, growth factors, nutrient status, and oxygen availability. PI3K/AKT and mitogen-activated protein kinase (MAPK) pathways are the two main pathways involved in the regulation of translation by RPS6 phosphorylation (Mok et al., 2013). RPS6 has five serine residues at the C-terminus that can be phosphorylated by several protein kinases (Nakashima & Tamanoi, 2010). The main signaling pathway that phosphorylates RPS6 in mammalian cells is the PI3K/AKT/mTORC1/S6K pathway (de la Cruz López et al., 2019). All the serine residues are phosphorylated by S6K1, starting with S236, and progressing on to S235, S240, S244, and S247. RPS6 can also be phosphorylated at S235 and S236 by p90 ribosomal S6 kinase (RSK) via the Ras-Raf-MEK-ERK (MAP Kinase) signaling cascade. Thus, RPS6 serves as a node of convergence for the PI3K/AKT/mTORC1/S6K and MAPK pathways (Figure 1.2). Furthermore, synergistic crosstalk between mTORC1 and MAPK signaling has been reported in the regulation of RPS6 phosphorylation in several studies. Oncogenic MAPK signaling was shown to increase mTORC1 activity through RSK-mediated inhibitory phosphorylation of TSC2 (Carrière et al., 2008). Another study reported that ERK phosphorylation could increase S6K activity (Mukhopadhyay et al., 1992). Moreover, ERK is known to activate mTORC1 indirectly by RSK-mediated phosphorylation of RAPTOR (Ma et al., 2005).

RPS6 is also associated with several extra-ribosomal functions. For example, it was demonstrated that RPS6 deficiency could induce p53-dependent cell cycle arrest in several tissues (Fumagalli et al., 2009; Panić et al., 2006; Sulic et al., 2005). Additionally, the knockdown of RPS6 in lung cancer cells was shown to decrease tumorigenicity (Chen et al., 2014). RPS6 overexpression and phosphorylation were shown to increase cell proliferation with concurrent increases in the level of cyclins and decrease the number of cells in the G0/G1 phase (Chen et al., 2015). Moreover, cells expressing hypo-phosphorylated RPS6 were more sensitive to apoptosis

induction by tumor necrosis factor-related apoptosis-inducing ligand (TRAIL) (Jeon et al., 2008). In another study, a negative regulation between phosphorylated RPS6 and DNA damage-regulated autophagy modulator protein 1 (DRAM1) was reported to decrease cell viability and colony formation in CRC cell line SW480 (Lu et al., 2019).

Cancer cells showing overexpression of RPS6 display intrinsic or acquired drug resistance. RPS6 has been linked to drug resistance by increasing the translation of nuclear factor erythroid 2-related factor 2 (NRF2), a transcription factor that targets Aldo keto reductase (AKR) family 1 member, which are NAD(P)H-dependent oxidoreductases, and their overexpression results in drug resistance (Gambardella et al., 2019; Penning, 2017).

Since the phosphorylation of RPS6 is associated with oncogenic signaling, it may play a role in tumorigenesis and could be used as a therapeutic target. For example, conditions such as hypoxia, a key inducer of neoangiogenesis, can activate RPS6 in endothelial cells via vascular endothelial growth factor (VEGF) secretion from the tumor cells which activates Akt expression and activation in endothelial cells (Pedersen et al., 2017). A knock-in mouse model of a non-phosphorylatable RPS6 mutant (rpS6P-/-) has shown that RPS6 phosphorylation is required for the development of pancreatic ductal adenocarcinoma (PDAC) in the KRASG12D mutation background (Khalaileh et al., 2013). A role of RPS6 phosphorylation on tumorogenesis was also shown in mice expressing constitutively active AKT; moreover, hypo-phosphorylation of RPS6 could reduce constitutively active AKT-induced tumor formation in insulinoma (Polyak et al., 1994).

RPS6 phosphorylation and/or overexpression have been observed in a variety of cancers, suggesting that RPS6 may serve as a predictive biomarker in cancer. The expression or phosphorylation of RPS6 was also linked to pathological grade and/or disease progression in various human cancers. Thus, phosphorylated RPS6 levels can be monitored to predict drug resistance and disease progression after drug treatment (Yi et al., 2022).

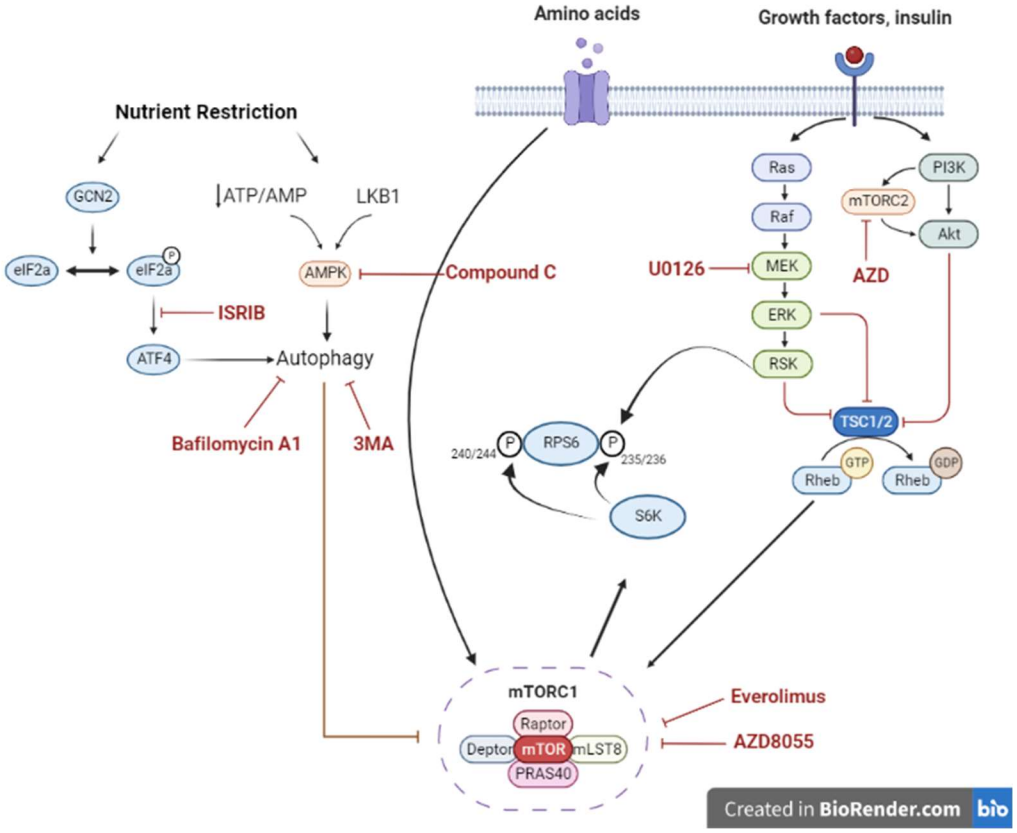

Figure 1.2 Signaling Pathways for the Activation of RPS6 and ATF4

Induction of ISR following nutrient restriction can encourage cap-independent translation of stress response proteins while inhibiting global translation. Additionally, nutrient restriction or Ca^{++}-mediated signaling can activate AMP Kinase (AMPK) and autophagy, which inhibits the mTOR pathway. RPS6 participates in 5' cap-dependent translation as well as cell proliferation, and cell growth when phosphorylated. Growth factors and insulin activate both MAPK and PI3K/Akt pathways. Activated MAPK pathway (Ras-Raf-MEK-ERK-RSK) contributes to the phosphorylation of RPS6 at Ser 235/236 as well as Ser 240/244 through the inhibition of TSC1/2 complex which inhibits mTORC1. PI3K activation also results in mTORC1 activation via Akt, which inhibits TSC2 and thus promotes Rheb GTP-loading. Specific inhibitors that can block critical nodes of this signaling mechanism have also been shown. Created with BioRender.com.

1.6 Scope, Aim, and Novelty of This Study

Many rapidly growing tumors are in a nutrient and oxygen-deficient environment; however, whether the activation of the stress response, as well as anabolic and catabolic nutrient sensing pathways in cancer cells subjected to prolonged starvation, is required for cell survival has not been adequately addressed. Nutrient restriction can activate a variety of common stress response pathways in cells (Wortel et al., 2017); however, the effect of limited nutrient availability on the activation of nutrient-sensing pathways like mTOR or AMPK has been unequivocally demonstrated (Condon & Sabatini, 2019).

Therefore, we incubated several colorectal cancer cell lines in glucose and glutamine-free RPMI medium supplemented with 1% FBS, 0.1g/L glucose, and 0.2mM L-glutamine which was optimized as a nutrient-restricted medium in the capacity of a TÜBİTAK 1001 project (118Z116) by our lab. We observed that the LoVo cell line showed the concurrent activation of AMPK (via phosphorylation at T172) and ribosomal protein (RP) S6.

The activation of RPS6 despite ongoing starvation in LoVo indicated a major overhaul of nutrient-sensing pathways, most likely to gain survival advantages. Based on the concurrent activation of RPS6 and AMPK in nutrient-restricted LoVo cells, I hypothesized that co-activation of RPS6 and AMPK may provide survival and growth advantages. To address this hypothesis, I examined the following:

What is the upstream activator of RPS6 in nutrient-restricted cells?

Is there a cross-talk between the activation of RPS6 and AMPK?

Whether RPS6 activation in nutrient-restricted cells could affect the cells' sensitivity to a chemotherapeutic agent, and whether RPS6 inhibition would make the cells more sensitive to chemotherapy.

Overall, this study showed for the first time that treatment of LoVo cells with physiologically relevant nutrient-restricted medium activates RPS6 which can be

inhibited by AMPK inhibitor Compound C, autophagy inhibitor 3MA, and MEK1/2 inhibitor U0126. This finding suggests complex signaling mechanisms that regulate RPS6 activation under nutrient restriction and provides us a unique opportunity to assess which mechanisms result in drug resistance and allow cell survival in nutrient-restricted conditions.

CHAPTER 2

MATERIALS AND METHODS

2.1 Cell Culture

Colorectal cancer (CRC) cell lines LoVo, T84, and RKO were purchased from the American Type Culture Collection (ATCC) (Middlesex, UK), HCT-116 cells were purchased from DKFZ (Heidelberg, Germany), Caco-2 cells were purchased from ŞAP Enstitüsü (Ankara, Turkey). HCT-116 and LoVo cells were grown in RPMI-1640 Medium (Biological Industries) supplemented with 10% fetal bovine serum (FBS), 2 mM L-Glutamine, and 1% Penicillin-Streptomycin (P/S). Caco-2 cells were cultured in Eagle's minimum essential medium (EMEM) supplemented with 1 g/L glucose and 20% FBS, 2 mM L-glutamine, 0.1 mM non-essential amino acids (NEAA), 1% P/S, and 1mM sodium pyruvate. T84 cells were cultured in DMEM - HAM'S F12 medium supplemented with 10% FBS, 2 Mm L-Glutamine, and 1% P/S. RKO cells were cultured in Eagle's Minimum Essential Medium (EMEM) containing 2 mM L-Glutamine, 1 mM sodium pyruvate, 0.1 mM NEAA, 10% FBS, and 1% P/S. All cell lines were cultured in an incubator with 95% air and 5% CO2 at 37oC. The cells were routinely tested for mycoplasma contamination by PCR (Young et al., 2010). Plasmocin (Invitrogen, France) was added to the culture medium at a concentration of 2.5 mg/ml to prevent any mycoplasma contamination.

Cell pellets were resuspended in media containing 5% DMSO (dimethyl sulfoxide) (Sigma, cat#: 154938) for long-term storage. Plastic consumables used in cell culture were purchased from Sarstedt (Germany).

2.1.1 LoVo Cell Line

LoVo is a cell line derived from the large intestine of a 56-year-old Caucasian man with grade IV Duke's C colorectal cancer. These cells are microsatellite instable, with the G13D; A14V KRAS mutation, and wilt type BRAF, PI3KC1, PTEN, and TP53. (Ahmed et al., 2013).

2.1.2 Caco-2 Cell Line

Caco-2 cells, which were isolated from a patient with colon adenocarcinoma, have the ability to spontaneously differentiate in cell culture (Sambuy et al., 2005). It is Duke's grade C colorectal cancer. These cells are microsatellite stable, with the E204X TP53 mutation, and wild-type BRAF, PTEN, KRAS, and PI3KC1 (Ahmed et al., 2013).

2.1.3 HCT-116 Cell Line

HCT-116 cell line was derived from an adult male's colon as three subpopulations (Fine WD, Brattain MG, Thompson J, Khaled FM, 1981) with grade Duke's D colorectal cancer. These cells are microsatellite instable, with the G13D KRAS, H1047R PI3KC1 mutation, and wild-type BRAF, PTEN, and TP53 (Ahmed et al., 2013).

2.1.4 RKO Cell Line

RKO is a colon carcinoma cell line that is poorly differentiated colorectal cancer. These cells are microsatellite instable, with the E204X TP53 and wild-type BRAF, PI3KC1, PTEN, KRAS, and TP53 (Ahmed et al., 2013).

2.1.5 T84 Cell Line

T84 is a transplantable derived from a lung metastasis in a 72-year-old man. . These cells are microsatellite stable, with TP53 and KRAS mutation (Sigma Aldrich, USA).

2.2 Nutrient Restriction Protocol

The nutrient restriction medium was prepared by using glucose and glutamine-free RPMI-1640 that was supplemented with 1% FBS, 0.2 mM L-glutamine, 0.1 g/L glucose, and 1% Penicillin-Streptomycin. Cells were seeded into 6-well plates or tissue culture flasks and allowed to attach overnight. The following day, the complete growth medium was removed, and the cells were washed with PBS before the starvation nutrient restriction medium was added and incubated for 48 h unless otherwise stated. For replenishment treatment, after 48 hours of treatment with nutrient restriction medium, the medium was replaced with the complete growth medium for 24 hours.

For the acute starvation of cells used in immunofluorescence experiments, LoVo cells were incubated with Earle's Balanced Salt Solution (EBSS) (Thermo Fisher) for 2 h.

2.3 Treatments

Drug treatment of LoVo cells was carried out in the following manner: cells were treated for 48h with 1 μM Everolimus (in DMSO), 5 μM AZD8055 (in DMSO), 100 nM Bafilomycin A1 (in DMSO), 5 mM 3-MA (in culture medium), 20 μM 5-FU (in DMSO), 5mg/mL Cisplatin (in PBS, 0.24%) and 5 μM Compound C (in DMSO), for 24h with 0.5 μM U0126 (in DMSO) and for 2h with 100 nM ISRIB (in DMSO) in either complete or in nutrient restriction medium. 48-hour drug treatments began simultaneously with nutrient restriction, and 24- and 2-hour drug treatments were

started after 24h and 46h of nutrient restriction respectively. The total duration of treatment or nutrient restriction did not exceed 48h. Table 2.1 provides a list of the drugs used in the study.

Table 2.1 Chemicals Used in This Study

Chemical	Function	Mechanism of Action	Vehicle	Concentration
Everolimus	mTORC1 inhibitor	Forms drug complex with FKBP-12 that inhibits the activation of mTORC1	DMSO (0.01%)	1 μM
AZD8055	mTOR inhibitor	ATP-competitive inhibitor	DMSO (0.01%)	5 μM
Compound C	AMPK inhibitor	ATP-competitive inhibitor	DMSO (0.01%)	5 μM
Bafilomycin A1	Autophagy inhibitor	Lysosomal V-ATPase inhibition	DMSO (0.01%)	100 nM
3-Methyladenine (3-MA)	Autophagy inhibitor	Class III PI3K inhibition	Medium (100%)	5 mM
ISRIB	Integrated stress inhibitor	Activates eIF2B enabling recycling of eIF2	DMSO (0.01%)	100 nM
U0126	MEK1/2 inhibitor	MEK1/2 kinase inhibitor	DMSO (0.01%)	0.5 μM

Table 2.1 (cont'd)

5-Fluorouracil (5-FU)	Anti-cancer agent	Thymidylate synthase inhibition	DMSO (0.05%)	20 µM
Cisplatin	Anti-cancer agent	DNA damage	PBS (0.24%)	5mg/mL

2.4 RNA Isolation and cDNA Synthesis

Cells were collected and washed with PBS after centrifuging at 1500 x *g* for 5 minutes at 4ºC. Total RNA was isolated using the NucleoSpin RNA Kit (Macherey Nagel, Germany) according to the manufacturer's protocol and stored at -80 °C until use. cDNA was synthesized from 1 µg RNA using the RevertAid First Strand cDNA Synthesis Kit (Thermo Scientific) and random hexamers. DNase I treatment was performed according to the kit's protocol, and the synthesized cDNAs were stored at -80 °C.

2.5 Quantitative Real-time PCR (qRT-PCR)

qRT-PCR was performed in Rotor GeneQ 6000 series (Qiagen) tubes with 100 µL 4-strip Rotor Gene style. The real-time PCR reactions were prepared with 5 µl of 2X GoTaq qPCR Master Mix (Promega, Madison, WI, USA), 1µM forward and reverse primers and 2 µl cDNA to a final volume of 10µl. Standard curves for each primer pair were generated. Threshold cycle (Ct) values were determined after 45 cycles using the relative standard curve method. The Pfaffl method was used to calculate the fold change in transcriptional expressions (Pfaffl, 2001).

Table 2.2 List of the Primers Used in This Study

Gene	Forward Primer Sequence	Reverse Primer Sequence	TM (°C)
ACTB Beta(β)-actin	TGTCCACCTTCCAGCAGATGT	AGCTCAGTAACAGTCCGCCTAGA	59
RAB5	CAAGGCCGACCTAGCAAATAA	GATGTTTTAGCGGATGTCTCCAT	56
RAB7A	AGTGTTGCTGAAGGTTATCATCC	TTCCTGTCCTGCTGTGTCC	56
SQSTM1 p62	ATGAGGACGGGGACTTGGTT	TTGCAGCCATCGCAGATCA	57
MCOLN1 Mucolipin-1	CATGAGTCCCTGCGACAAGT	ACCACGGACATACGCATACC	60

Table 2.3 List of NCBI Reference Sequence of the Primers

Gene	NCBI Reference Sequence
ACTB	NM_001101
RAB5	NM_001292048.2 NM_004162.5
RAB7A	NM_004637.6
SQSTM1	NM_001142298.2 NM_001142299.2 NM_003900.5
MCOLN1	NM_020533.3

2.6 Protein Isolation and Western Blot

2.6.1 Total Protein Isolation & Quantification

Total protein isolation was performed according to the manufacturer's instructions using Mammalian Protein Extraction Reagent M-PER (Thermo Fisher Scientific, USA) supplemented with PhosSTOP Phosphatase Inhibitor and complete Mini EDTA-free Protease Inhibitor Cocktail (Roche, Germany). The protein concentration of the isolated protein was determined with the Bradford assay using Coomassie Protein Assay Reagent (Thermo Fisher Scientific, USA). In a plastic cuvette, 5 µl of total protein was mixed with 1.5 ml of Coomassie Protein Assay Reagent, and the absorbance value was measured at 595 nm using a Multiskan-GO microplate reader (Thermo Fisher Scientific, USA). After that, the protein concentration was determined by comparing the reading to a standard curve generated with bovine serum albumin (BSA).

2.6.2 Cytoplasmic and Nuclear Protein Isolation

The collected cells were washed twice with 0.3 ml of hypotonic PBS and centrifuged at 500 x *g* for 5 min at 4 °C. The lysed cells were combined with 75 µl of 10% NP-40 (Pan-Reac AppliChem, Darmstadt, Germany) and incubated on ice for 15 minutes. The tubes were centrifuged at the highest speed for 30 seconds at 4 °C and the supernatant, containing the cytosolic proteins, was added to a fresh Eppendorf tube. The remaining pellet was resuspended in 80 µl of a nuclear extraction buffer. The mixture was vortexed for 30 seconds and incubated on ice for 15 minutes on an orbital shaker. This procedure was carried out twice. The mixture was centrifuged at 14000 x *g* for 10 minutes at 4 °C, and the supernatant containing the nuclear fraction was collected in a fresh Eppendorf tube.

2.6.3 Western Blot

The expression of proteins of interest in the cell lines was verified using the Western blot method. 6X Laemmli Buffer was added to 30 µg of isolated total protein and boiled for 10 minutes at 95 °C and then loaded onto 12% SDS-polyacrylamide gel. Proteins were separated by SDS Polyacrylamide Gel Electrophoresis (SDS-PAGE) at 90 V for 1.5 h. PageRuler Plus Prestained Protein Ladder (Thermo Fisher Scientific, USA) was used as a marker for proteins with molecular weights between 10 to 250 kDa. After separation, the proteins were transferred from the gel to a Polyvinylidene Fluoride (PVDF) membrane for 1 hour 15 minutes at 115 V at 4 °C. Membrane blocking was carried out in a TBS-T buffer containing 5% skimmed milk for 1 hour at room temperature. The membranes were incubated with the primary antibody (Table 1) overnight at 4 °C, then properly rinsed with TBS-T, and afterward incubated with the appropriate secondary antibody for 1 hour at room temperature, followed by another TBS-T rinse. The membranes were then incubated with Clarity ECL Substrate (BioRad, USA) as the visualization agent for approximately 1 minute and visualized in a Chemi-Doc MP (BioRad, USA).

The membranes were stripped where necessary by incubating for 10 minutes at 60 °C in mild stripping buffer and then properly rinsed with TBS-T before incubating the membrane with a different antibody. To confirm similar protein loading, β-actin or GAPDH antibody was employed as a loading control.

Table 2.4 List of Antibodies Used in This Study

Antibody	**Size (kDa)**	**Origin**	**Brand**	**Catalog Number**
ß-actin (C4)	45	Mouse	Santa Cruz Biotechnolgy	sc-47778
GAPDH (FL-335)	37	Rabbit	Santa Cruz Biotechnolgy	sc-25778
Lamin B1	66	Mouse	ProteinTech	66095-1-Ig

Table 2.4 (cont'd)

Tubulin	55	Mouse	Santa Cruz Biotechnology	sc-5286
LC3 A/B (D3U4C)	14,16	Rabbit	Cell Signaling Technology	12741S
SNAP29	29	Mouse	R&D Systems	MAB7869
p62/SQSTM1	62	Mouse	Santa Cruz Biotechnology	sc-28359
RAB5	25	Rabbit	Cell Signaling Technology	3547
RAB7a	23	Rat	Biolegend	850401
LAMP1 (H4A3)	90, 120	Mouse	Santa Cruz Biotechnology	sc-20011
RPS6 (S235/236)	32	Rabbit	Cell Signaling Technology	2211S
RPS6 (S240/244)	36	Rabbit	St John's Laboratory	STJ113488
p70S6K (49DS7)	70, 85	Rabbit	Cell Signaling Technology	2708P
p70S6K (T289)	70, 85	Rabbit	Cell Signaling Technology	9234S
ULK1 (S757)	140, 150	Rabbit	Cell Signaling Technology	6888S
4E-BP1 (Ser65)	15, 20	Rabbit	Cell Signaling Technology	9451S
AMPKα1/2	62	Mouse	Santa Cruz Biotechnology	sc-74461
AMPKα (T172)	62	Rabbit	Cell Signaling Technology	2535S

Table 2.4 (cont'd)

TFEB	65,70	Mouse	Biolegend	852001
eIF2α (Ser51)	38	Rabbit	St John's Laboratory	STJ11102562
ATF4	49	Rabbit	St John's Laboratory	STJ92467
p90RSK (Thr573)	90	Rabbit	Cell Signaling Technology	9346
ERK 1/2 (Thr 202/Tyr 204)	42, 44	Rabbit	Santa Cruz Biotechnology	sc-16982
Goat α-Rabbit				R05071 500
Goat α-Mouse				R05072 500
Goat α-Rat				R05075 500

2.7 Chorioallantoic Membrane (CAM) Assay

Fertilized Leghorn eggs were purchased from Ankara Tavukçuluk Araştırma Enstitüsü and delivered at an ambient temperature of 12 ºC. The eggs were cleaned with distilled water before putting them into a dedicated incubator at 37 ºC with 60-70% humidity for 8 days. On day 8, a window of about 1 cm was opened into the more rounded pole of the egg. A drop of sterile PBS was placed on the eggshell membrane, and the membrane was pinched to allow the PBS to flow and the eggshell membrane was removed. A piece of silk tape was used to seal the window and eggs were left in the incubator overnight. Next, LoVo cells (1x106) were embedded in Matrigel at a 1:1 ratio (v/v) with culture medium in a total volume of 40 µl for each egg. The cell suspension embedded in Matrigel was incubated for 10 minutes at room temperature and 1h at 37 ºC and then placed on the CAM of the developing embryos. The eggs were moved to the incubator at 37ºC with 60-70% humidity and incubated

for another 5 days. Microtumors were harvested and measured in terms of height, width, and length for tumor volume calculation according to the following formula:

Tumor volume = pellet length*width*height* × 0.52 (Böhm et al., 2019).

A minimum of 8 fertilized eggs were used for each experiment.

2.7.1 Protein Isolation of CAM Microtumors

Each isolated microtumor was incubated in 200 µl of Recovery solution (Corning, USA). The microtumors could also be pooled, in that case, the amount of recovery solution was scaled up accordingly. The tube containing microtumors and the recovery solution was mixed gently and incubated on ice for 60-90 minutes until the Matrigel was completely dissolved. The mixture was then centrifuged at 300 x *g* for 5 min at 4 °C, the supernatant was discarded, and the remaining pellet was washed with cold PBS and centrifuged again at 500 x *g* for 5 min at 4 °C. The last two steps were repeated twice. The resulting pellet was used for total protein isolation as described above.

2.8 Immunofluorescence (IF)

LoVo cells were seeded on 12mm sterile coverslips placed in the wells of a 12-well plate and allowed to attach overnight. The appropriate treatment was performed on these cells on the following day. At the end of the treatment, the cells attached to the coverslips were fixed in 4% paraformaldehyde (PFA) in phosphate buffer for 2h and then washed with PBS twice. The fixed cells were then treated with 0.1% Triton for 10 minutes for permeabilization. The cells were incubated in 0.15% Glycine solution for 10 minutes to bleach the autofluorescence of PFA and blocked with 1% BSA for 10 minutes. The primary antibodies diluted in 1% BSA in PBS were added to the cells and incubated for 1h at room temperature. Next, the cells were washed with PBS three times and incubated with the secondary antibody in 1% BSA for 30

minutes and washed with PBS three times. Diluted Phalloidin-488 in 1% BSA was added to the cells and incubated for 60 minutes and washed with PBS three times and once with H2O. The coverslips were mounted on microscope slides using prolong gold (Thermo Fisher, USA) and dried overnight at room temperature. Table 2.4 provides a list of the antibodies used in the immunofluorescence experiment.

Table 2.5 Antibodies Used in Immunofluorescence Experiment

Antibody	Fluorescence	Origin	Reactivity	Dilution	Brand	Catalog Number
LAMP1	-	Mouse	Human	1:500	BD Pharmingen	555798
TFEB	-	Rabbit	Human	1:200	Cell Signaling Technology	4240
mTOR	-	Rabbit	Human	1:50	Cell Signaling Technology	2972
Phalloidin_488	488 (green channel)	-	-	-	Life Technologies	A12379
DαM_488	488 (green channel)	Donkey	Mouse	1:250	Life Technologies	A21202
DαR_568	568 (red channel)	Donkey	Rabbit	1:250	Life Technologies	A10042

2.9 Proliferation Assay – MTT

An MTT [3-(4, 5-dimethylthiazol-2-yl)-2,5-diphenyltetrazolium bromide] assay was used to measure cell viability according to the manufacturer's instructions (Thermo Fisher, USA). In a 96-well plate, 10,000 cells per well were seeded and allowed to attach for 24 hours after which treatments were started. 12 mM MTT solution was prepared by dissolving 5mg MTT in 1 mL of PBS and further diluted with the cell

culture medium to 1.2 mM MTT solution (100 µL for each well). At the end of the treatment, the drug or vehicle containing cell culture medium was aspirated and 100 µL of 1.2 mM MTT solution was added to wells. After 4 hours of incubation, 100 µL 1 % SDS- 0.01M HCl solution was added to the MTT-added wells and incubated for another 18 hours at 37 ºC. A Multiskan-GO spectrophotometer was used to measure the absorbance at 570 nm.

2.10 Colony Formation Assay

6-well plates were seeded with 1000 cells per well and the cells were allowed to attach overnight. After washing the cells with PBS once, the appropriate treatments dissolved in the culture mediums were added to the wells on the following day. The cells were incubated in a humidified incubator containing 5% CO2 at 37ºC, and their medium was changed every 48 h. When the colonies were large enough to be seen with the naked eye, the medium was removed, and the colonies were washed once with PBS. Then 4% paraformaldehyde (PFA) was used for the fixation of the cells for 15 minutes at room temperature. The PFA was aspirated and the cells were washed with PBS. Next, 1 ml of 0.5% crystal violet in methanol (Sigma Aldrich, USA) was added to the wells and incubated for 20 minutes at room temperature on a rocker. Following that, wells were washed with tap water gently to remove the excess crystal violet solution and left to air-dry. The colonies were imaged and counted manually using the white tray of the ChemiDoc Imaging system and Image Lab software (BioRad, USA).

2.11 Statistical Analysis

Every experiment contained at least two biological replicates each having at least two technical replicates. For data analysis, GraphPad Prism 6.1 (GraphPad Software Inc., USA) was used. To evaluate significance, one-way ANOVA or Student's t-test was used. Statistical significance was defined as a p-value of less than 0.05.

CHAPTER 3

RESULTS

3.1 Activation of Nutrient Sensing Pathways in Nutrient Restricted CRC Cells

Tumor development is dependent on metabolic activities that need energy, such as the biosynthesis of proteins, nucleotides, and lipids. Many tumor-associated conditions like hypoxic microenvironment and low nutrient availability occur as a result of poor vascularization and fast growth. Under such challenging circumstances, cancer cells must adapt their metabolism in order to maintain cellular homeostasis and survive (Robles-Flores et al., 2021). Both hypoxia and nutrient restriction can activate a number of common stress response pathways in cells (Wortel et al., 2017). However, the activation of nutrient-sensing pathways such as mTOR and AMPK has been unequivocally shown when cells are grown under varying nutrient availability (Condon & Sabatini, 2019).

Therefore, we incubated 5 colorectal cancer cell lines in a nutrient-restricted medium (glucose and glutamine-free RPMI medium supplemented with 1% FBS, 0.1g/L glucose, and 0.2mM L-glutamine) which was optimized in the capacity of a TÜBİTAK 1001 project (118Z116) by graduate students Aliye Ezgi Güleç and Hepşen Hazal Hüsnügil in our lab. The withdrawal of three major sources of energy abrogated the possibility of compensatory nutrient acquisition from other sources. We observed that all 5 CRC showed the activation of the nutrient sensor AMP Kinase (AMPK at T172) suggesting an increase in the AMP/ATP ratio and inhibition of p70S6 Kinase (p70S6K at T389), as expected. Interestingly, despite p70S6K inhibition, phosphorylation of RPS6 at S235/236, a residue known to be phosphorylated by both p70S6K and RSK, and S240/244, a site that can only be

phosphorylated by p70S6K(Yi et al., 2022), was found to be increased only in LoVo cells (Figure 3.1).

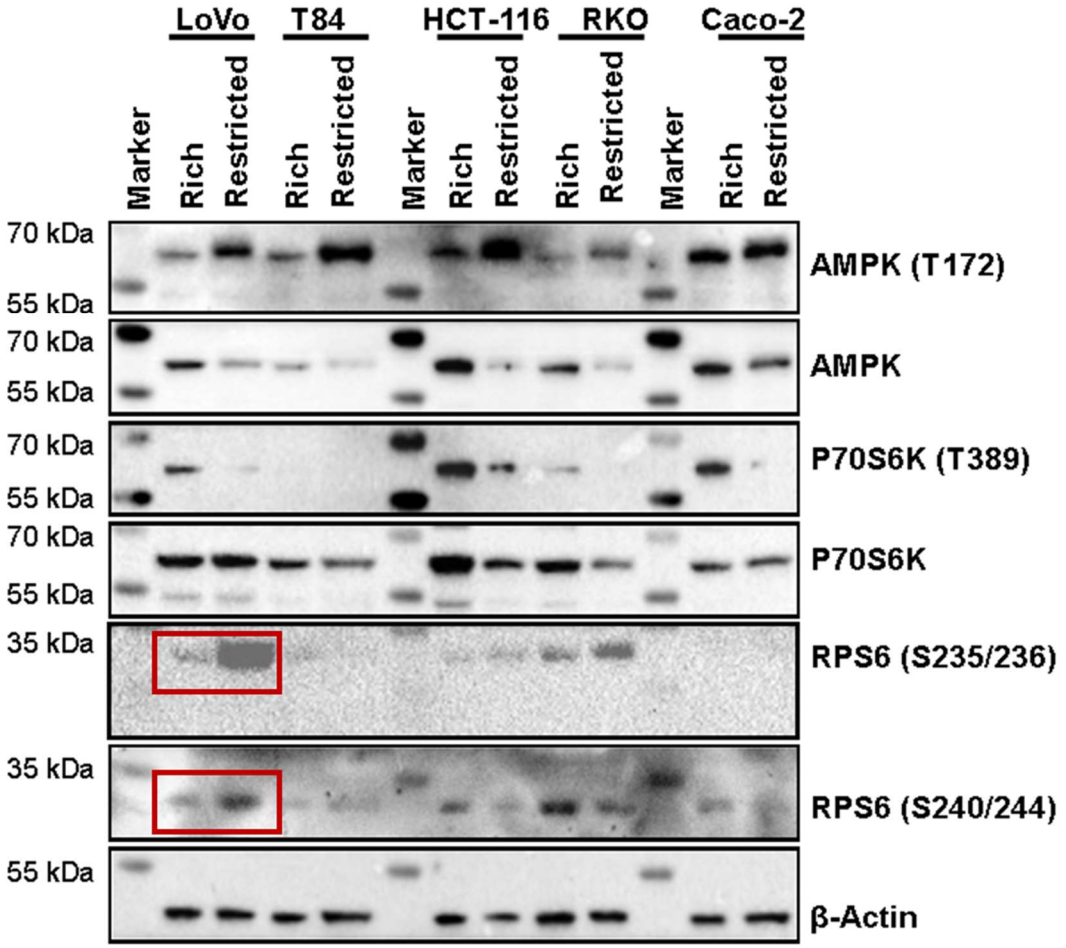

Figure 3.1 Co-activation of AMPK and RPS6 in Nutrient-restricted LoVo Cells

5 colorectal cancer cell lines were incubated with either complete (RPMI medium supplemented with 10% FBS, 2mM L-Glutamine, 1g/L glucose) or nutrient-restricted medium (glucose and glutamine free RPMI medium supplemented with 1% FBS, 0.1g/L glucose and 0.2mM L-glutamine) for 48h. cells were collected for protein isolation. 30 µg proteins were loaded on 12% SDS-PAGE gel. β-Actin was used as a loading control. Representative blot from 3 independent biological replicates is shown.

To determine the shortest duration of nutrient restriction (NR) for the co-activation of AMPK and RPS6, a time course study was performed with LoVo cells incubated with NR medium for 2, 6, 24, and 48h and collected at each time point.

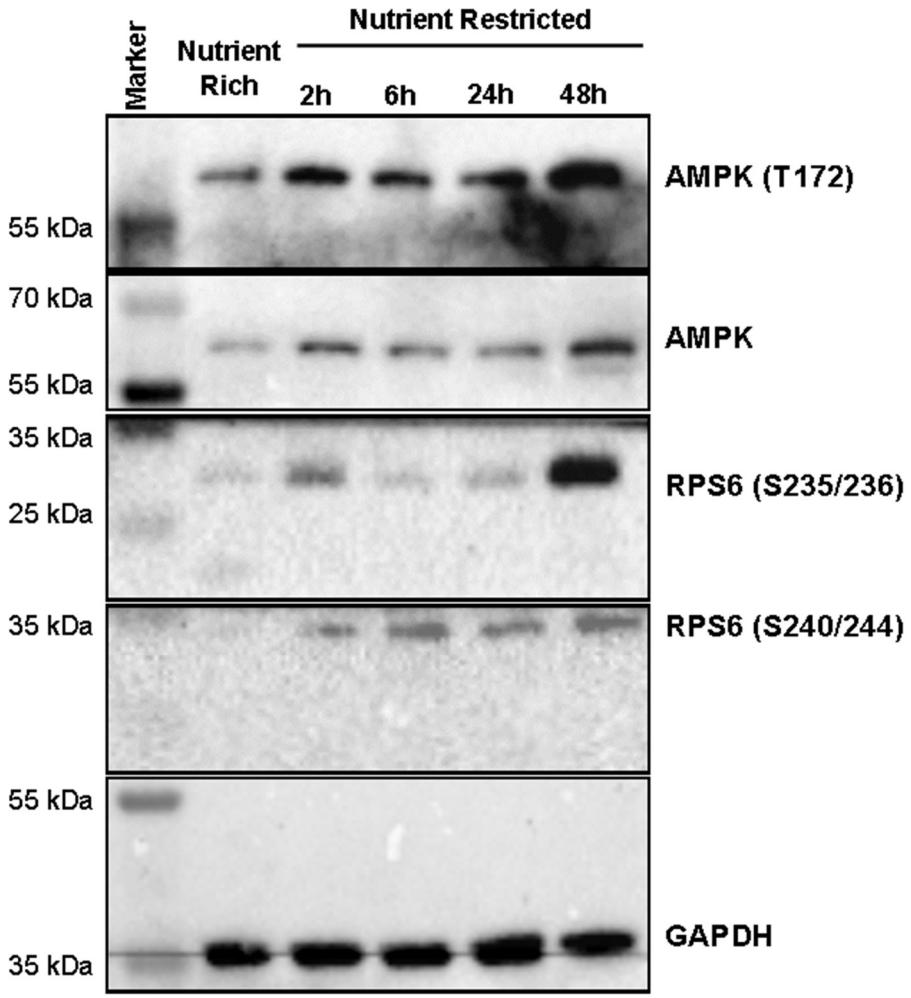

Figure 3.2 Time Course Study to Determine The Shortest Duration of Incubation with NR Medium for the Co-Activation of RPS6 and AMPK

LoVo cells were cultured with NR media for 2, 6, 24, and 48 hours, and nutrient-rich medium for 48 hours as a control and collected for protein isolation. 30 µg proteins were loaded on 12% SDS-PAGE gel. GAPDH was used as a loading control. Representative blot from 4 independent biological replicates is shown.

The time course study showed that, although the phosphorylation of AMPK increased in a time-dependent manner starting within 2h of nutrient restriction, RPS6 was activated after 48h of starvation (Figure 3.2). Thus, 48h of nutrient restriction was determined as the shortest duration of incubation for the co-activation of AMPK and RPS6 and further experiments were performed accordingly.

3.2 Evaluation of Interdependence of AMPK Pathway and RPS6 Activation in LoVo Cells Grown Under Nutrient Restriction

The major signaling pathway that phosphorylates RPS6 in mammalian cells is the PI3K/AKT/mTORC1/ p70S6K pathway. RPS6 was first reported as a p70S6K substrate and phosphorylation of RPS6 is often attributed to the activation of the mTORC1 pathway (Yi et al., 2022).

Therefore, we used two different mTOR inhibitors to determine whether the phosphorylation of RPS6 was a readout of mTOR activity and whether inhibiting the mTOR pathway caused a change in AMPK phosphorylation levels (Figure 3.3). Everolimus is a selective mTORC1 inhibitor that forms a complex with intracellular receptor FK506-binding protein (FKBP-12) that inhibits the mTORC1 activation (Y. Zhang et al., 2018). Recent research, however, showed that selective mTORC1 inhibition causes feedback activation of AKT at S473 via mTORC2, limiting the anticancer efficacy of this method (Lu et al., 2020) Therefore, we also used AZD8055, an mTOR ATP-competitive inhibitor that can inhibit both mTORC1 and mTORC2 (Y. Zhang et al., 2018).

Nutrient-rich and restricted LoVo cells were co-treated with either 1 µM Everolimus or 5 µM AZD8055 for 48h. Phosphorylation of 4EBP1 (S65), ULK1 (S757) and p70S6K (T389) were evaluated as downstream effectors of mTORC1. Phosphorylation of 4EBP1 (S65) by mTORC1 leads to its inhibition and abrogates its role as a negative regulator of translation. This leads to the dissociation of 4E-

BP1 from eIF-4E and cap-dependent translation of many proteins involved in cell growth, proliferation and cell cycle regulation can be initiated (Qin et al., 2016).

ULK1 was identified as a direct target of both mTORC1 and AMPK. Under nutrient-restricted conditions activated AMPK phosphorylates ULK1 at S317 and S777 and promotes autophagy. On the other hand, high mTOR activity hinders ULK1 activation by phosphorylating ULK1 at S757 which destroys the interaction between AMPK and ULK1 (Kim et al., 2011). Phosphorylation of S6K1 via mTORC1 can activate the 40S ribosomal protein (RP) S6 via phosphorylation at S240/244 as well as S235/236 (Roux et al., 2007).

EVE: mTORC1 inhibitor
AZD: mTOR inhibitor
Comp C: AMPK inhibitor

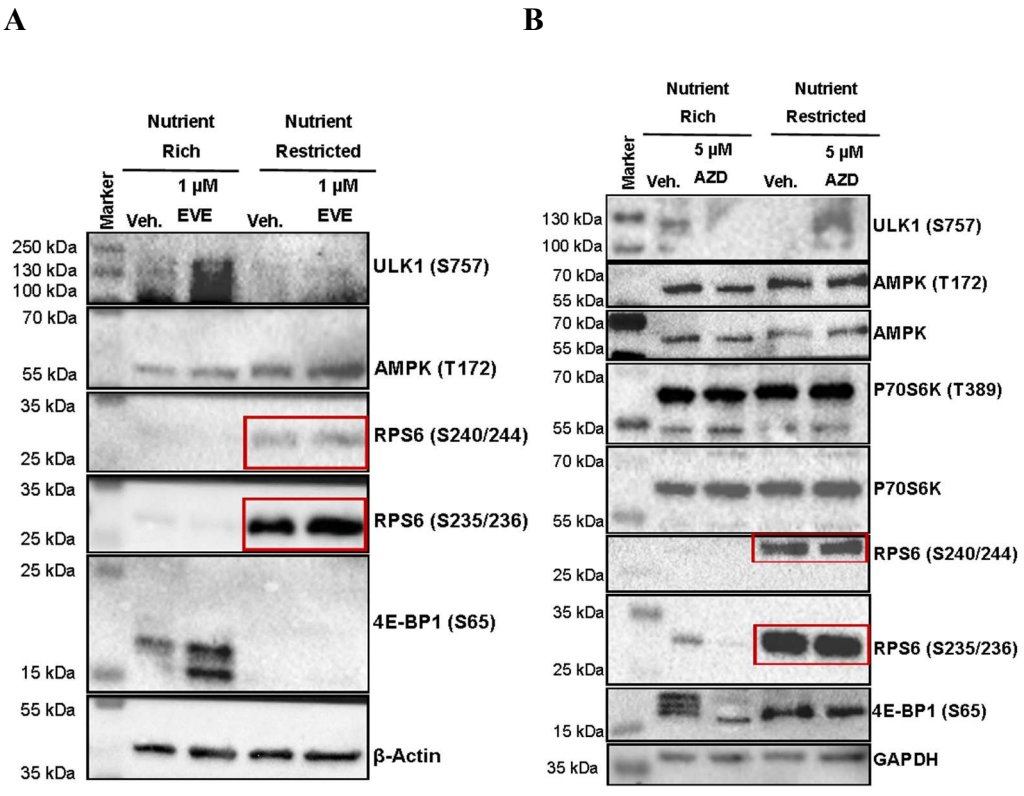

Figure 3.3 Effect of mTORC1 and AMPK Inhibitors on RPS6 Activation

C

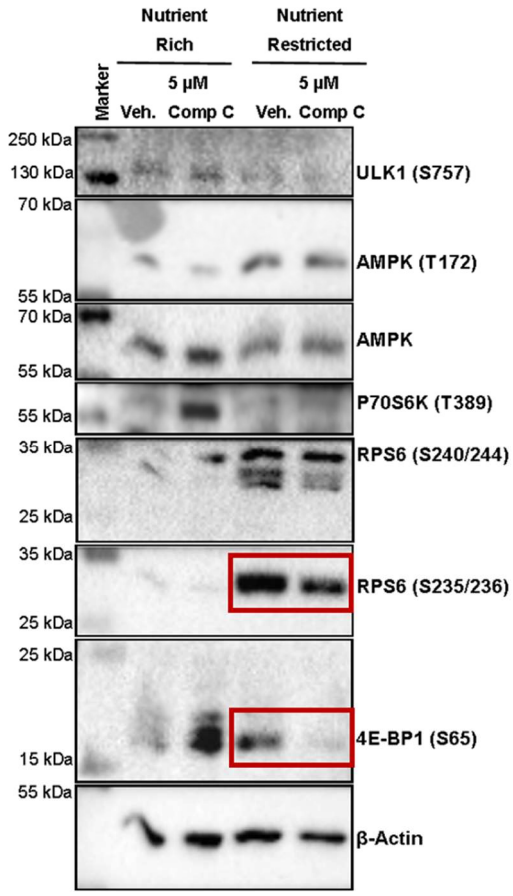

Figure 3.3 (cont'd) *Nutrient-rich and restricted LoVo cells were co-treated with (A) 1 µM Everolimus (B) 5 µM AZD8055 (C) 5 µM Compound C for 48h and collected for protein isolation. 30 µg proteins were loaded on 12% SDS-PAGE gel. Representative blot from 2 independent biological replicates is shown.*

In control cells, AZD8055 but not Everolimus decreased the phosphorylation levels of mTOR targets ULK1 and 4EBP1, indicating that AZD8055 effectively inhibited mTOR. However, phosphorylation levels of mTOR targets and RPS6 (S235/236 and S240/244) did not decrease in nutrient-restricted LoVo cells treated with AZD8055 or Everolimus. We also did not observe a change in AMPK phosphorylation after treatment with either of the mTOR inhibitors (Figure 3.3 A, B).

The AMPK pathway is activated in the presence of a high AMP/ATP ratio and enhances macromolecule catabolism for ATP production (Palm & Thompson, 2017). We used Compound C as a pharmacological AMPK inhibitor that efficiently blocks the metabolic actions of AMPK to determine whether RPS6 phosphorylation was dependent on AMPK activation. Nutrient-rich and restricted LoVo cells were treated with 5 μM Compound C for 24h. Interestingly, Compound C treatment was able to decrease phosphorylation levels of 4E-BP-1 together with RPS6 S235/236, particularly in nutrient-restricted cells. These data suggest that the activation of RPS6 in starved cells might be dependent on the activation of the AMPK pathway.

3.3 Role of Autophagy in Co-activation of RPS6 and AMPK in Nutrient-restricted LoVo Cells

mTORC1 is known to respond to amino acids taken into the cytosol and those generated by protein degradation in the lysosome. Therefore, when cytosolic amino acids are scarce (such as during starvation), mTORC1 signaling is inhibited and autophagy is initiated to restore lysosomal amino acid pools through protein degradation. Release of these amino acids into the cytosol can reactivate mTORC1. Therefore, long-term starvation can lead to the reactivation of mTORC1 in an autophagy-dependent manner (Condon & Sabatini, 2019).

Therefore, we assessed the induction of autophagy in nutrient-restricted LoVo cells (Figure 3.4 A). LoVo cells were cultured for 48 h in either a nutrient-rich or nutrient-restricted medium. Autophagy induction in response to nutrient restriction was shown by the increase in LC3-II levels. The expression of the cargo protein p62 is expected to decrease in cells undergoing autophagic flux. However, we observed an increase in p62 levels with starvation, suggesting either autophagic flux inhibition or an increase in endo-lysosomal trafficking. Supporting the latter, we observed an increase in the protein levels of the early endosomal marker RAB5 and the late endosomal marker RAB7, while the protein levels of the lysosomal marker LAMP1 did not change.

Next, we evaluated the time course for the initiation of autophagy and endolysosomal signaling (Figure 3.4 B). LoVo cells were incubated with NR medium for 2, 6, 24, and 48h and collected at each time point. Cells cultured in the nutrient-rich medium was collected as the control. Autophagy markers p62, Beclin-1, LC3, and endo-lysosomal trafficking markers LAMP1, RAB5, and RAB7a showed an increase in a time-dependent manner in nutrient restriction starting from the 2h timepoint.

To evaluate whether the activation of autophagy with nutrient restriction was also manifested *in vivo,* we inoculated the 48h nutrient-restricted and control LoVo cells to the chorioallantoic membrane (CAM) of fertilized chicken eggs. The tumors were allowed to form over a period of 5 days, excised from the CAM tissue, and processed for protein isolation. Western blot analysis of these proteins showed that nutrient-restricted microtumors generated in CAM tissue showed an increased level of LAMP1 and a decrease in p62, supporting high lysosomal activity and active autophagy. However, we were unable to observe any dramatic difference in the levels of RAB5, RAB7, or LC3-II in the nutrient-restricted microtumors compared to controls (Figure 3.4 C). Of note, the expression of all of these markers was higher in the microtumors generated from both nutrient-restricted and control cells (labeled as post-inoculation) compared to the LoVo cells grown in 2D culture plates (labeled as pre-inoculation).

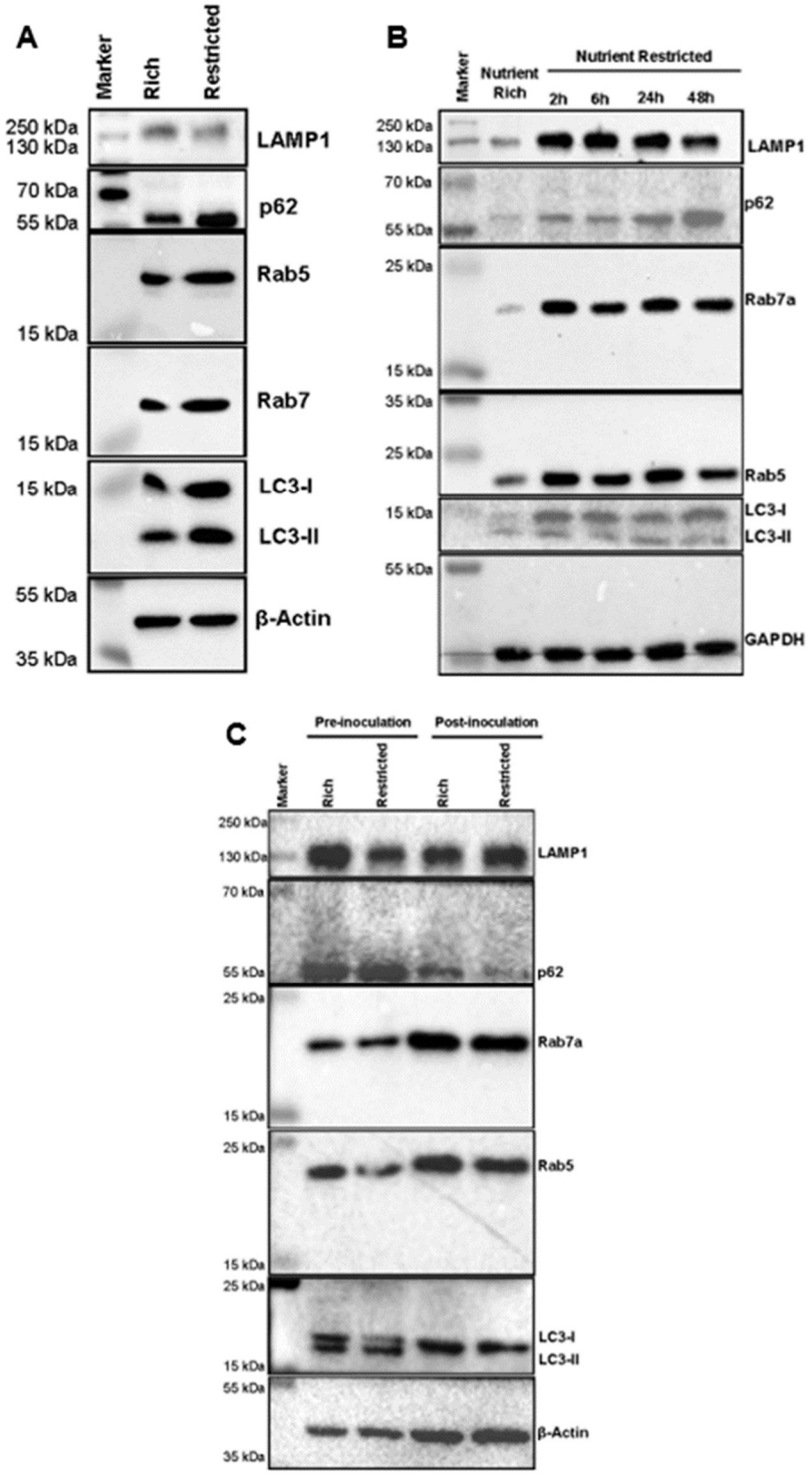

Figure 3.4 Determination of Autophagy Induction and Endolysosomal Marker Levels of LoVo Cells Upon Nutrient Restriction

Figure 3.4 (cont'd) *(A)LoVo cells were cultured either in a nutrient-restriction medium or a nutrient-rich medium. (B)LoVo cells were cultured with NR medium for 2, 6, 24, and 48 hours, and nutrient-rich medium for 48 hours as a control and collected for protein isolation. (C) LoVo cells were cultured with either a nutrient-restriction medium or nutrient-rich medium for 48h and a CAM assay was performed. Microtumors were harvested for protein isolation. 30 µg proteins were loaded on 12% SDS-PAGE gel. A representative blot from 4 independent biological replicates for (A) and (B) and 10 biological replicates for (C) is shown.*

3.4 Determination of Autophagic Flux in LoVo Cells – Use of Bafilomycin A1

It is now accepted autophagic degradation activity (flux) cannot be evaluated simply by examining the protein levels of the autophagy markers. Increasing autophagosome numbers might indicate both rapid generation and reduced clearance (Juhász, 2012). Nutrient-rich and restricted LoVo cells were treated with 100 nM Bafilomycin A1 (BafA1) for 48h which inhibits the vacuolar-type v-ATPase complex necessary for lysosomal acidification (Wang et al., 2021). BafA1 treatment, therefore, inhibits autophagic degradation in the lysosome downstream of autophagosome formation. Therefore, the accumulation of autophagic markers after treatment of BafA1 is considered as an indication of autophagic flux. We observed that treatment with BafA1 resulted in the accumulation of all autophagy (p62, Beclin-1, LC3) and endo-lysosomal trafficking markers (LAMP1, RAB5, RAB7a); removal of the BafA1 medium and replenishment with complete medium reduced the levels of all markers in nutrient-rich cells. In nutrient-restricted cells, the replacement of Baf A1 also led to a reduction in levels of the markers. However, this reduction was modest in comparison to the reduction in nutrient-rich cells. This suggests that autophagic flux was slowed down rather than inhibited in nutrient-restricted LoVo cells (Figure 3.5).

Baf: Autophagy inhibitor

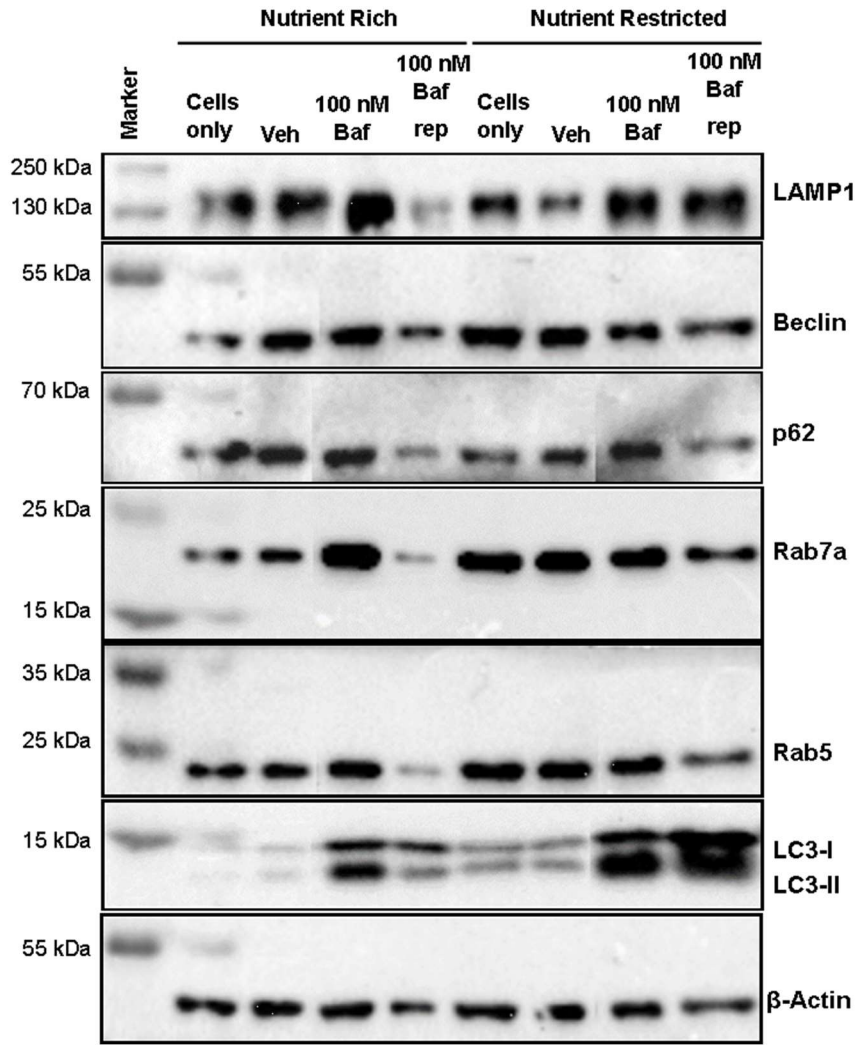

Figure 3.5 Determination of Autophagic Flux in Nutrient-rich and Nutrient-restricted LoVo Cells

LoVo cells were incubated in either nutrient-rich or restricted medium containing vehicle (DMSO) or 100 nM Bafilomycin A1 for 48 h. For Bafilomycin A1 replacement, cells were incubated in Bafilomycin A1 containing nutrient-rich or restricted medium and then incubated in nutrient-rich and restricted medium respectively for 24 h. Representative blot from 3 independent biological replicates is shown.

3.5 Analysis of Possible Reasons for Flux Impairment in LoVo Cells

There might be numerous mechanisms for the impairment of autophagic flux. We examined whether the deregulation was at the level of autophagosome-lysosome fusion, lysosome biogenesis, or lysosomal alkalinization.

3.5.1 Autophagosomes-lysosomes Fusion

Three protein families including Rab GTPases, SNAREs, and tethering factors, are necessary for autophagosome-lysosome fusion. Rab proteins bind to endosomal membranes and recruit tethering complexes to regulate membrane traffic. Among them, RAB7 has been reported to be involved in incomplete autophagy (Lőrincz & Juhász, 2020). Among the SNAREs, SNAP29 is the key adaptor protein that governs autophagosome-lysosome fusion by interacting with STX17 which targets autophagosomes, and VAMP8, which is found on the lysosomal membrane(Tang et al., 2021) Here, we investigated the abundance of RAB7a and SNAP29 in a time-dependent manner. A robust increase in RAB7a protein levels was observed even after 2h of starvation. SNAP29 protein levels were also observed to increase after 6h of starvation and reached their highest level at 48h (Figure 3.6). Given the elevated levels of RAB7a and SNAP29, we concluded that inhibition of autophagosome-lysosome fusion may not be the reason for impaired autophagy.

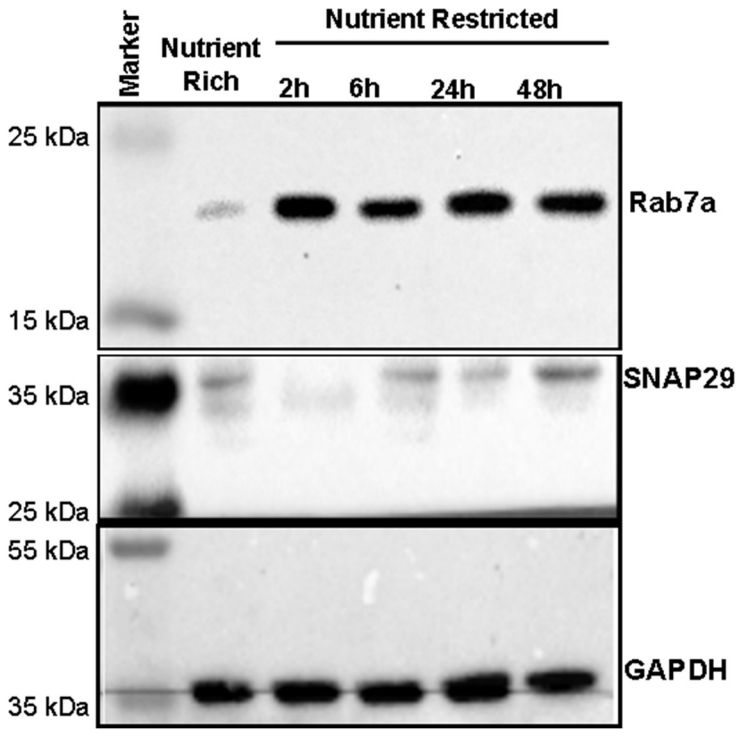

Figure 3.6 Autophagosomes-lysosomes Fusion

LoVo cells were cultured with NR media for 2, 6, 24, and 48 hours, and nutrient-rich medium for 48 hours as a control. Both RAB7a and SNAP29 protein levels increased with starvation. Representative blot from 4 independent biological replicates is shown.

3.5.2 Lysosome Biogenesis

Lysosomal biogenesis and autophagy are controlled by transcription factor EB (TFEB). The activation of TFEB, which is primarily regulated by nuclear translocation, is necessary for the enhanced expression of genes involved in lysosome biogenesis and function. It is known that compounds that inhibit the nuclear translocation of TFEB result in incomplete autophagy due to lysosomal dysfunction. This suggests that suppression of lysosome biogenesis by the cytosolic retention of TFEB can induce incomplete autophagy (Puertollano et al., 2018). Moreover, TFEB is known to upregulate the transcription of lysosomal proteins

under nutrient-restricted conditions. Therefore, we determined the cytoplasmic and nuclear protein levels of TFEB. Interestingly, nuclear to cytoplasmic levels of TFEB decreased with nutrient restriction and remained unchanged upon nutrient replenishment for 24h (Figure 3.7 A). We also determined the mRNA levels of TFEB target genes including *MCOLN1, RAB7a, RAB5, and SQSTM1* (Palmieri et al., 2011) While *MCOLN1, RAB7a,* and *RAB5* mRNA levels didn't change significantly, mRNA levels of *SQSTM1* increased 4-fold with nutrient restriction. Moreover, mRNA levels of all target genes except *MCOLN1* decreased significantly with nutrient replenishment (Figure 3.7 B).

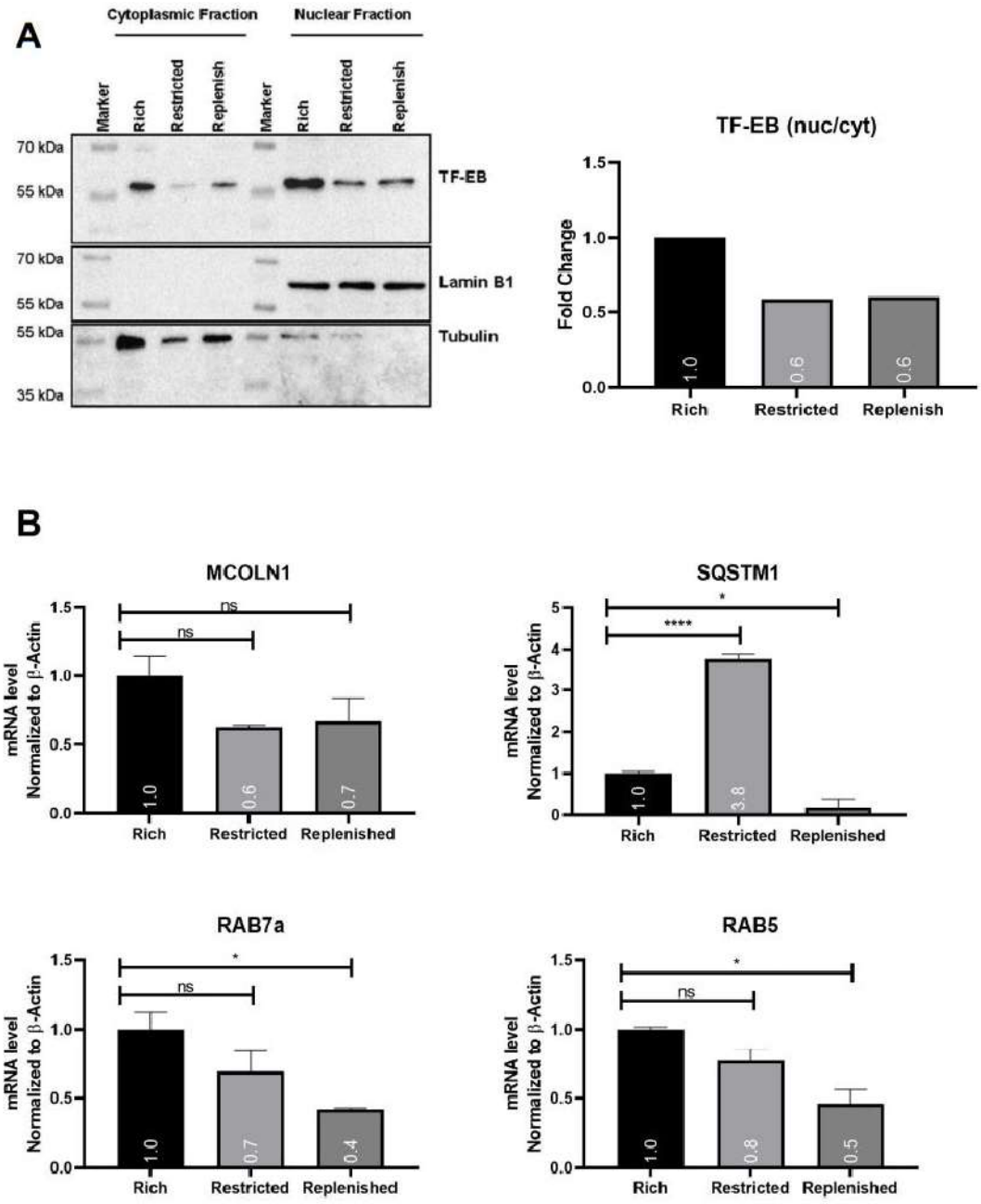

Figure 3.7 Analysis of Lysosome Biogenesis

LoVo cells were cultured with either nutrient restriction medium or nutrient-rich medium for 48h for the replenishment group, cells were cultured in nutrient restricted medium for 48h and then cultured in the nutrient-rich medium for 24h. (A) Nuclear to cytoplasmic levels of TFEB decreased with nutrient restriction and replenishment group. Lamin B1 and tubulin were used for nuclear and cytoplasmic

Figure 3.7 (cont'd) *normalization respectively. (B) Nutrient-rich, Nutrient restricted, and replenished cells were collected for RNA isolation and RT-qPCR. Representative data from 2 independent biological replicates are shown. Statistical analyses were carried out using ANOVA followed by Tukey's multiple comparison test (****p< 0.0001, *p<0.05, ns: not significant).*

It is known that mTORC1 regulates nuclear localization and activity of the TFEB. Under nutrient-rich conditions, TFEB is phosphorylated by mTORC1 in Ser211 and Ser142 which keeps the TFEB in the cytosol and inactive (Martina et al., 2012). Additional kinases such as ERK can also regulate TFEB activity by phosphorylating the mTOR-dependent site (Ser142) and modulating TFEB localization (Napolitano et al., 2018). Thus, to further confirm the subcellular localization of TFEB, we performed an immunofluorescence experiment with nutrient-rich and restricted LoVo cells. As a positive control, we have included cells that are starved acutely by culturing in EBSS for 2h (Figure 3.8). Supporting the Westen Blot data (Figure 3.7 A) both nutrient-rich and restricted cells showed staining of TFEB in the cytoplasm. In contrast, acute starvation induced a significant accumulation of TFEB in the nucleus. This may imply that during starvation in LoVo cells, activation of signaling pathways via mTORC1 or MAPK can phosphorylate and keep TFEB in the cytosol. This is also supportive of the activation of RPS6 observed with nutrient restriction in these cells.

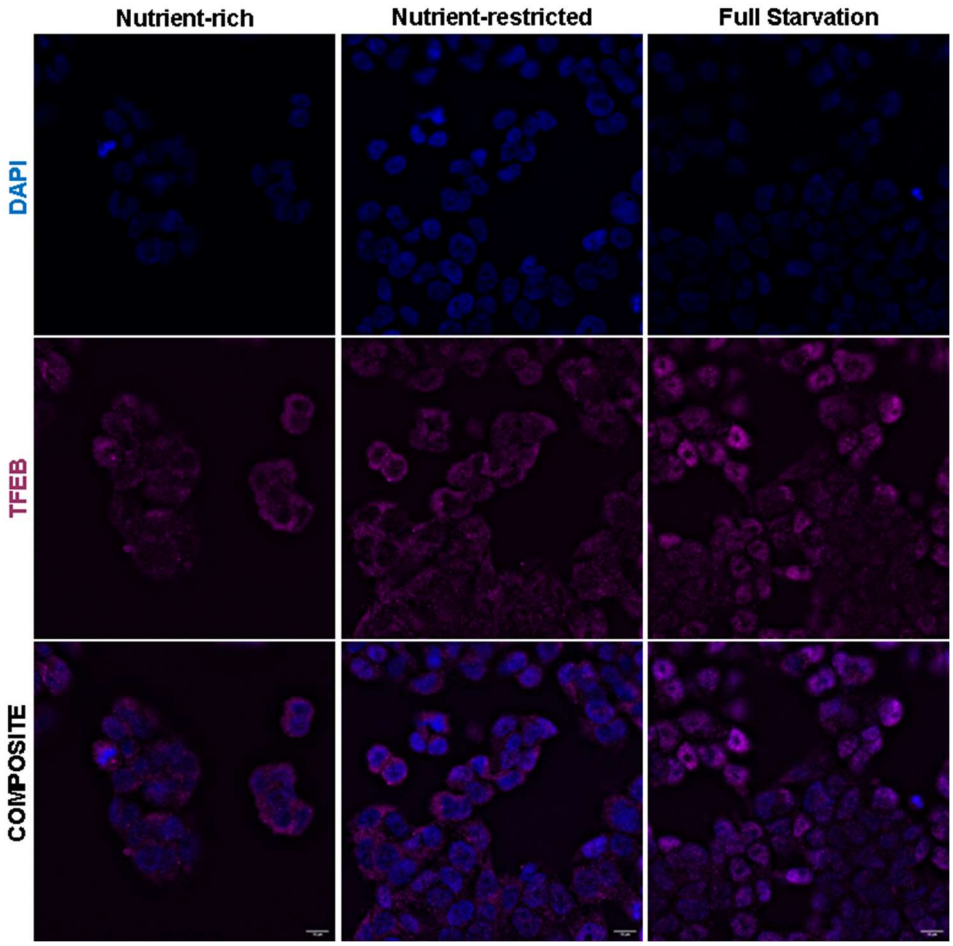

Figure 3.8 Subcellular Localization of TFEB

Immunofluorescence microscopy showing nuclear localization of TFEB in LoVo cells incubated with either nutrient restriction or nutrient restricted medium for 48h and as a positive control, cells were treated with EBSS for 2h. TFEB is shown in magenta and cell nuclei (DAPI) is shown in blue. Scale bar: 10µm. The microscopic fields imaged were chosen randomly. The experiments were replicated three times. These data were generated by Aliye Ezgi Güleç.

3.5.3 Alkalinization of Lysosomal pH

Although it is known that lysosomal acidification is not required for autophagosome-lysosome fusion (Mauvezin et al., 2015) degradative enzymes in the lysosomes have acidic pH optima; hence, the degradative capacity of the enzymes is decreased in alkalinized lysosomes (Johnson et al., 2016). It is well known that alkalinizing the lysosomal pH can induce incomplete autophagy (Q. Zhang et al., 2022). We determined the changes in lysosomal acidity upon nutrient restriction via LysoTrcaker staining in LoVo cells. 100 nM Bafilomycin A1 treated cells for 24 and 48h were used as positive controls (Figure 3.9). Although Lysotracker output was significantly lower in nutrient-restricted cells with respect to nutrient-rich cells, it was also significantly higher in nutrient-restricted cells with respect to Bafilomycin A1 treated nutrient-restricted cells.

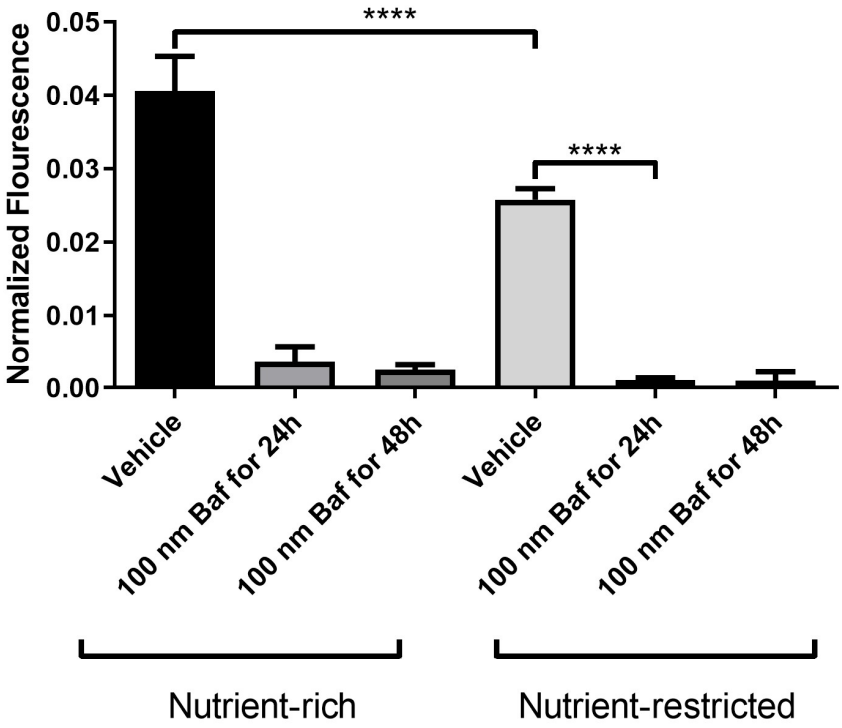

Figure 3.9 Determination of Changes in the Lysosomal Acidity via LysoTrcaker Staining

*LysoTracker and Hoechst staining (for normalization) were performed to determine the lysosomal acidification of nutrient-restricted and rich cells. 24 and 48h 100nm Bafilomycin A1 treated cells were used as positive controls. Baf: Bafilomycin A1, DMSO is the vehicle. Representative data is an average of 2 independent biological replicates. Statistical analyses were carried out using ANOVA followed by Tukey's multiple comparison test (****$p<0.0001$).*

3.5.4 Position of Lysosomes within the Cell

It is widely accepted that the luminal pH of individual lysosomes varies with their position within the cell with juxtanuclear lysosomes being more acidic than

peripheral lysosomes (Johnson et al., 2016). During starvation lysosomes preferentially cluster in the perinuclear area to facilitate lysosome-autophagosome fusion (Poüs & Codogno, 2011). We evaluated the location of lysosomes in nutrient-rich and restricted LoVo cells by staining the cells for the lysosomal marker Lamp1 (Figure 3.10). Upon nutrient restriction, peripheral lysosomes that were positioned distal to the nucleus were lost while the perinuclear lysosomes were increased. Since nutrient starvation is expected to increase lysosomal activity, the perinuclear location of the lysosomes also confirms the presence of acidic and active lysosomes in LoVo cells.

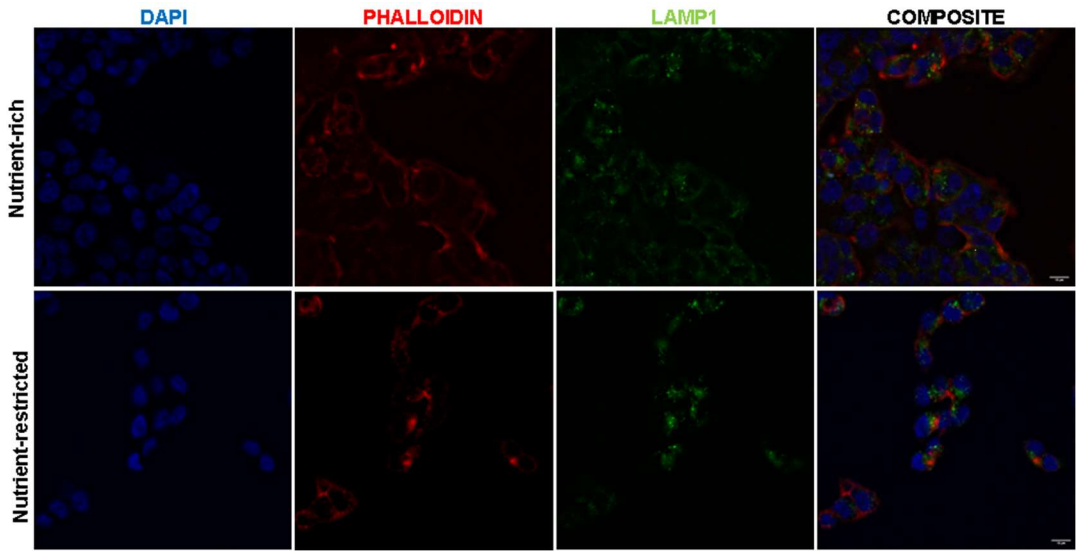

Figure 3.10 Lysosomal Distribution in Nutrient-rich and Nutrient-restricted LoVo Cells

Immunofluorescence microscopy showing subcellular localization of lysosomes in LoVo cells incubated with either nutrient-rich or nutrient-restricted medium for 24h. Cell boundaries are depicted in red (phalloidin), cell nuclei (DAPI) is shown in blue, and lysosomes were visualized with an anti-LAMP-1 antibody. The scale bar corresponds to 10μm. The microscopic fields imaged were chosen randomly. The experiments were replicated three times. This data was generated by Aliye Ezgi Güleç.

The lysosome surface serves as a platform for the activation of mTORC1 where Rag-GTPases recruit mTOR only when nutrient levels are sufficient (Mutvei et al., 2020). Since our data showed with nutrient restriction the activation of RPS6 at Serine residues that are phosphorylated upon mTORC1 signaling, we investigated whether mTORC1 was localized on the lysosomes and therefore also active when the cells were starved (Figure 3.11). We observed that mTORC1 was localized to LAMP1-positive lysosomal membranes in both nutrient-rich and restricted LoVo cells. These data suggest that despite long-term nutrient restriction, mTORC1 was located on the lysosomes and may remain active in LoVo cells.

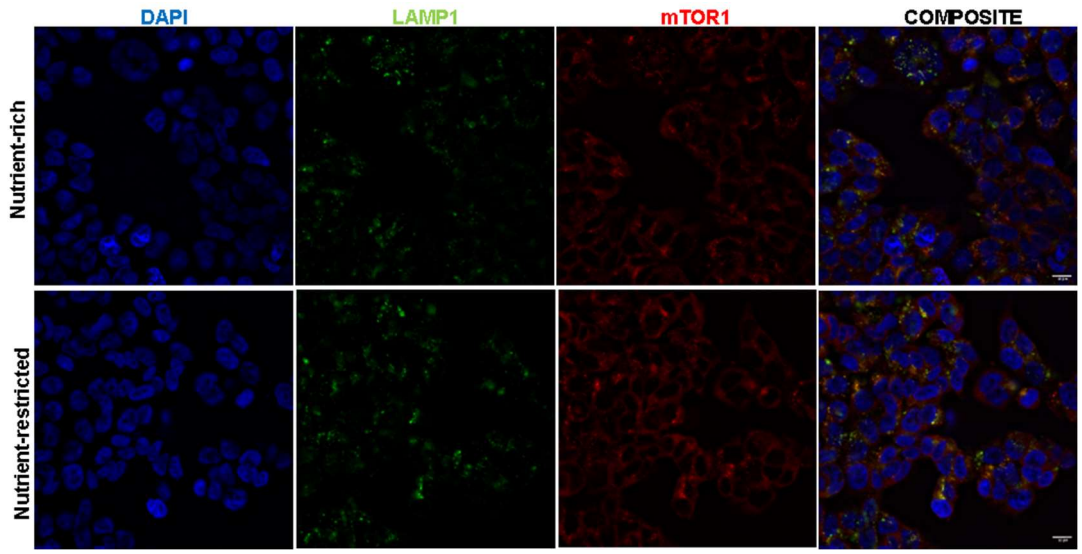

Figure 3.11 mTORC1 Lysosomal Localization

Immunofluorescence microscopy showing mTORC1 (Red), LAMP1 (green), and cell nuclei (DAPI in blue) in LoVo cells incubated with either nutrient-rich or nutrient-restricted medium for 24h. The scale bar corresponds to 10µm. The microscopic fields imaged were chosen randomly. The experiments were replicated three times. These data were generated by Aliye Ezgi Güleç.

3.6 Effect of Autophagy Inhibition on Activation of RPS6 in Nutrient-restricted LoVo Cells

To understand whether nutrient-restricted LoVo cells showed the activation of autophagy and whether this activation could be implicated in the phosphorylation of RPS6, we treated starved and control cells with 2 different autophagy inhibitors. 3MA (5 mM concentration) was employed as an early-stage autophagy inhibitor via the inhibition of type III Phosphatidylinositol 3-kinases (PI-3K), this event in turn inhibits autophagosome formation. Bafilomycin A1 (100 nM) was employed as a later-stage autophagy inhibitor via inhibition of lysosomal V-ATPases and alkalinization of lysosomes (Xie et al., 2014) (Liu et al., 2020).

LC3 lipidation was first monitored as a general means to assess autophagy. As expected, LC3 expression was decreased with 3MA due to an inhibition in the formation of the autophagosome. LC3 levels were increased with Bafilomycin A1 treatment in nutrient-restricted LoVo cells as expected because of an inability of the alkaline lysosomes to degrade the autophagosomes. Additionally, p62 protein levels were increased with both 3MA and Bafilomycin A1 confirming that inhibition of autophagy also led to a decrease in autophagic flux (Su et al., 2015).

Next, we determined the S235/236 and S240/244 phosphorylations of RPS6. The S240/244 phosphorylation is solely mediated by p70S6K while the phosphorylation at S235/236 can be mediated by many other kinases in addition to p70S6K. The S240/244 phosphorylation of RPS6 is therefore considered to be a direct read out of mTORC1 activity. 3MA treatment was able to decrease phosphorylation of RPS6 at both S235/236 and S240/244, suggesting the possibility of autophagy induction plays role in RPS6 activation in nutrient-restricted LoVo cells, perhaps via the concurrent activation of mTORC1 and/or other kinases. No change in the phosphorylation of RPS6 (either S235/236 or S240/244) was observed in the cells treated with BafA1 in both nutrient-restricted and control cells, suggesting a greater contribution of the regulation of RPS6 activation at the initial rather than later stages of autophagy.

3MA: Early-stage autophagy inhibitor
Baf: Late-stage autophagy inhibitor

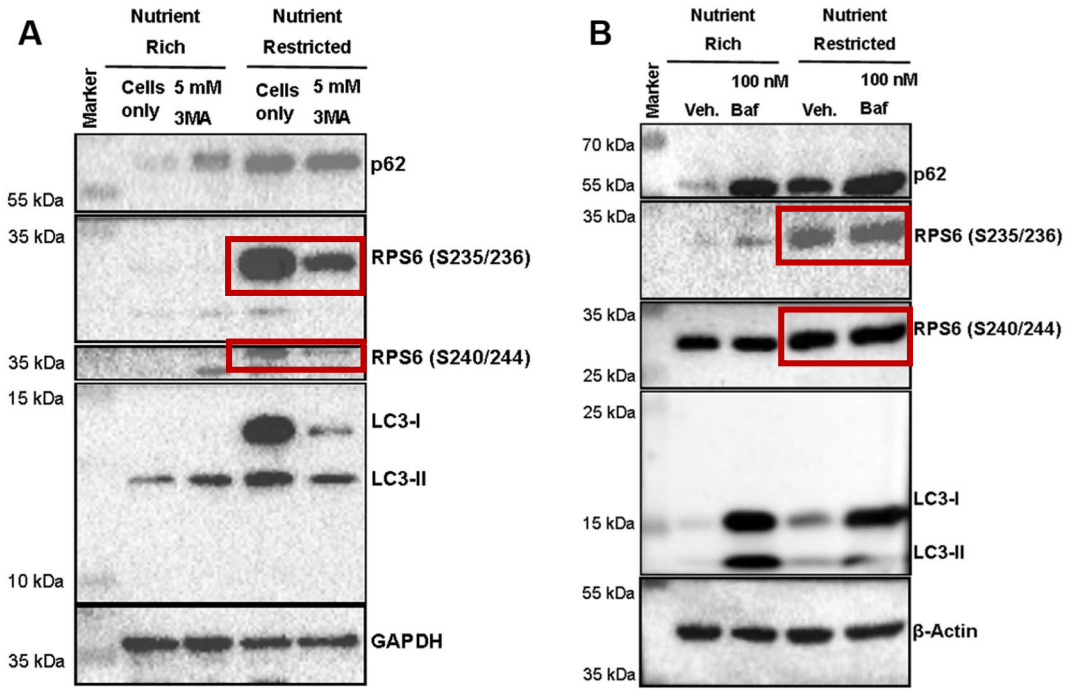

Figure 3.12 Effect of Autophagy Inhibitors on RPS6 Activation

LoVo cells were incubated in the nutrient-rich or nutrient-restricted medium and co-treated with (A) 5 mM 3MA (B) Vehicle (DMSO) or 100 nM Bafilomycin A1 and collected for protein isolation. 30 µg proteins were loaded on 12% SDS-PAGE gel. Representative blot from 2 independent biological replicates (A) and 3 independent biological replicates (B) is shown.

3.7 Induction of Integrated Stress Response (ISR) in Nutrient-restricted LoVo Cells

It is known that the integrated stress response (ISR) pathway can be activated under nutrient, oxidative or hypoxic stress (Sela et al., 2022). A core member of ISR is

eIF2α which is phosphorylated at Serine 51, which results in the inhibition of 5'cap-dependent translation. This causes a global decrease in protein synthesis thereby decreasing the consumption of macromolecules such as amino acids at times of shortage. However, mRNAs like the transcription factor ATF4 that participate in the cell's response to stress are unaffected or even increased in the presence of eIF2 phosphorylation(Chu et al., 2021). To identify whether the ISR pathway was activated in nutrient-restricted LoVo cells, we evaluated the phosphorylation of eIF2α as well as the expression of ATF4. Although phosphorylation levels of eIF2α remained the same upon nutrient restriction, we observed an increase in ATF4 levels. This suggests that ATF4 levels may have increased independent of eIF2α activation. To further evaluate the activation of ISR, we incubated the cells in the nutrient-rich or restricted medium for 48h and co-treated with 100 nM ISR inhibitor (ISRIB) for the last 2h of 48h. We found that ISRIB treatment did not alter the phosphorylation levels of eIF2α in both nutrient-rich and restricted cells which was expected since ISRIB acts downstream of the phosphorylation of eIF2α (Pavitt, 2013). However, the treatment had no effect on ATF4 levels either, suggesting that there might be an alternative mechanism to canonical ISR pathway activation by eIF2α phosphorylation that can regulate ATF4 and its target genes. A very recent study has shown ATF4 to be a downstream target of mTORC1 signaling, resulting in increased expression of part of the ATF4 target genes including those involved in amino acid uptake, synthesis, and tRNA charging (Torrence et al., 2021). We speculate that the expression of ATF4 may be a reflection of active mTORC1 in nutrient-starved cells, rather than the activation of ISR.

ISRIB: Integrated Stress Response inhibitor

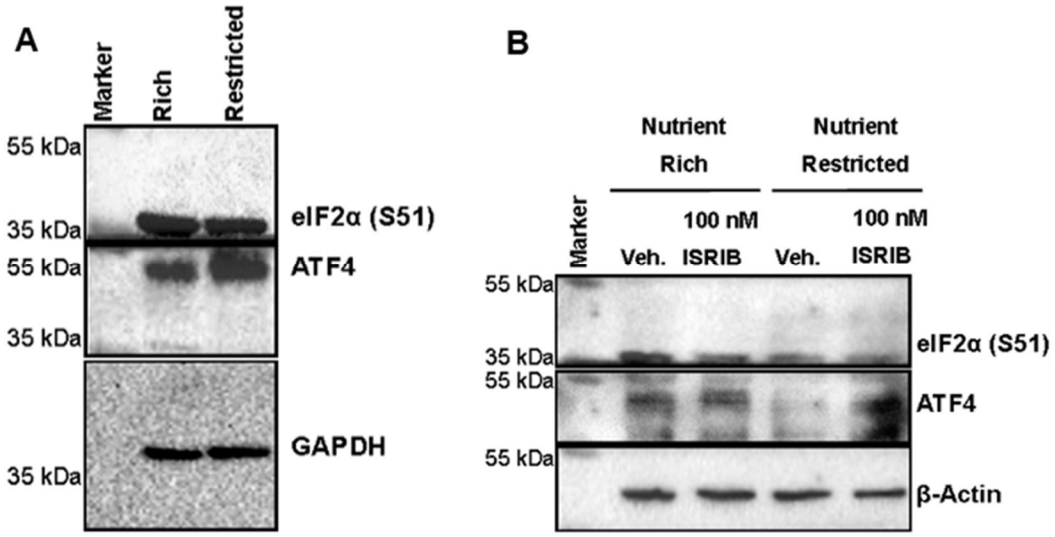

Figure 3.13 Evaluation of ISR Activation Upon Nutrient Restriction

(A)LoVo cells were cultured with either the nutrient-restriction medium or the nutrient-rich medium. (B) LoVo cells were cultured with either nutrient restriction medium or nutrient-rich medium containing for 48h and 100nm ISRIB or vehicle (DMSO) was added in the last 2h. 30 µg proteins loaded on 12% SDS-PAGE gel. Representative blot from 3 independent biological replicates is shown.

3.8 Role of MAP Kinase Pathway on RPS6 Activation in Nutrient-restricted LoVo Cells

Mitogen-activated protein kinase (MAPK) pathways are kinase modules that link extracellular signals to the machinery that governs essential cellular functions such as growth, proliferation, differentiation, migration, and cell death (Dhillon et al., 2007). The MAPK pathway includes kinases such as RAS, RAF, MEK, and ERK.

One of the kinases that can phosphorylate RPS6 at Ser235/236 is the Ribosomal S6 Kinase (RSK) proteins, which are downstream effectors of the MAPK pathway

(Roux et al., 2007). To determine whether the MAPK signaling pathway was contributing to RPS6 activation, we checked the phosphorylation levels of ERK1/2 at Thr202/204 as a function of nutrient availability. Upon nutrient restriction, the ERK1/2 was activated in LoVo cells. To further evaluate the activation of the ERK signaling pathway we treated the cells with 0.5 μM of the MEK1/2 inhibitor U0126 for the last 24h of 48h starvation. Since MEK1/2 is the upstream activator kinase of ERK1/2, U0126 treatment led to a decrease in the phosphorylation level of ERK1/2 at Thr202/204 in nutrient-rich and restricted groups as expected. Interestingly, both S235/236 and S240/244 phosphorylations of RPS6 showed a decrease with the U0126 treatment, suggesting that activation of RPS6 can be indeed activated as a result of the activation of the MAPK pathway. However, we did not observe any difference in the phosphorylation of RSK1/2 at T573 with either starvation or upon treatment with the MEK inhibitor.

U0126: MEK inhibitor

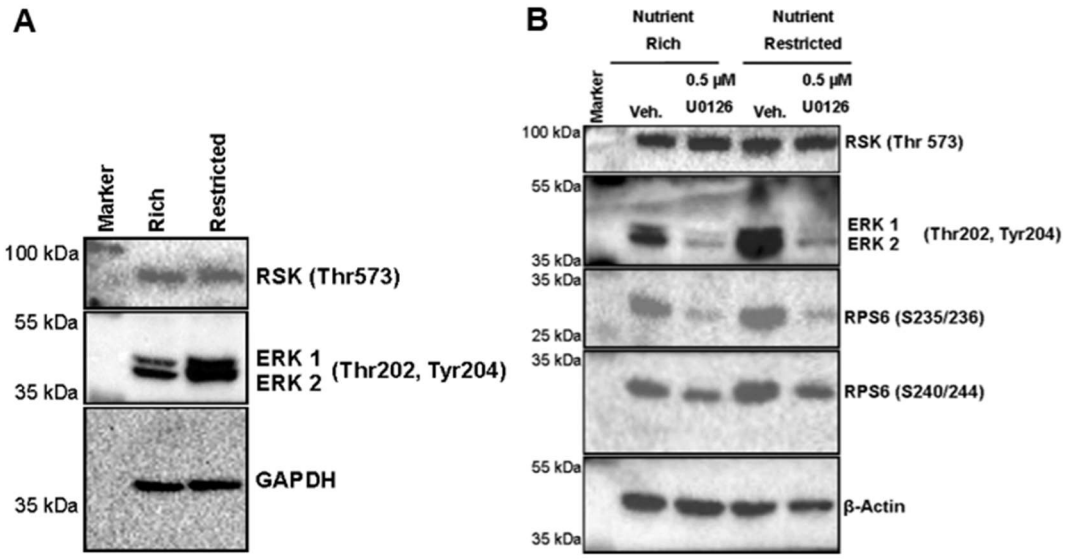

Figure 3.14 Evaluation of the Role of MAPK Signaling Pathway to RPS6 Activation Upon Nutrient Restriction

(A)LoVo cells were cultured with either the nutrient-restriction medium or the nutrient-rich medium. (B) LoVo cells were cultured with either nutrient restriction

Figure 3.14 (cont'd) *medium or nutrient-rich medium containing for 48h and 0.5 μM U0126 or vehicle (DMSO) was added for the last 24h of 48h. 30 μg proteins were loaded on 12% SDS-PAGE gel. Representative blot from 2 independent biological replicates is shown.*

3.9 In Silico Investigation of the Effect of Co-activation of AMPK and RPS6 on Patient Survival

The activation of RPS6 in cells that have low nutrient availability is likely to be a mechanism for cell survival. We particularly examined this hypothesis since the surviving LoVo cells after 48h of nutrient restriction were highly viable. We sought to examine if the co-activation of nutrition-sensing pathways such as AMPK and RPS6 was associated with the development of CRC tumors. For this, we evaluated publicly available reverse phase protein array (RPPA) data for a subset of patients from the colon adenocarcinoma (COAD) cohort from The Cancer Genome Atlas (TCGA). The analysis included 347 patients who had follow-up and RPPA data available. AMPK (T172) phosphorylation as a robust marker for nutrition restriction and RPS6 (S240/244 and S235/236) phosphorylation were divided into 25% quadrants, and tumors with the highest phosphorylation of both RPS6 and AMPK were further investigated. We found that AMPK and RPS6 were co-activated in 6% (22/347) of CRC tumors. When the proteins currently available in the RPPA for COAD were analyzed in these patients, we found a significant enrichment of proteins associated with the MAPK pathway (MEK, Src, p38), growth factors (Akt, IGFBP2), oncogenic transcription factors (NF-B), fatty acid oxidation (ACC), and stress response (YB1) compared to patients with high AMPK but low RPS6 phosphorylation. This shows that the tumors with AMPK and RPS6 coactivation displayed both growth (anabolic) and catabolic signals. The same tumors also showed a down-regulation in tumor suppressive proteins such as caveolin-2 (which inhibits growth factor signaling), Annexin-1 (which is implicated in apoptosis), and

collagen (cell-matrix interaction). More interestingly, patients with high AMPK and RPS6 phosphorylation had lower overall survival compared to patients with high p-AMPK and low p-RPS6; nevertheless, the difference failed to reach statistical significance (p=0.27) due to the small patient number (Figure 3.15).

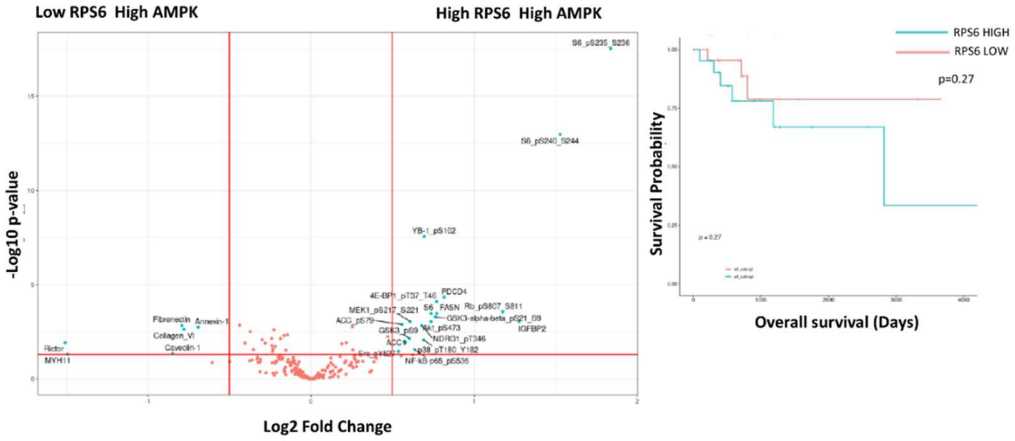

Figure 3.15 Major Deregulation in the Expression of Metabolic Genes in Colon Adenocarcinoma Tumors (COAD) from The Cancer Genome Atlas (TCGA).

Tumors with high phospho (p)-AMPK (T172) and p-RPS6 (S240/244& S235/236) showed increased expression of many critical growth and catabolism-related genes versus tumors with high p-AMPK versus low p-RPS6. Patients with high p-AMPK and p-RPS6 showed a trend for worse survival compared to patients with high p-AMPK and low p-RPS6 (right panel). The difference did not reach statistical significance (p=0.27) due to the low patient number (n=22). The data analysis and figure were generated by Ilir Sheraj.

3.10 Could RPS6 Activation in Nutrient-restricted Cells Provide Survival Advantages?

Next, we evaluated the survival of LoVo cells over a period of 72 hours with nutrient restriction and observed that 76% of the LoVo cells remained metabolically active

after 48h of nutrient restriction (Figure 3.16 A). The high viability of the cells after 48h of nutrient restriction suggested that this time point was ideally suited to determine pathways that could keep these cells alive despite the low availability of nutrients. Furthermore, we also evaluated the effect of long-term starvation (up to 8 days) on proliferation with a colony formation assay (Figure 3.16 B). Starvation for up to 8 days caused complete cell death that could be reversed with 2 days of starvation and 6 days of recovery.

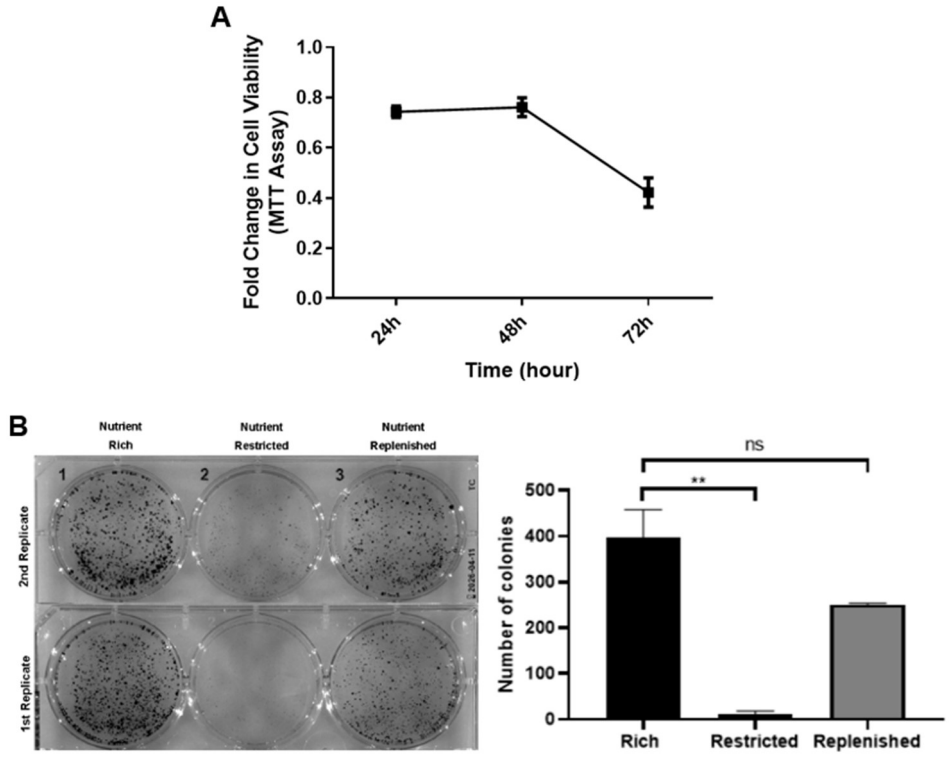

Figure 3.16 The Proliferation of Nutrient-restricted LoVo with Prolonged Nutrient Restriction was Evaluated

with MTT Assay (A) and Colony Formation Assay (B) 1000 LoVo cells per well were plated in a 6-well plate. Cells were cultured with nutrient-rich or nutrient-restricted medium for 8 days. The nutrient-replenished cells were cultured with a nutrient-restricted medium for 2 days and then a nutrient-rich medium for the next 6 days. The medium was renewed every 48 hours. After 8 days, cells were fixed with 4% PFA and stained with 0.5% crystal violet solution. The mean of 2 independent biological

Figure 3.16 (cont'd) *replicates is shown for the MTT assay. Each group's two technical replicates are shown for colony formation assay.*

Next, we investigated the *in vivo* impact of nutrient restriction by examining the size of the microtumors formed with a CAM assay (Figure 3.17). For this, LoVo cells grown for 48h in the nutrient-restricted or nutrient-rich medium were inoculated in fertilized chicken eggs and the size of the tumor was determined after 5 days. We observed that nutrient-restricted CAM microtumors were comparable in size to nutrient-rich CAM microtumors. This supports our *in vitro* data of no change in the viability of LoVo cells with nutrient-restriction.

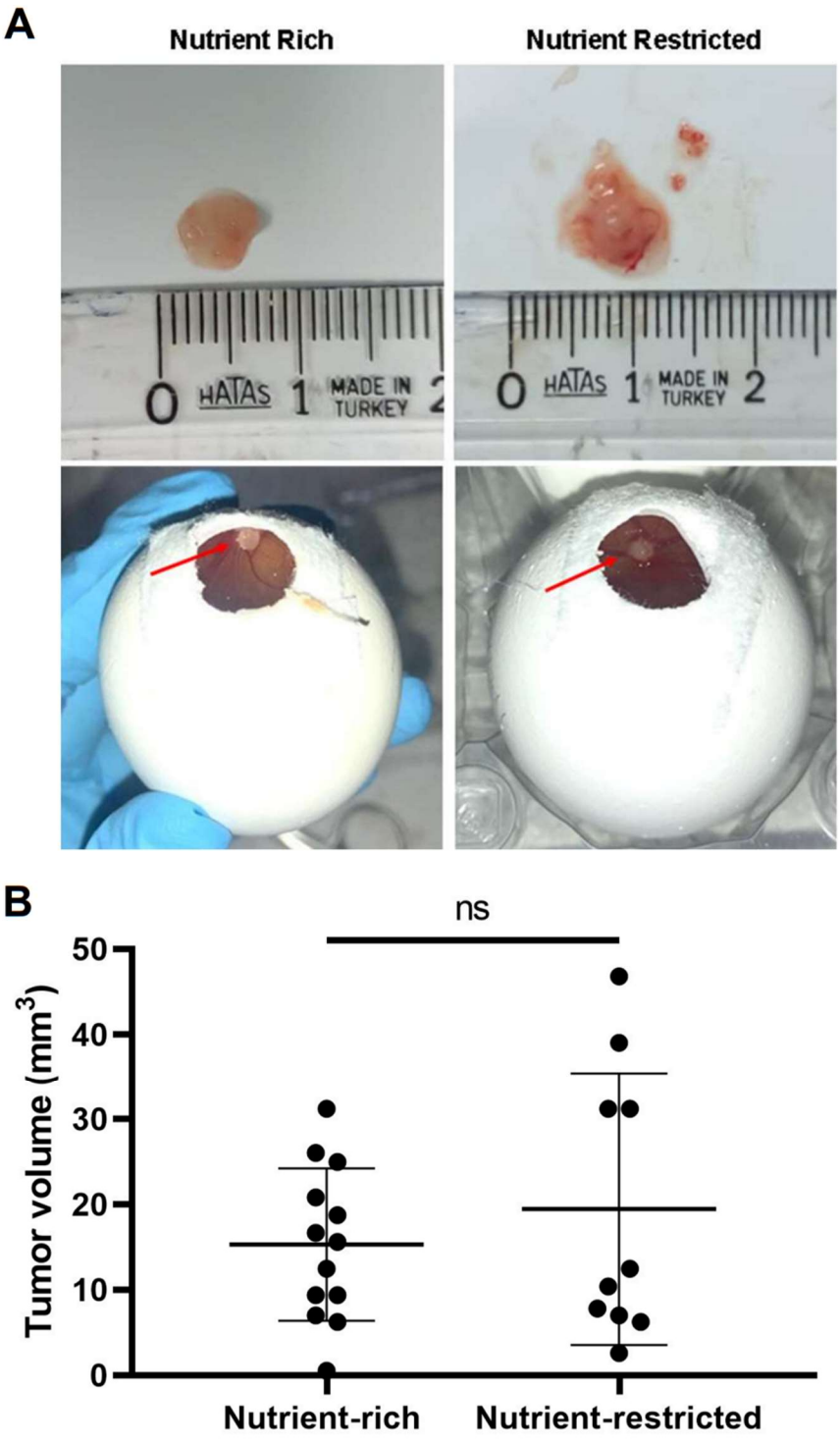

Figure 3.17 Evaluation of Nutrient Restriction on Tumor Size *in vivo* Using the CAM Assay

Figure 3.17 (cont'd) *(A) Representative CAM microtumor images (red arrows). (B) Tumor volume of LoVo CAM assay microtumors nutrient-rich (n= 12) and nutrient-restricted (n= 9). Statistical analyses were carried out using Mann–Whitney test (ns: not significant).*

3.11 The Effect of 5-FU and Cisplatin on Cell Viability

To determine whether the activation of RPS6 in nutrient-restricted LoVo cells also altered the sensitivity of the cells to chemotherapy drugs, an MTT assay was carried out with LoVo cells treated with two well-known chemotherapeutic drugs, 5-FU (20 μM) and cisplatin (5 μg/mL) (Figure 3.18 A, B). Treatment with both 5-FU and cisplatin decreased cell viability in nutrient-rich LoVo cells. However, neither 5-FU nor cisplatin significantly reduced cell viability in nutrient-restricted LoVo cells, suggesting that nutrient-restricted LoVo cells were insensitive to both 5-FU and cisplatin treatment.

To determine whether the activation of RPS6 in nutrient-restricted LoVo cells also causes chemoresistance MTT analysis was performed with 20 uM 5-FU and 5mg/mL cisplatin two well-known chemotherapeutic drugs. Both 5-FU and cisplatin treatment decreased the cell viability in nutrient-rich LoVo cells. However, neither 5-FU nor cisplatin significantly reduced cell viability in nutrient-restricted LoVo cells. Suggesting that, nutrient-restricted LoVo cells are insensitive to both 5-FU and cisplatin treatment.

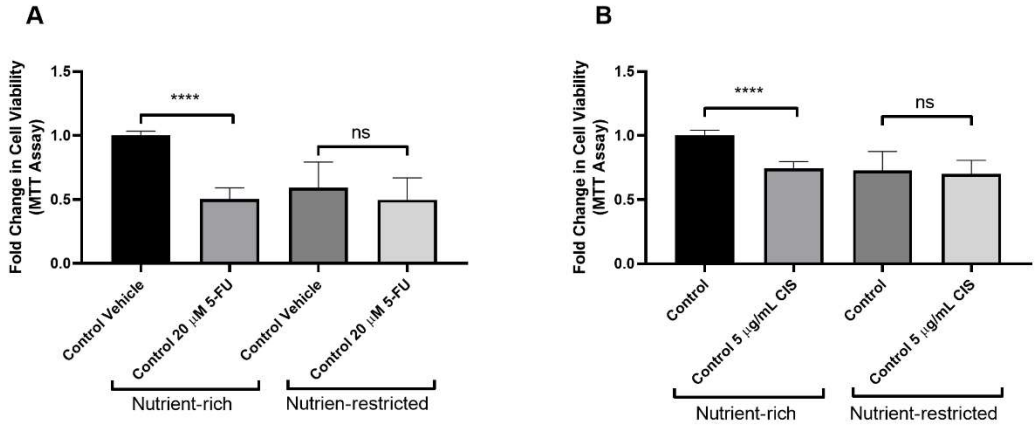

Figure 3.18 The Effect of 5-FU and Cisplatin on Cell Viability in Nutrient-rich and Nutrient-restricted LoVo Cells

*The MTT assay shows that while nutrient-rich LoVo cells were sensitive to both 5-FU and cisplatin treatment nutrient restricted LoVo cells were insensitive to both chemotherapeutic drugs. A representative graph from the mean of 5 independent biological replicates is shown. Statistical analyses were carried out using ANOVA followed by Tukey's multiple comparison test (****p<0.0001, *p<0.05, ns: not significant).*

We also investigated the *in vivo* impact of the chemotherapeutic drug (5-FU) on the size of the microtumors formed with a CAM assay (Figure 3.19). Nutrient-restricted LoVo cells were co-treated with 20 μM 5-FU for 48 hours before being inoculated in fertilized chicken eggs, and the size of the tumor was measured after 5 days, with nutrient-rich LoVo cells serving as a control.

Similarly to MTT data, 5-FU treated nutrient-restricted CAM tumors did not differ significantly from nutrient-restricted or nutrient-rich microtumors.

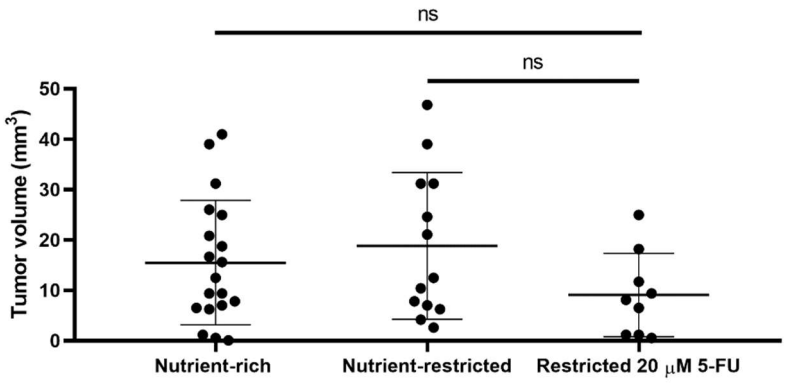

Figure 3.19 The Effect of 5-FU Treatment on Tumor Size *in vivo* Using the CAM Assay

Tumor volume of LoVo CAM assay microtumors nutrient-rich (n= 19) and nutrient restricted (n= 13), nutrient restricted 20 μM 5-FU (n= 9). Statistical analyses were carried out using ANOVA followed by Tukey's multiple comparison test (ns: not significant).

3.12 The Investigation of Whether AMPK or mTOR Inhibition Causes Metabolic Vulnerability in Nutrient-restricted LoVo Cells

The co-activation of AMPK and RPS6 in nutrient-restricted cancer cells is likely to activate pathways that can enable survival. Such information would not only provide us with mechanistic insights into the cross-talk between divergent metabolic pathways but may also enable us to identify gene signatures that can be used in the future for patient stratification and therapy. Therefore, we evaluated the proliferation of nutrient-restricted LoVo cells treated with the AMPK inhibitor Compound C, mTORC1 inhibitor Everolimus, or AZD8055 (mTOR ATP-competitive inhibitor) in combination with the chemotherapeutic drugs 5-FU and cisplatin. The inhibition of AMPK by Compound C, or of mTOR by Everolimus or AZD8055 did not lead to any change in cell proliferation either in nutrient-rich or in nutrient-restricted LoVo

cells, and sensitivity of the cells to 5-FU and cisplatin remained the same when co-treated with Everolimus or AZD8055. Interestingly, only co-treatment of nutrient-restricted cells with compound C and cisplatin increased the nutrient-restricted cells' sensitivity to cisplatin. Recent research has shown that cisplatin induces protective autophagy, which contributes to the development of cisplatin resistance (Lin et al., 2017). Inhibiting autophagy with compound C in the early stages by inhibiting AMPK could potentially overcome cisplatin resistance caused by autophagy induction.

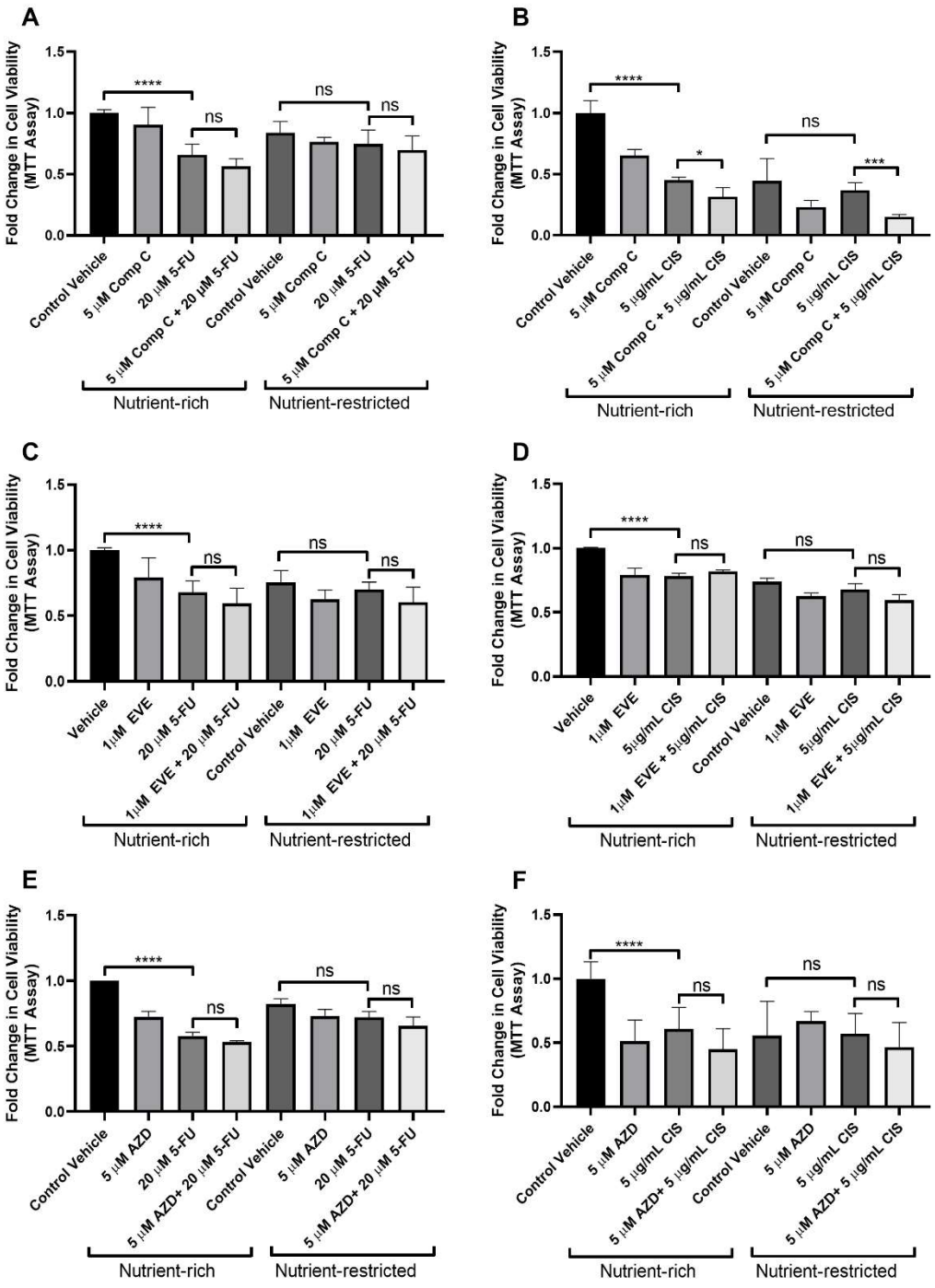

Figure 3.20 The Effect of AMPK or mTOR Inhibition on Cell Viability

MTT assay was used to assess the effect of AMPK inhibitor Compound C (A-B), mTORC1 inhibitor Everolimus (C-D), AZD8055 mTOR ATP-competitive inhibitor

Figure 3.20 (cont'd) *(E-F) on cell viability and the effect of inhibitors on the sensitivity of cells to 5-FU and Cisplatin was evaluated with MTT assay. A representative graph from the mean of 2 independent biological replicates is shown. Statistical analyses were carried out using ANOVA followed by Tukey's multiple comparison test (****p<0.0001, ns: not significant).*

3.13 The Investigation of Whether Autophagy Inhibition Causes Metabolic Vulnerability in Nutrient-restricted LoVo Cells

It is evident that various cancers depend on functional autophagy for growth, survival, and the development of malignancy. Autophagy likely plays a pro-tumorigenic role in human tumors given the low frequency of mutations in critical autophagy genes in human cancers (Hernandez & Perera, 2022). Therefore, to test the effect of autophagy inhibition on the survival of LoVo cells upon nutrient restriction we evaluated the proliferation of nutrient-restricted LoVo cells treated with 5 mM 3MA as an early-stage autophagy inhibitor and 100 nM Bafilomycin A1 as a late-stage autophagy inhibitor in combination with the chemotherapeutic drugs 5-FU and cisplatin. Neither 3MA nor Bafilomycin combined with 5-FU killed the nutrient-rich or restricted LoVo cells. This suggests that the resistance mechanism activated by the nutrient restriction medium was not associated with autophagy induction or autophagic flux. However, 3MA combined with cisplatin significantly reduced the cell viability in both nutrient-rich and restricted LoVo cells. Suggest that, cisplatin resistance can be overcome by inhibition of autophagy at early stages like with 3MA or Compound C, but not later stages like with Bafilomycin.

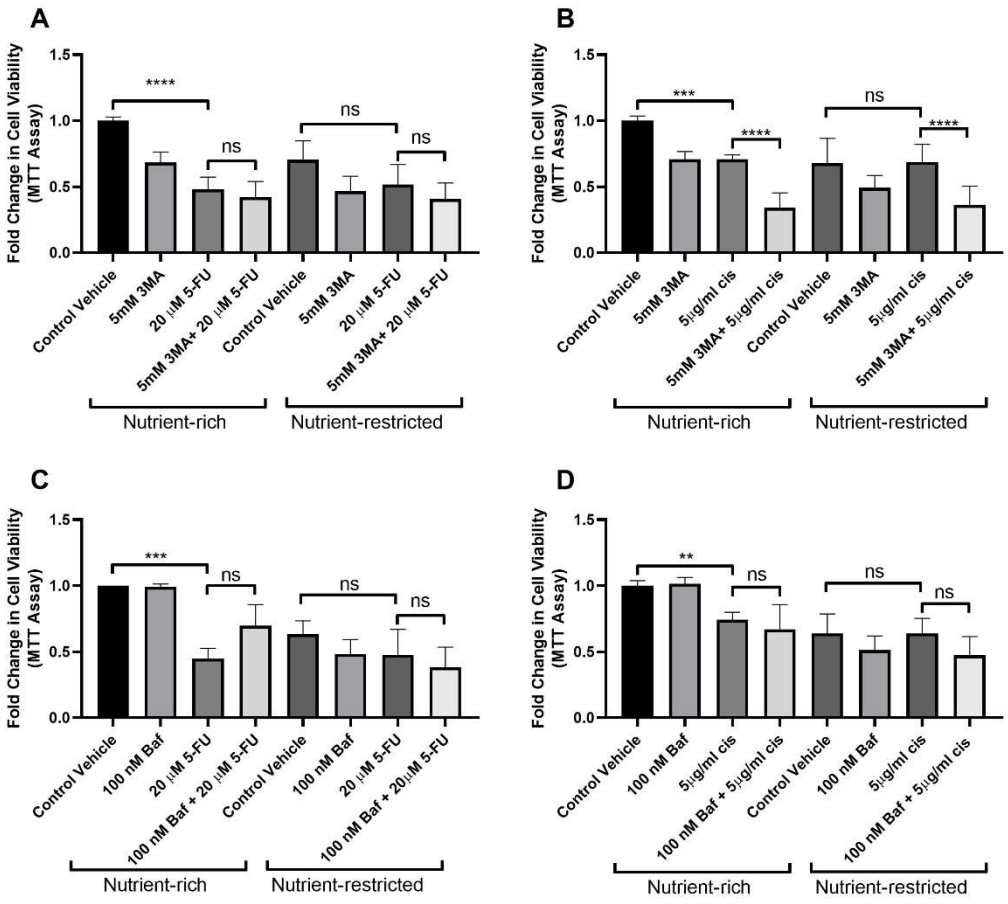

Figure 3.21 The Effect of Autophagy Inhibition on Cell Viability

*MTT assay was used to assess the effect of early-stage autophagy inhibitor 3MA (A-B) and late-stage autophagy inhibitor Bafilomycin A1 (C-D) on cell viability and the effect of inhibitors on the sensitivity of cells to 5-FU and Cisplatin was evaluated with MTT assay. A representative graph from the mean of 2 independent biological replicates (A-B-D) 3 independent biological replicates (C) is shown. Statistical analyses were carried out using ANOVA followed by Tukey's multiple comparison test (****p< 0.0001, ***p<0.001, **p<0.01, ns: not significant).*

3.14 Evaluation of Whether Integrated Stress Response Inhibition Causes Metabolic Vulnerability in Nutrient-restricted LoVo Cells

The ISR, along with other cellular adaptation pathways, contributes significantly to the cellular defense strategy in response to stress and it is considered primarily a pro-survival, homeostatic program (Tian et al., 2021). To test the effect of ISR suppression on the survival of LoVo cells, we treated the nutrient-rich and nutrient-restricted LoVo cells with 100 nM of the small-molecule ISR inhibitor ISRIB as well as chemotherapeutic drugs 5-FU and cisplatin. Neither nutrient-rich nor nutrient-restricted LoVo cells were sensitive to ISR pathway suppression, and their sensitivity did not increase with additional chemotherapy agent treatment. This suggested that the resistance mechanism activated by the nutrient restriction medium was not associated with ISR.

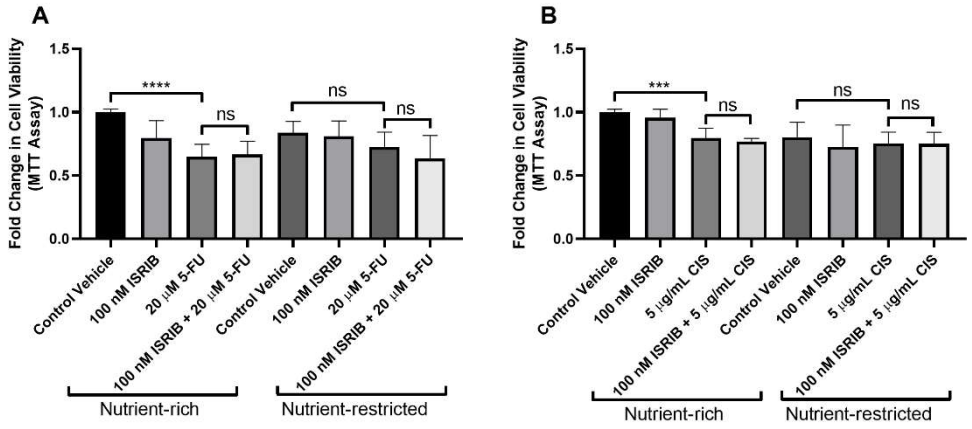

Figure 3.22 The Effect of ISR Suppression on Cell Viability

*The MTT assay was used to assess the change in cell viability of LoVo cells in response to ISR suppression. The effect of ISR suppression on the sensitivity of LoVo cells to 5-FU (A) and cisplatin (B) was evaluated. Data represent 2 independent biological replicates. Statistical analyses were carried out using ANOVA followed by Tukey's multiple comparison test (****p<0.0001, ns: not significant).*

3.15 Evaluation of Whether MAP Kinase (MAPK) Pathway Inhibition Causes Metabolic Vulnerability in Nutrient-restricted LoVo Cells

The Ras/Raf/MAPK (MEK)/ERK signaling cascade is the most important signaling cascade among all MAPK signal transduction pathways and is essential for tumor cell survival and development. The activation of the ERK/MAPK signaling cascade promotes proliferation while also inhibiting apoptosis (Guo et al., 2020). Since we observed that nutrient restriction could activate the phosphorylation of ERK1/2 (Figure 3.14), we treated both nutrient-rich and restricted LoVo cells with different concentrations of the specific MEK inhibitor U0126 (Figure 3.23 A). We observed that the effect of U0126 on cell viability was more pronounced in nutrient-restricted LoVo cells, whereas nutrient-rich LoVo cells were completely insensitive to U0126 treatment. Next, we decided to treat the cells with 10 μM U0126, in combination with a chemotherapy agent 5-FU or Cisplatin evaluate whether any additional overwhelming stress was required to kill the cells (Figure 3.23 B, C). We discovered that the decrease in proliferation in nutrient-restricted cells was primarily mediated by U0126, as the chemotherapy drugs had no additive effect on cell proliferation.

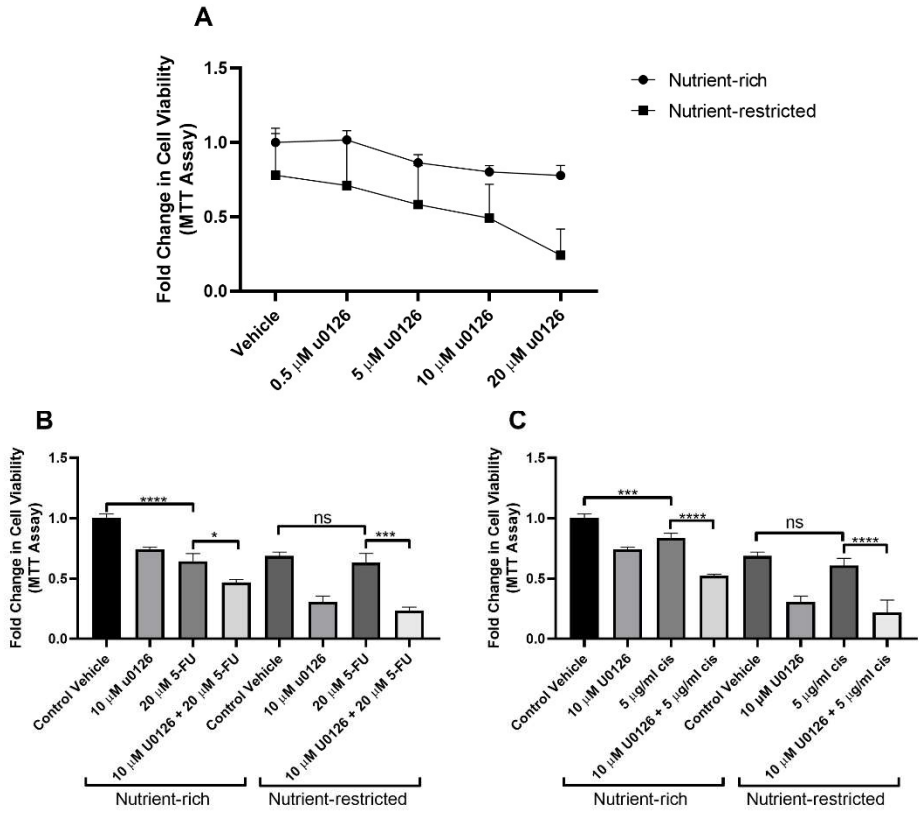

Figure 3.23 The Effect of MAPK Pathway Inhibition on Cell Viability

*(A) The sensitivity of nutrient-rich and nutrient-restricted LoVo cells to U0126 was evaluated in a dose-dependent manner. The effect of MAPK pathway inhibition with 10 μM U0126 on the sensitivity of LoVo cells to (B) 5-FU and (C) Cisplatin was evaluated. Data represent 2 independent biological replicates. Statistical analyses were carried out using ANOVA followed by Tukey's multiple comparison test (****p< 0.0001, ns: not significant).*

.

An overall summary of the effect of different inhibitors on LoVo cells grown in nutrient-rich and nutrient-restricted culture medium is shown in Table 3.1. We observed that Bafilomycin A1 and AZD8055 did not re-sensitize cells to either chemotherapy drug. Inhibition of AMPK with Compound C and activation of early stages of autophagy with 3MA could re-sensitize nutrient-restricted LoVo cells to Cisplatin, but not to 5FU. The ınhibition of the MAPK pathway with U0126 could successfully resensitize cells to both 5-FU and Cisplatin. Table 3.1 provides MTT data summary for LoVo cells treated with various inhibitors in combination with chemotherapeutic drugs.

Table 3.1 The Effect of Different Inhibitors on Chemoresistance

		Comp C	3MA	Baf	AZD	U0126
5-FU	**Nutrient-rich**	No (ns)	No (ns)	No (ns)	No (ns)	Yes (*)
	Nutrient-restricted	No (ns)	No (ns)	No (ns)	No (ns)	Yes (***)
CIS	**Nutrient-rich**	Yes (*)	Yes (****)	No (ns)	No (ns)	Yes (****)
	Nutrient-restricted	Yes (***)	Yes (****)	No (ns)	No (ns)	Yes (****)

Comp C: AMPK inhibitor
3MA: Early-stage autophagy inhibitor
Baf: Late-stage autophagy inhibitor
AZD: mTOR inhibitor
U0126: MEK inhibitor

CHAPTER 4

DISCUSSION

Cancer cells are frequently subjected to nutrient and oxygen deprivation, either due to their location in the tumor's center, which may be "arid," or because the vasculature is insufficient to ensure blood supply. Despite these unfavorable conditions, cancer cells continue to survive and proliferate (E. Y. Liu & Ryan, 2012). In this study, we incubated 5 colorectal cancer cell lines in a nutrient-restricted medium containing reduced amounts of glucose, glutamine, and serum to investigate how cancer cells survive in a nutrient-deficient environment. The majority of starvation protocols in the literature rely on the complete or partial removal of nutrients such as glucose, serum, and amino acids alone or in combination, which does not reflect the actual physiological condition to which the cancer cells are subjected.

This study demonstrated for the first time the surprising result that culture of LoVo cells in the nutrient-restricted medium containing resulted in the activation of AMP Kinase (AMPK), a nutrient sensing protein that is activated when cells are starved. However, these cells also showed the activation of ribosomal protein S6 (RPS6), a downstream target of the mTOR pathway that is generally functional under nutrient replete conditions (Figure 3.1). We also showed that Mitogen Activated Protein Kinase (MAPK) pathway was the upstream activator for mTOR.

Energy stress caused by starvation (with high AMP/ATP ratio in the cell) or hypoxia activates the upstream kinase Liver Kinase B1 (LKB1), which phosphorylates and activates AMPK at Thr -172 (Shackelford & Shaw, 2009). Alternatively, calmodulin-dependent protein kinase kinase 2 (CAMKK2) can activate AMPK in a cytosolic Ca^{2+} concentration dependent manner, which can prepare the cell for energy utilization (Carling et al., 2008). Activation of AMPK can initiate stress

response pathways to maintain cellular homeostasis, while also providing metabolites and energy by activating autophagy. The induction of autophagy allows cancer cells to survive by maintaining energy homeostasis and removing damaged organelles and proteins (Puissant et al., 2010).

mTOR is a key regulator of cell growth and division. Dysregulation of mTOR signaling has been demonstrated in many human diseases, particularly a wide range of human cancers, and is reported to be aberrantly overactivated in more than 70% of cancers (Forbes et al., 2011). Abnormally activated mTOR in tumor cells sends signals that encourage tumor cells to grow, proliferate, and metastasize (Hsieh et al., 2012). Therefore, mTOR inhibitors are frequently used in the study of targeted therapy for tumors.

Among the many upstream signals that can regulate mTORC1, the MAPK signaling pathway tightly regulates mTOR activity via the inhibition of tuberous sclerosis complex 2 (TSC2). A link between abnormal MAPK- mTOR pathway activation and tumorigenesis has also been established (Carracedo et al., 2008; L. Ma et al., 2005; Miyazaki & Takemasa, 2017; Nakashima & Tamanoi, 2010).

4.1 Co-activation of AMPK and RPS6 in Nutrient-restricted LoVo Cells

We first established whether the co-activation of AMPK and RPS6 was of clinical significance and not just a cell line observation. For this, using publicly available RPPA data from the TCGA cohort, we examined the correlation between high AMPK and RPS6 phosphorylation and the overall survival (OS) of the patients. We found that the cohort of patients showing high levels of both p-AMPK and p-RPS6 showed a trend for lower OS compared to patients with high p-AMPK and low p-RPS6 (Figure 3.15). Moreover, these tumors also showed significant enrichment of proteins associated with the MAPK pathway, growth factors, oncogenic transcription factors, and stress response in tumors. This further suggested the biological

importance of the oncogenic MAPK and mTOR pathways in human colorectal cancer.

An intriguing corollary question is what advantage RPS6 activation would provide tumor cells under nutrient stress. In order to cope with stress conditions, tumor cells enhance signaling pathways that regulate nutrient availability, flux, cell cycle progression, and cell survival through altered metabolic pathways (Darling & Cook, 2014). Cancer cells are vulnerable to fluctuations in the microenvironment due to metabolic rewiring. Nutrient availability, in particular, has a significant impact on the metabolism and survival of cancer cells (Muir & vander Heiden, 2018).

We observed that LoVo cells grown for 48h under nutrient restriction led to some cell death; however, the surviving cells were all highly viable and were able to form tumors in a CAM assay (Figure 3.16, Figure 3.17). RPS6 activation in nutrient-restricted cells may reflect the activation of oncogenic signaling pathways such as the PI3K/AKT/mTOR, MYC or MAPK pathway upon metabolic rewiring to increase their survival and tumorigenicity. For example, Ma et al showed that cells with constitutively activated ERK along with high mTOR activity showed higher tumorigenicity in athymic nude mice (L. Ma et al., 2005).

The mTORC1/p70S6K signaling pathway is primarily implicated in the phosphorylation of RPS6 in mammalian cells, although several other kinases including the Ras-MAPK pathway can also activate this protein (Yi et al., 2022). The mTOR and AMPK pathways are generally activated in an antagonistic manner with mTOR activating anabolic reactions and AMPK activating catabolic reactions (Robles-Flores et al., 2021). Since nutrient-restricted LoVo cells showed the activation of both AMPK and RPS6, we first aimed to establish the primary pathway for the activation of RPS6 (Figure 3.3 A, B).

Cells treated with selective mTORC1 inhibitor Everolimus did not show any inhibition of mTORC1 in both nutrient-rich and restricted LoVo cells, which can be explained by the possibility of feedback activation of mTORC2, which can reactivate mTORC1 via AKT (Y. Zhang et al., 2018). To circumvent this, we also used

AZD8055, an ATP-competitive mTOR inhibitor capable of inhibiting both mTORC1 and mTORC2 activity (Y. Zhang et al., 2018). Interestingly, while AZD8055 decreased the phosphorylation levels of mTOR targets ULK1 and 4EBP1 in nutrient-rich cells, as expected, the phosphorylation of RPS6 at both known sites of phosphorylation (S235/236 and S240/244) remained unaffected, suggesting that RPS6 could be phosphorylated by alternative kinases. We also evaluated whether mTOR inhibition could reverse the survival of LoVo cells under prolonged starvation with an MTT assay (Figure 3.19 C, D, E, F). The inhibition of the mTOR pathway did not reverse the survival nor did it re-sensitize nutrient-restricted cells to chemotherapy, supporting the fact that mTOR may not be a key kinase for the phosphorylation of RPS6 under nutrient restriction. However, imaging studies indicated that mTOR could colocalize with LAMP1, suggesting the presence of active mTOR on lysosomes in nutrient-restricted cells. Additionally, while the phosphorylation of p70S6K at T389, a direct downstream target of mTOR, was inhibited in the nutrient-restricted LoVo cells, the phosphorylation of 4EBP1 remained reasonably high. Therefore, it is likely that signaling via mTORC1 remains partially active in nutrient-restricted LoVo cells.

We next used compound C to inhibit AMPK, which decreased the p-AMPK levels in nutrient-rich but not in nutrient-restricted LoVo cells (Figure 3.3 C). Interestingly, Compound C treatment was able to reduce phosphorylation levels of the downstream effectors of mTORC1 including RPS6 at S235/236 in nutrient-restricted LoVo cells, suggesting that activation of the AMPK pathway and its downstream effectors could lead to the activation of RPS6. We also evaluated the proliferation of nutrient-restricted LoVo cells treated with Compound C (Figure 3.19 A, B) and observed a reversal of the survival.

The MAPK pathway is known to contribute to the phosphorylation of RPS6 via Ras/ERK signaling (Roux et al., 2007). We also observed the activation of ERK1/2 in response to nutrient restriction (Figure 3.14). To further establish whether ERK1/2 signaling was contributing to RPS6 activation, the cells were treated with the MEK1/2 inhibitor U0126. We showed that ERK1/2 phosphorylation was efficiently

blocked by the U0126, which also significantly reduced the S235/236 phosphorylation of RPS6, supporting our hypothesis. Of note, phosphorylation of RPS6 at S240/244 was also affected significantly upon treatment with U0126. Indeed, it is well defined in the literature that while RPS6 S235/236 phosphorylation occurs via both mTOR and MEK1/2 activity, S240/244 phosphorylation is regulated exclusively via mTOR (Roux et al., 2007a, 2007b; Yi et al., 2022). A crosstalk between MAPK and mTOR also exists since the activation of MEK/ERK by an agonist was shown to activate mTORC1 signaling via phosphorylation of the upstream regulator tuberous sclerosis 2 (TSC2) in C2C12 myoblasts (Miyazaki & Takemasa, 2017). Yet another study has identified the Ras/MAPK pathway as an upstream kinase of the inhibitory TSC complex, with MAPK activation enhancing mTOR signaling, leading to cell proliferation and oncogenic transformation (L. Ma et al., 2005). Therefore, we can conclude that the mTOR pathway could be activated via several components of the MAPK pathway, resulting in both S235/236 and S240/244 phosphorylation of RPS6. To further evaluate this, we examined the phosphorylation of RSK, a downstream kinase of ERK1/2 that was shown to phosphorylate RPS6, especially at S235 /236 (Carrière et al., 2008; Roux et al., 2007). However, we observed that the phosphorylation of RSK at T573 remained unchanged in the nutrient-restricted LoVo cells in comparison to control cells, suggesting either that ERK1/2 can directly phosphorylate RPS6 or the presence of an alternative kinase that can act as an intermediate. Further studies are needed to elucidate how these two pathways interact to modulate RPS6 and other downstream targets to support cell growth and survival.

4.2 Lysosomal Turnover and Acidity in Nutrient-restricted LoVo Cells

Cancer cells must maintain a fine balance between anabolic and catabolic pathways (Robles-Flores et al., 2021). It has been reported that lysosomal amino acid pools restored through the catabolic autophagic process can reactivate the anabolic mTORC1 pathway during long-term starvation (Condon & Sabatini, 2019; Yu et al.,

2010). LoVo cells incubated in the nutrient restriction medium lead to an increase in autophagy, as shown by the increase in LC3-II. In addition, we observed an increase in the endo-lysosomal trafficking markers RAB5 and RAB7a and the lysosomal protein LAMP1 (Figure 3.4 A). Interestingly, a time course study of nutrient restriction revealed that LAMP1 levels increased as early as 2 hours of nutrient restriction and then decreased over the next 48 hours (Figure 3.4 B). During prolonged starvation, lysosomes can be consumed via the generation of autolysosomes, which may have led to a decrease in the LAMP1 signal. Reactivation of mTORC1 under long-term starvation can be a mechanism of lysosomal reformation via a pathway called autophagic lysosome reformation (ALR), in which proto-lysosomal tubules are formed from autolysosomes and the generated vesicles mature into a restored pool of lysosomes (Y. Chen & Yu, 2017; Yu et al., 2010).

To better evaluate the process of autophagy and its flux in the nutrient-restricted cells, we used the late-stage autophagy inhibitor Bafilomycin A1 (Baf) to inhibit autophagic degradation. The accumulation of autophagic markers after Baf treatment was expected since autophagic flux is inhibited. When we removed Baf from the culture, we observed a modest decrease in the expression of autophagic markers in the nutrient-restricted cells while a robust decrease was observed in the nutrient-rich cells (Figure 3.5). This suggests that autophagic flux was slowed rather than inhibited in nutrient-restricted LoVo cells.

Autophagic flux can be slowed down by various mechanisms, including deregulation at the autophagosome-lysosome fusion, inhibition of nuclear translocation of Transcription Factor EB (TFEB) that transcriptionally upregulates the Coordinated Lysosomal Expression and Regulation (CLEAR) gene network, or lysosomal alkalinization (Q. Zhang et al., 2022). To evaluate whether the starved LoVo cells had impaired autophagosome-lysosome fusion, we determined the expression of the late lysosomal protein RAB7 and Synaptosome Associated Protein 29 (SNAP29), a protein that mediates the fusion of autophagosomes to lysosomes. We observed robust and high levels of both proteins in the nutrient-restricted cells (Figure 3.6).

Therefore, it was unlikely for the cells to have impaired autophagosome-lysosome fusion.

Under nutrient-rich conditions, TFEB is found in the cytoplasm, while nutrient restriction can rapidly cause the nuclear translocation of the protein (Settembre et al., 2011). Inhibition of nuclear translocation of TFEB can lead to incomplete autophagy due to lysosomal dysfunction. Thus, cytosolic retention of TFEB can induce incomplete autophagy by suppressing lysosome biogenesis. We observed that nuclear TFEB levels were lower in nutrient-restricted LoVo cells (Figure 3.6 A); additionally, cytoplasmic TFEB was present in both nutrient-rich and restricted cells when observed with immunofluorescence microscopy (Figure 3.8).

Supporting the high levels of cytosolic TFEB in nutrient-restricted LoVo cells, mRNA levels of the TFEB targets MCOLN1, RAB7a, and RAB5 were decreased slightly but not significantly in response to the nutrient restriction (Figure 3.6 B). However, p62 (encoded by the gene *SQSTM1*) was the only TFEB target that showed significantly higher mRNA levels in nutrient-restricted LoVo cells, reflecting the high protein levels also observed in these cells. *SQSTM1* expression is regulated by transcription factors other than TFEB as well. Indeed, it was shown that Ras-transformed fibroblasts expressed a high level of *SQSTM1* mRNA, which was lost after the AP-1 binding site located upstream on the promoter was removed. This suggests that a constitutively active Ras/MEK/ERK1/2 pathway can regulate *SQSTM1* transcription via the AP-1 binding domain in its promoter (Duran et al., 2008). Induction of *SQSTM1* by Ras is important for the activation of NF-κB which enhances cell survival and increases tumorigenicity, and indeed increase in p62 levels and Ras activity has been reported in several human tumor tissues (Duran et al., 2008). LoVo cells have a G13D; A14V KRAS mutation (Ahmed et al., 2013) which increases the accumulation of active RAS and leads to the constitutive activation of downstream pathways (Tong et al., 2014). We also demonstrated the activation of ERK1/2 upon nutrient restriction (Figure 3.14), implying that activation of the Ras/MEK/ERK1/2 pathway, rather than TFEB nuclear translocation, may have caused the transcriptional upregulation of *SQSTM1*.

mTORC1 plays a critical role in the regulation of nuclear localization and activity of TFEB. mTOR needs to be recruited to the lysosome for activation and the amino acid-induced recruitment of this complex is primarily transmitted via Rag-GTPases (Mutvei et al., 2020). vacuolar H+-adenosine triphosphatase ATPases (v-ATPases) are known to be required for the amino acid mediated activation of mTORC1, which are also necessary for lysosome acidification (Zoncu et al., 2011). Under nutrient-rich conditions, lysosomal recruitment and activation of mTORC1 result in the phosphorylation of TFEB at Ser211 and Ser142 which retains the transcription factor in the cytoplasm and inactivates it (Chao et al., 2018). We observed both cytosolic retention of TFEB and phosphorylation of RPS6 at S240/244 by western blot; the latter phosphorylation is specific to mTORC1, suggesting the activation of mTORC1 in spite of nutrient restriction. To further confirm this, we evaluated the subcellular localization of mTORC1 in LoVo cells grown in the nutrient-rich and restricted medium by immunofluorescence assay (Figure 3.11). mTORC1 was co-localized on LAMP1-positive lysosomal membranes in nutrient-restricted LoVo cells, similar to nutrient-rich conditions. This suggests that despite long-term nutrient restriction, lysosomally localized mTORC1 may remain active in LoVo cells. This could be a survival mechanism; thus, the mTORC1 pathway is inhibited under nutrient stress, allowing autophagy to be triggered, this provides macromolecules such as amino acids leading to the reactivation of mTORC1 and cell survival under adverse conditions (Cabezudo et al., 2021; Condon & Sabatini, 2019; Kim & Guan, 2019).

TFEB activity can also be regulated by other kinases, such as ERK1/2, which phosphorylates TFEB at Ser142 and modulates its subcellular localization (Napolitano et al., 2022). Furthermore, it has been shown that ERK1/2 knock-down induced TFEB translocation to the nucleus to a similar extent as serum starvation in HeLa cells (Settembre et al., 2011). Therefore, supporting the activation of RPS6 in nutrient-restricted cells, it can be suggested that the activation of either mTORC1 or MAPK may prevent nuclear translocation of TFEB even during prolonged starvation.

Lysosomal alkalinization can cause incomplete autophagy since it reduces the degradative capacity of lysosomal enzymes which have acidic pH optima (Johnson et al., 2016). Therefore, we used Lysotracker (LTR) staining to detect the acidification of lysosomes after treatment of cells with the lysosomal v-ATPase inhibitor Baf (Figure 3.9). Under both nutrient-rich and restricted conditions, the LTR signal was almost completely lost in the Baf-treated cells, indicating a loss of lysosomal acidification, as expected. On the other hand, an unexpected decrease in the LTR signal was observed in nutrient-restricted LoVo cells compared to the nutrient-rich controls. The pH of the lysosomes can vary with their subcellular localization; perinuclear lysosomes are known to be more acidic than lysosomes localized closer to the membranes (Johnson et al., 2016). For this reason, we evaluated the location of lysosomes in nutrient-rich and restricted LoVo cells by immunofluorescence (Figure 3.10). We observed that upon nutrient restriction lysosomes were clustered in the perinuclear region, where autophagosome-lysosome fusion is known to take place and is suggestive of adequately acidic lysosomes (Poüs & Codogno, 2011). The level of LTR signal in cells is determined by lysosomal acidity as well as lysosome number and/or area (Guha et al., 2014). Therefore, it is possible that a decrease in lysosome numbers, reflected by the decreased expression of LAMP1 may have led to the decreased Lysotracker activity.

So far we have established that both autophagy and mTOR were co-activated in nutrient-restricted LoVo cells. To determine whether mTOR reactivation was autophagy-dependent, we inhibited the autophagy with two different autophagy inhibitors, 3MA and Bafilomycin (Figure 3.12). Based on our hypothesis we would expect to see a decrease in RPS6 phosphorylation levels upon autophagy inhibition. We observed that while nutrient-restricted LoVo cells treated with 3MA could indeed show a reduction in RPS6 phosphorylation (both at S235 /236 and S240/244) and cells treated with Baf did not. Baf is a late-stage autophagy inhibitor that induces lysosomal alkalinization, whereas 3MA is a type III PI-3K inhibitor and therefore an early-stage autophagy inhibitor (T. Liu et al., 2020; Xie et al., 2014). Thus, a decrease in RPS6 activation following treatment with an early-stage autophagy

inhibitor but not with a later-stage inhibitor could imply that the regulation of RPS6 activation occurs earlier rather than later in the autophagy process. In fact, LoVo cells responded very rapidly to nutrient restriction, increasing the levels of RPS6 and endolysosomal markers within 2h, implying that induction of autophagy may be critical for the increase in RPS6 phosphorylation. Furthermore, it has been shown that 3MA treatment inhibited ERK1/2 phosphorylation in human peritoneal mesothelial cells (Shi et al., 2021). Therefore, inhibition of ERK1/2 by 3MA may also lead to a decrease in RPS6 phosphorylation levels.

The lack of any inhibition of RPS6 phosphorylation in nutrient-restricted LoVo cells treated with Baf could be attributed to the activation of RPS6 via alternative pathways such as the MAPK pathway. Treatment of colorectal cancer cells with Baf was shown to increase the phosphorylation of ERK1/2 (Wu et al., 2009). These examples highlight the possibility that the phosphorylation of RPS6 could be via an interplay between mTORC1 and ERK1/2, allowing the cell to tightly regulate these crucial signaling pathways.

4.3 Chemoresistance in Nutrient-restricted LoVo Cells

Rapidly proliferating cells, such as cancer cells, enhance signaling pathways that regulate nutrient availability and flux of carbons and nitrogens through metabolic pathways to accommodate the increased demand for macromolecules (Zhu & Thompson, 2019). Nutrient availability, therefore, has a significant impact on the survival of cancer cells as well as on how they react to chemotherapy (Muir & vander Heiden, 2018). Autophagy certainly can play a pro-tumorigenic role in human tumors, given the low frequency of mutations observed in critical autophagy genes in human cancers (Hernandez & Perera, 2022).

Activation of RPS6 was shown to be associated with intrinsic or acquired drug resistance (Gambardella et al., 2019; Penning, 2017). In our study, we observed that nutrient-restricted LoVo cells were insensitive to the chemotherapeutic drug 5-FU

and cisplatin compared to their nutrient-rich counterparts (Figure 3.18). Additionally, despite the long-term nutrient restriction (48h), the cells remained viable (Figure 3.16). We also compared the *in vivo* tumor-forming ability of these cells using the CAM assay. Tumorigenicity of nutrient-restricted cells *in vivo* appeared to be similar compared to nutrient-rich cells (Figure 3.17) and treatment of nutrient-restricted LoVo cells with 5-FU did not inhibit the tumor-forming ability of these cells. These cells also maintained high viability with the inhibition of the later stage of autophagy with Baf in the presence of 5-FU or cisplatin (Figure 3.20). However, when the initiation of autophagy was inhibited with 3MA, the cells became more responsive to cisplatin, but not 5-FU. A similar sensitization to cisplatin but not 5FU was observed in nutrient-restricted LoVo cells treated with compound C. Recent research has shown that cisplatin induces protective autophagy, which contributes to the development of cisplatin resistance and cell survival via the upregulation of BECN1 (Lin et al., 2017). However, the relationship between cisplatin treatment and BECN1 upregulation needs to be studied further. For example, upon apoptotic stimuli, caspases can cleave BECN1 and prevent autophagy (Kang et al., 2011). Furthermore, apoptosis can be inhibited by autophagy by degradation of caspase-8. It has been also suggested that BECN1 may interact with the anti-apoptotic proteins Bcl-2 or Bcl-xL, which are thought to act as a switch between autophagy and apoptosis (Maiuri et al., 2007). However, another study found that the anti-apoptotic function of Bcl-2 is maintained when it interacts with Beclin 1 (Ciechomska et al., 2009). It appears that cisplatin resistance caused by nutrient restriction can be overcome by inhibiting autophagy at the early stages with either 3MA or compound C but not at later stages as with Baf. Supporting this, autophagy inhibition was shown to reverse cisplatin resistance and promote cisplatin-induced apoptosis (J. Chen et al., 2018; Galluzzi et al., 2014; Kang et al., 2011; Lin et al., 2017). Intriguingly, after 3MA treatment of nutrient-restricted cells, RPS6 phosphorylation at both S235/236 and S240/244 was decreased, supporting the idea that RPS6 activation could be implicated in drug resistance.

The activation of ERK signaling during nutrient restriction is also likely to be relevant during the metabolic reprogramming of cancer cells and is important for survival. We, therefore, evaluated cell proliferation and viability upon ERK1/2 inhibition with U0126 (Figure 3.22). ERK1/2 inhibition resulted in a dose-dependent decrease in cell viability of both nutrient-rich and restricted cells. However, cell viability in the nutrient-restricted cells was more remarkably decreased in the presence of U0126 compared to nutrient-rich cells (Figure 3.22 A). While the viability of nutrient-rich cells was 90% at the highest concentration of U0126 used (20 μM), it decreased to 30% in nutrient-restricted cells. This suggests that the high viability of nutrient-restricted cells was mediated mainly by the MAPK pathway. ERK1/2 activation has been reported to mediate chemoresistance in several cancers including colon (Li et al., 2018), breast (D. Chen et al., 2018), and liver (J. Ma et al., 2017). We observed less proliferation of nutrient-restricted LoVo cells treated with a combination of 5FU or Cisplatin and U0126 compared to 5FU or Cisplatin alone. However, it also needs to be mentioned that the decrease in proliferation was mediated primarily by U0126 as there was no additive effect of the chemotherapy drugs on U0126. The MTT assay relies on mitochondrial enzyme activity, which may not be the most suitable method to evaluate cell proliferation in cells under nutrient stress. Future experiments using cell counting and *in vivo* experiments using the CAM assay will be necessary to determine whether the combination of U0126 and 5FU or cisplatin has additive effects or not. Moreover, the mechanism of how ERK1/2 mediates cell survival should be investigated further.

Signaling via ERK1/2 can mediate chemoresistance through a variety of mechanisms. These include decreased apoptosis by decreasing Bcl-2 or decreasing the levels of reactive oxygen species, increased cell proliferation by inducing cyclins, and up-regulation of drug efflux transporters like multidrug resistance-related proteins (MRP) and ABC transporters (Salaroglio et al., 2019). For example, doxorubicin resistance in breast cancer was shown to be related to the overexpression of fibroblast growth factor receptor 4 (FGFR4), which activated ERK1/2 and induced doxorubicin resistance (Xu et al., 2018). Furthermore, extracellular ATP was shown

to promote the expression of MRP2 by increasing MEK/ERK1/2 signaling in transformed colon cells (Vinette et al., 2015). Combined treatment of LoVo cells with U0126 and cisplatin caused significant cell death under both nutrient-rich and restricted conditions. Cisplatin treatment was shown to induce ERK1/2 activation and subsequently activate autophagy. Inhibiting ERK activation with MEK inhibitors or knocking down ERK expression with siRNA was able to reduce cisplatin-induced autophagy, making ovarian cancer cells more susceptible to cisplatin-induced apoptosis (Wang & Wu, 2014). Therefore, higher levels of ERK activation may be associated with the induction of autophagy and decreased cisplatin-induced apoptosis. More importantly, inhibition of ERK with U0126 sensitized the cells to cisplatin-induced death. Hence, we can conclude that inhibiting ERK1/2 activation can make resistant cells more sensitive to cisplatin.

4.4 Induction of Integrated Stress Response (ISR) in Nutrient-restricted LoVo Cells

The ISR pathway is known to be activated in response to several stress conditions including nutrient stress. In response to stress, the eukaryotic initiation factor eIF2, a key component of the ISR, is phosphorylated at S51, which inhibits 5'cap-dependent translation. This results in a global decrease in protein synthesis, which reduces the consumption of macromolecules such as amino acids during times of scarcity. However, mRNAs that participate in the cell's response to stress, such as the transcription factor ATF4, remain unaffected or even increased in the presence of ISR. In the present work, we examined whether the nutrient restriction in LoVo cells led to the activation of the ISR pathway. The rationale for this hypothesis comes from the observation that ATF4 expression levels were increased in LoVo cells upon nutrient restriction (Figure 3.13 A). Activation of eIF2α by phosphorylation is the canonical path to ATF4 activation; however, we did not observe any change in this phosphorylation in LoVo cells upon nutrient restriction (Figure 3.13 B).

The observation of very high basal levels of eIF2 phosphorylation even in nutrient-rich conditions can be explained by the increased proliferation of cancer cells, which also leads to increased protein synthesis, which leads to a high basal level of ISR compared to normal cells. This is the rationale for the selective targeting of cancer cells by ISR inducers (McConkey, 2017; Tameire et al., 2019). To further investigate whether the increase in ATF4 expression was an outcome of ISR, we used the small molecule ISR inhibitor ISRIB, which acts downstream of eIF2α phosphorylation (Pavitt, 2013). However, we didn't observe any decrease in ATF4 expression upon ISRIB treatment (Figure 3.13 B) suggesting an alternative mechanism of ATF4 activation in nutrient-restricted cells. Park et al. reported that mTOR inhibitors could inhibit ATF4 target genes via a mechanism that was independent of eIF2 activation and involved mTOR-dependent stabilization of ATF4 by eIF4E-BP1 (Park et al., 2017). Similarly, a very recent study showed that methionine restriction resulted in an mTOR and ERK1/2-dependent, but eIF2-independent stress response that was linked to ATF4 in HepG2 cells (Stone et al., 2021). Notably, both ATF4 and p-RPS6 levels were increased by nutrient restriction in LoVo cells (Figure 3.13 A, Figure 3.1).

Activation of ERK1/2 upon nutrient restriction (Figure 3.14) also suggests an involvement of ERK1/2 in this regulatory pathway in nutrient-restricted LoVo cells. We, therefore, treated LoVo cells with a U0126 and observed that the inhibition of p-ERK1/2 could decrease ATF4 levels, suggesting that nutrient restriction mediated activation of ERK1/2 may provide an alternative pathway to regulate the induction ATF4 by nutrient restriction (Supp. Figure 2). Collectively, our findings provide appealing new evidence that nutrient restriction acutely regulates mTOR and ERK1/2 may provide regulatory input to ISR in LoVo cells.

Although the ISR is primarily an adaptive, pro-survival, homeostatic program, severe stress overwhelms the capacity of adaptive response and can cause signaling that leads to cell death. It accomplishes this primarily by altering global protein synthesis and by regulating genes that promote pro-survival signaling, such as autophagy activation, or pathways that interact with cell death processes, such as

apoptosis or proteotoxicity (Pakos-Zebrucka et al., 2016). Interestingly, ISR has been shown to have a cytoprotective function in conditions that mimic viral infection or induce ER stress by activating cell survival pathways such as PI3K and its downstream target Akt/mTOR (Kazemi et al., 2007). In fact, the cytoprotective ISR can be activated in response to anticancer therapies, resulting in the development of chemoresistance, as seen in pancreatic ductal carcinoma cells and an orthotopic mouse model treated with gemcitabine (Palam et al., 2015). However, in our study inhibition of ISR with ISRIB did not increase cell death in LoVo cells in response to chemotherapeutic drugs (Figure 3.21). A recent study showed that when intracellular p-eIF2 levels exceeded a critical threshold, ISRIB was not potent enough to inhibit ISR and concluded while ISRIB can reduce the negative consequences of low-level ISR activation, it leaves cytoprotective effects of acute ISR activation intact (Rabouw et al., 2019) Therefore, considering the high basal levels of p-eIF2 even in nutrient-rich LoVo cells (Figure 3.13 A), we can argue that the lack of chemosensitization could be a consequence of lack of ISR inhibition by ISRIB. We are planning to stably silence ATF4 in LoVo cells to determine whether this can increase chemosensitivity.

Overall, we have shown in this study that nutrient restriction can activate both anabolic and catabolic pathways in LoVo cells, leading to cell survival and chemoresistance. The MAPK pathway appears to be critical not only for the survival of nutrient-restricted cells but also for the activation of corollary pathways such as the mTOR pathway and ISR, both of which can help the cells cope with the stress of limited nutrient availability and contribute towards cell survival and tumorigenicity. Inhibition of the MAPK, AMPK, or early stages of autophagy, but not mTOR or ISR, could reverse the high viability and chemoresistance observed in these cells.

CHAPTER 5

CONCLUSION AND FUTURE STUDIES

The primary findings of this thesis study are as follows (Figure 5.1):

1- LoVo cells grown in a nutrient-restricted medium containing 1% FBS, 0.1g/L glucose, and 0.2mM L-glutamine showed a time-dependent increase in the phosphorylation of RPS6 and a concomitant activation of AMPK. RPS6 phosphorylation at both S235/236 and S240/244 suggests that the kinase activity of both mTOR and ERK1/2 may have regulated its activation under nutrient restriction (Yi et al., 2022).

2- mTORC1 was found to be located on the LAMP1-positive lysosomes in nutrient-restricted LoVo cells along with cytoplasmic retention of TFEB, similar to the nutrient-rich counterparts, suggesting the presence of active mTOR despite limited nutrient availability.

3- The MAPK pathway was activated in LoVo cells in response to nutrient restriction. The phosphorylation of RPS6 at both S235/236 and S240/244 could be prevented by the MEK inhibitor U0126. It is known that while phosphorylation at S235/236 could be mediated via both mTOR and MEK1/2, the S240/244 phosphorylation is exclusively mediated by mTOR (Yi et al., 2022). Our data suggest that the mTOR pathway could be activated via the MAPK pathway in nutrient-restricted cells, resulting in Ser240/244 phosphorylation of RPS6. ERK1/2 inhibition with U0126 treatment resulted in a dose-dependent decrease in cell viability and could also reverse the cells' insensitivity to chemotherapy drugs.

4- Nutrient restriction induced autophagy by increasing LC3-II, p62, and endolysosomal marker levels, all of which are indicators of nutrient stress (Kim et al., 2011). However, the lysosomal marker LAMP1 levels appeared

to decrease in a time-dependent manner during the nutrient restriction, consistent with the interpretation that lysosomes were consumed during long-term starvation. Reactivation of the mTOR pathway is required for the activation of the lysosomal reformation pathway, which could be a reason for the activation of mTOR observed in nutrient-restricted LoVo cells (Chen & Yu, 2017; Yu et al., 2010).

5- We observed an increase in the protein levels of the autophagic cargo protein p62 at both mRNA and protein levels. In general, the protein levels of p62 decrease with autophagy as it is degraded along with the cargo. An increase in p62 protein levels is therefore associated either with the inhibition of autophagic flux or an increase in endo-lysosomal trafficking. Therefore, we evaluated several pathways of flux inhibition including deregulation at the autophagosome-lysosome fusion, cytosolic localization of TFEB, or lysosomal alkalinization. We observed robust levels of RAB7a and SNAP29 suggesting the efficient formation of a tethering complex for autophagosome-lysosome fusion. We also did not observe any remarkable change in lysosomal acidity. The modest decrease in the Lysotracker signal, a reporter for lysosomal acidity, was attributed to a decrease in lysosome numbers with prolonged starvation. On the contrary, nuclear TFEB levels were lower in nutrient-restricted cells compared to LoVo cells undergoing acute starvation. These data suggest that signaling pathways that play a critical role in the regulation of nuclear localization and activity of TFEB such as mTOR and MAPK were activated by the starvation medium used in the current study. These pathways may have prevented the nuclear localization of TFEB even in the presence of long-term starvation.

6- Nutrient-restricted LoVo cells were highly viable and were also resistant to the chemotherapeutic drugs cisplatin and 5-FU. Increased autophagic activity (such as observed with nutrient restriction) is often correlated with increased chemotherapeutic drug resistance (Wang & Wu, 2014). Inhibition of autophagy induction at early stages with 3MA or with the AMPK inhibitor

Compound C, but not the late-stage autophagy inhibitor Bafilomycin led to sensitization of nutrient-restricted cells to cisplatin-induced cell death and also a decrease in RPS6 activation. Thus, the activation of RPS6 was mediated early rather than later in the autophagy process and inhibition of early stages of autophagy could render resistant cells sensitive to cisplatin.

7- Stress factors such as poor nutrient availability or ER stress can lead to the activation of an integrated stress response (ISR). The canonical path for the activation of the ISR marker ATF4 is the phosphorylation of the eukaryotic initiation factor eIF2 (Stone et al., 2021). We observed very high basal levels of eIF2α in LoVo cells under nutrient-rich conditions, which did not increase any further when the cells were cultured in the nutrient-restricted medium. Recent studies suggest that ATF4 can be activated via mTOR signaling. Therefore, we speculate that the increase in ATF4 levels observed in nutrient-restricted LoVo cells could have been mediated via an mTOR or ERK1/2-dependent and eIF2-independent stress response.

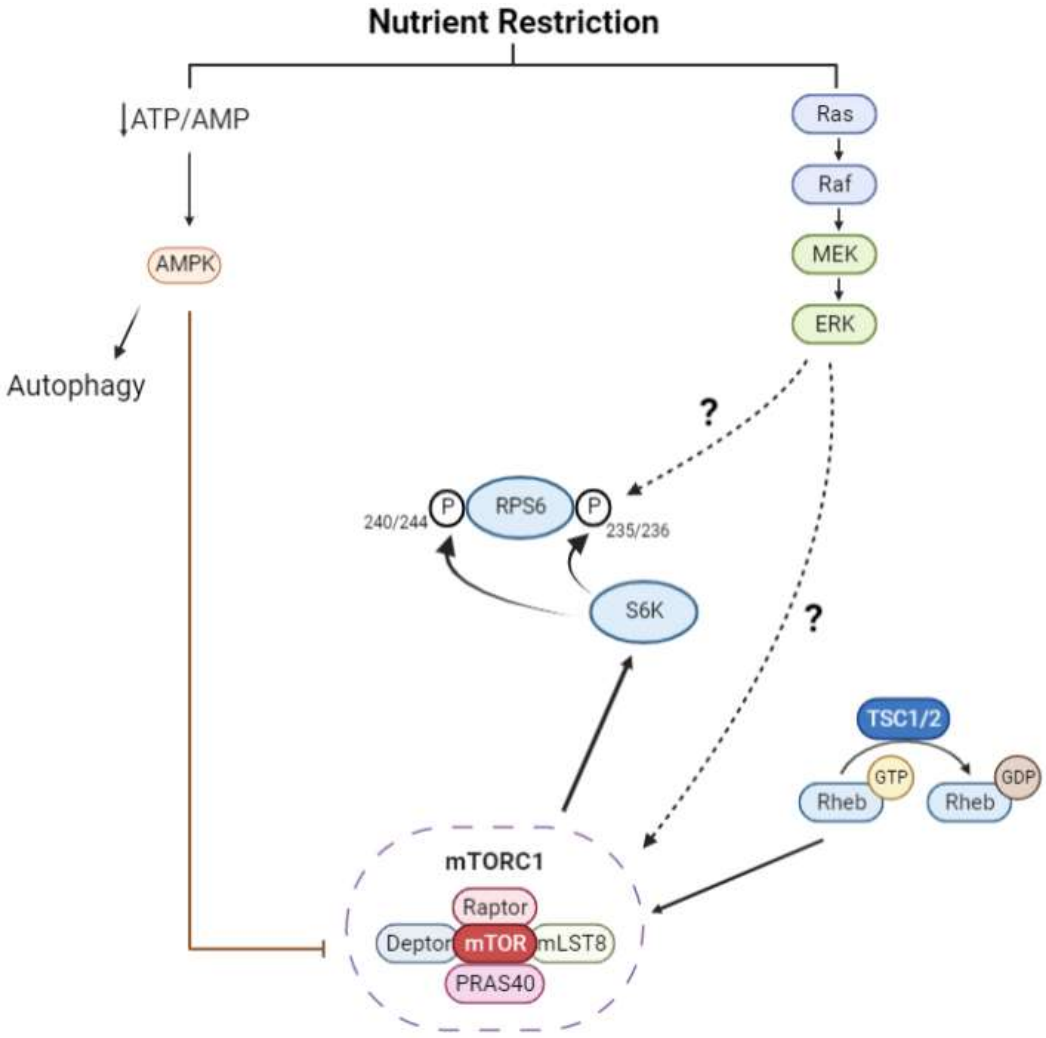

Figure 5.1 The MAPK and mTORC1 Pathways Regulate RPS6 Activation by a Twofold Mechanism

Although mTORC1 and MAPK pathways are known to activate RPS6 directly via S6K and RSK respectively, neither intermediate was activated in the nutrient-restricted LoVo cells. Thus, our data suggest the presence of alternative pathways that can lead to the activation of RPS6. Created with BioRender.com.

Given the importance of mTOR and ERK signaling in various cancers, the present study investigated the possibility of cross-talk between these two main oncogenic pathways in colorectal cancer. Our findings highlight the interdependence of the Ras/MAPK and mTOR pathways, both of which are frequently deregulated in human

cancers. mTOR hyperactivation has been reported in several cancers with oncogenic Ras activation (LoVo cells KRAS mutated), and mTORC1 activity has been shown to be required for Ras-mediated proliferation and transformation (Carrière et al., 2008). Although the molecular mechanisms underlying mTOR hyperactivation in cancer cells remain unknown, the constitutive Raptor phosphorylation observed in cells expressing oncogenic forms of Ras and MEK suggests that MAPK inhibition may offer an alternative strategy for treating patients with activating mutations in the Ras/MAPK pathway. Moreover, the use of a combination of MAPK and mTORC1 inhibitors in the treatment of cancer with KRAS mutations might improve the efficacy of each compound alone. Finally, our findings raise significant concerns about the use of RPS6 phospho- antibodies as biomarkers for mTOR/PI3K pathway activation when staining tissue samples from tumor biopsies, as is a common practice (Roux et al., 2007). Although phosphorylation of RPS6 is primarily regulated via mTOR/PI3K/S6K signaling, tumors with mutated KRAS and BRAF may mediate the activation of Ser235/236 even in the absence of mTOR signaling. Such information could lead to an incorrect conclusion about the involvement of specific signaling pathways in tumorigenesis. Targeted therapies in the future may rely on specific biomarkers such as p-ERK1/2 or p-RSK to reflect Ras/Raf activation and RPS6 phospho-Ser240/244 antibodies to reflect PI3K/mTOR activation. Furthermore, the use of mTOR inhibitors in the treatment of the disease may result in the development of mTOR inhibitor-resistant cancers due to compensatory mechanisms by the Ras/Raf pathway. In these circumstances, inhibitors of the MAPK pathway will be therapeutically useful. Given the additional roles of ERK1/2 in cell survival and drug resistance, ERK1/2 or MEK inhibitors may be beneficial for the treatment of cancers with mTOR activation.

Although our findings are intriguing, several unanswered questions remain. Future experiments that can be carried out to further substantiate the findings of this thesis include the following:

1- In order to understand how the mTOR and MAPK pathways cross-talk to modulate RPS6 activation to promote cell growth, survival, and chemoresistance, cell viability assays should be performed by using a combination of MAPK and mTORC1 inhibitors together with chemotherapeutic drugs used *in vivo* and *in vitro* models.
2- Mechanisms for the development of drug resistance such as the expression of efflux proteins need to be determined.
3- The ERK/MAPK signaling pathway is known to promote cell survival by regulating the activity of apoptotic proteins like BIM, PUMA, and BMF. In order to understand how ERK1/2 activation promotes cell survival in nutrient-restricted cells, apoptosis can be measured by evaluating the expression of pro and anti-apoptotic proteins, in addition to cell-based assays such as the Annexin V, Caspase, and TUNEL assays.
4- We suggest that the ERK/MAPK signaling pathway can regulate mTOR activity; however, the mechanism for this regulation is still unknown. Therefore, the key upstream regulatory mechanisms, which can impinge on mTOR regulators such as TSC2 or Raptor should be evaluated.
5- We did not observe any change in cell proliferation when ISR was inhibited with ISRIB in the nutrient-restricted or nutrient-rich cells. However, we are not confident of the efficacy of ISRIB since we did not observe any change in the activation (phosphorylation) of other markers of ISR such as p-PERK. Currently, there are no other commercially available inhibitors of ISR. Therefore, to establish whether ATF4 was activated via mTOR and/or ERK1/2 and not p-EIF2, we will carry out a stable shRNA mediated knockdown of ATF4. These cells will be treated with the mTOR inhibitor AZD8055, or the ERK1/2 inhibitor U0126 to determine any change in cell survival. Additionally, RNAseq followed by bioinformatic analysis can be used to interrogate the transcriptional responses downstream of ATF4 in these cells.

REFERENCES

Ahmadiankia, N. (2020). In vitro and in vivo studies of cancer cell behavior under nutrient deprivation. In *Cell Biology International* (Vol. 44, Issue 8, pp. 1588–1597). Wiley-Blackwell Publishing Ltd. https://doi.org/10.1002/cbin.11368

Ahmed, D., Eide, P. W., Eilertsen, I. A., Danielsen, S. A., Eknæs, M., Hektoen, M., Lind, G. E., & Lothe, R. A. (2013). Epigenetic and genetic features of 24 colon cancer cell lines. *Oncogenesis*, *2*. https://doi.org/10.1038/oncsis.2013.35

Alfarouk, K. O., Ahmed, S. B. M., Elliott, R. L., Benoit, A., Alqahtani, S. S., Ibrahim, M. E., Bashir, A. H. H., Alhoufie, S. T. S., Elhassan, G. O., Wales, C. C., Schwartz, L. H., Ali, H. S., Ahmed, A., Forde, P. F., Devesa, J., Cardone, R. A., Fais, S., Harguindey, S., & Reshkin, S. J. (2020). The Pentose Phosphate Pathway Dynamics in Cancer and Its Dependency on Intracellular pH. *Metabolites*, *10*(7), 1–16. https://doi.org/10.3390/METABO10070285

B'Chir, W., Maurin, A. C., Carraro, V., Averous, J., Jousse, C., Muranishi, Y., Parry, L., Stepien, G., Fafournoux, P., & Bruhat, A. (2013). The eIF2α/ATF4 pathway is essential for stress-induced autophagy gene expression. *Nucleic Acids Research*, *41*(16), 7683–7699. https://doi.org/10.1093/nar/gkt563

Böhm, J., Muenzner, J. K., Caliskan, A., Ndreshkjana, B., Erlenbach-Wünsch, K., Merkel, S., Croner, R., Rau, T. T., Geppert, C. I., Hartmann, A., Roehe, A. V., & Schneider-Stock, R. (2019). Loss of enhancer of zeste homologue 2 (EZH2) at tumor invasion front is correlated with higher aggressiveness in colorectal cancer cells. *Journal of Cancer Research and Clinical Oncology*, *145*(9), 2227–2240. https://doi.org/10.1007/s00432-019-02977-1

Boroughs, L. K., & Deberardinis, R. J. (2015). Metabolic pathways promoting cancer cell survival and growth. In *Nature Cell Biology* (Vol. 17, Issue 4, pp. 351–359). Nature Publishing Group. https://doi.org/10.1038/ncb3124

Bose, K., Chaudhari, P., Butler, A., Prebble, H., Moghiseh, M., Raja, A., & Anderson, A. (2019). Unravelling cancer signaling pathways: A multidisciplinary approach.

In *Unravelling Cancer Signaling Pathways: A Multidisciplinary Approach*. Springer Singapore. https://doi.org/10.1007/978-981-32-9816-3

Bose, S., Allen, A. E., & Locasale, J. W. (2020). The Molecular Link from Diet to Cancer Cell Metabolism. In *Molecular Cell* (Vol. 78, Issue 6, pp. 1034–1044). Cell Press. https://doi.org/10.1016/j.molcel.2020.05.018

Cabezudo, S., Sanz-Flores, M., Caballero, A., Tasset, I., Rebollo, E., Diaz, A., Aragay, A. M., Cuervo, A. M., Mayor, F., & Ribas, C. (2021). Gαq activation modulates autophagy by promoting mTORC1 signaling. *Nature Communications*, *12*(1). https://doi.org/10.1038/s41467-021-24811-4

Carling, D., Sanders, M. J., & Woods, A. (2008). The regulation of AMP-activated protein kinase by upstream kinases. In *International Journal of Obesity* (Vol. 32, pp. S55–S59). https://doi.org/10.1038/ijo.2008.124

Carracedo, A., Ma, L., Teruya-Feldstein, J., Rojo, F., Salmena, L., Alimonti, A., Egia, A., Sasaki, A. T., Thomas, G., Kozma, S. C., Papa, A., Nardella, C., Cantley, L. C., Baselga, J., & Pandolfi, P. P. (2008). Inhibition of mTORC1 leads to MAPK pathway activation through a PI3K-dependent feedback loop in human cancer. *Journal of Clinical Investigation*, *118*(9), 3065–3074. https://doi.org/10.1172/JCI34739

Carrière, A., Cargnello, M., Julien, L. A., Gao, H., Bonneil, É., Thibault, P., & Roux, P. P. (2008). Oncogenic MAPK Signaling Stimulates mTORC1 Activity by Promoting RSK-Mediated Raptor Phosphorylation. *Current Biology*, *18*(17), 1269–1277. https://doi.org/10.1016/j.cub.2008.07.078

Chao, X., Wang, S., Zhao, K., Li, Y., Williams, J. A., Li, T., Chavan, H., Krishnamurthy, P., He, X. C., Li, L., Ballabio, A., Ni, H.-M., & Ding, W.-X. (2018). Impaired TFEB-Mediated Lysosome Biogenesis and Autophagy Promote Chronic Ethanol-Induced Liver Injury and Steatosis in Mice. *Gastroenterology*, *155*(3), 865-879.e12. https://doi.org/https://doi.org/10.1053/j.gastro.2018.05.027

Chauvin, C., Koka, V., Nouschi, A., Mieulet, V., Hoareau-Aveilla, C., Dreazen, A., Cagnard, N., Carpentier, W., Kiss, T., Meyuhas, O., & Pende, M. (2014). Ribosomal protein S6 kinase activity controls the ribosome biogenesis transcriptional program. *Oncogene*, *33*(4), 474–483. https://doi.org/10.1038/onc.2012.606

Chen, B., Tan, Z., Gao, J., Wu, W., Liu, L., Jin, W., Cao, Y., Zhao, S., Zhang, W., Qiu, Z., Liu, D., Mo, X., & Li, W. (2015). Hyperphosphorylation of ribosomal protein S6 predicts unfavorable clinical survival in non-small cell lung cancer. *Journal of Experimental & Clinical Cancer Research : CR*, *34*, 126. https://doi.org/10.1186/s13046-015-0239-1

Chen, B., Zhang, W., Gao, J., Chen, H., Jiang, L., Liu, D., Cao, Y., Zhao, S., Qiu, Z., Zeng, J., Zhang, S., & Li, W. (2014). Downregulation of ribosomal protein S6 inhibits the growth of non-small cell lung cancer by inducing cell cycle arrest, rather than apoptosis. *Cancer Letters*, *354*(2), 378–389. https://doi.org/https://doi.org/10.1016/j.canlet.2014.08.045

Chen, D., Si, W., Shen, J., Du, C., Lou, W., Bao, C., Zheng, H., Pan, J., Zhong, G., Xu, L., Fu, P., & Fan, W. (2018). miR-27b-3p inhibits proliferation and potentially reverses multi-chemoresistance by targeting CBLB/GRB2 in breast cancer cells. *Cell Death & Disease*, *9*(2), 188. https://doi.org/10.1038/s41419-017-0211-4

Chen, J., Zhang, L., Zhou, H., Wang, W., Luo, Y., Yang, H., & Yi, H. (2018). Inhibition of autophagy promotes cisplatin-induced apoptotic cell death through Atg5 and Beclin 1 in A549 human lung cancer cells. *Molecular Medicine Reports*, *17*(5), 6859–6865. https://doi.org/10.3892/mmr.2018.8686

Chen, S., Fisher, R. C., Signs, S., Molina, L. A., Shenoy, A. K., Lopez, M.-C., Baker, H. v, Koomen, J. M., Chen, Y., Gittleman, H., Barnholtz-Sloan, J., Berg, A., Appelman, H. D., & Huang, E. H. (2016). Inhibition of PI3K/Akt/mTOR signaling in PI3KR2-overexpressing colon cancer stem cells reduces tumor growth due to

apoptosis. *Oncotarget*, *8*(31), 50476–50488. https://doi.org/10.18632/oncotarget.9919

Chen, Y., & Yu, L. (2017). Recent progress in autophagic lysosome reformation. In *Traffic* (Vol. 18, Issue 6, pp. 358–361). Blackwell Munksgaard. https://doi.org/10.1111/tra.12484

Chu, H. S., Peterson, C., Jun, A., & Foster, J. (2021). Targeting the integrated stress response in ophthalmology. In *Current Eye Research* (Vol. 46, Issue 8, pp. 1075–1088). Taylor and Francis Ltd. https://doi.org/10.1080/02713683.2020.1867748

Ciechomska, I. A., Goemans, G. C., Skepper, J. N., & Tolkovsky, A. M. (2009). Bcl-2 complexed with Beclin-1 maintains full anti-apoptotic function. *Oncogene*, *28*(21), 2128–2141. https://doi.org/10.1038/onc.2009.60

Conacci-Sorrell, M., Ngouenet, C., Anderson, S., Brabletz, T., & Eisenman, R. N. (2014). Stress-induced cleavage of Myc promotes cancer cell survival. *Genes & Development*, *28*(7), 689–707. https://doi.org/10.1101/GAD.231894.113

Condon, K. J., & Sabatini, D. M. (2019). Nutrient regulation of mTORC1 at a glance. *Journal of Cell Science*, *132*(21). https://doi.org/10.1242/JCS.222570

Darling, N. J., & Cook, S. J. (2014). The role of MAPK signalling pathways in the response to endoplasmic reticulum stress. In *Biochimica et Biophysica Acta - Molecular Cell Research* (Vol. 1843, Issue 10, pp. 2150–2163). Elsevier. https://doi.org/10.1016/j.bbamcr.2014.01.009

de Berardinis, R. J., & Chandel, N. S. (2016). Fundamentals of cancer metabolism. In *Science Advances* (Vol. 2, Issue 5). American Association for the Advancement of Science. https://doi.org/10.1126/sciadv.1600200

de la Cruz López, K. G., Guzmán, M. E. T., Sánchez, E. O., & Carrancá, A. G. (2019). mTORC1 as a Regulator of Mitochondrial Functions and a Therapeutic Target in Cancer. *Frontiers in Oncology*, *9*, 1373. https://doi.org/10.3389/FONC.2019.01373/BIBTEX

de Marval, P. L. M., Kim, S. H., & Rodriguez-Puebla, M. L. (2013). *Isolation and Characterization of a Stem Cell Side-Population from Mouse Hair Follicles* (pp. 259–268). https://doi.org/10.1007/7651_2013_61

DeBerardinis, C. T. H. A. N. D. A. T. W. A. N. D. R. J. (2013). Glutamine and cancer: cell biology, physiology, and clinical opportunities. *The Journal of Clinical Investigation*, *123*(9), 3678–3684. https://doi.org/10.1172/JCI69600

Dhillon, A. S., Hagan, S., Rath, O., & Kolch, W. (2007). MAP kinase signalling pathways in cancer. In *Oncogene* (Vol. 26, Issue 22, pp. 3279–3290). https://doi.org/10.1038/sj.onc.1210421

Ding, S., Li, C., Cheng, N., Cui, X., Xu, X., & Zhou, G. (2015). Redox Regulation in Cancer Stem Cells. *Oxidative Medicine and Cellular Longevity*, *2015*, 750798. https://doi.org/10.1155/2015/750798

Dufour, M., Dormond-Meuwly, A., Demartines, N., & Dormond, O. (2011). Targeting the mammalian target of rapamycin (mTOR) in cancer therapy: Lessons from past and future perspectives. In *Cancers* (Vol. 3, Issue 2, pp. 2478–2500). https://doi.org/10.3390/cancers3022478

Duran, A., Linares, J. F., Galvez, A. S., Wikenheiser, K., Flores, J. M., Diaz-Meco, M. T., & Moscat, J. (2008). The Signaling Adaptor p62 Is an Important NF-κB Mediator in Tumorigenesis. *Cancer Cell*, *13*(4), 343–354. https://doi.org/https://doi.org/10.1016/j.ccr.2008.02.001

Forbes, S. A., Bindal, N., Bamford, S., Cole, C., Kok, C. Y., Beare, D., Jia, M., Shepherd, R., Leung, K., Menzies, A., Teague, J. W., Campbell, P. J., Stratton, M. R., & Futreal, P. A. (2011). COSMIC: mining complete cancer genomes in the Catalogue of Somatic Mutations in Cancer. *Nucleic Acids Research*, *39*(Database issue), D945–D950. https://doi.org/10.1093/nar/gkq929

Fumagalli, S., di Cara, A., Neb-Gulati, A., Natt, F., Schwemberger, S., Hall, J., Babcock, G. F., Bernardi, R., Pandolfi, P. P., & Thomas, G. (2009). Absence of nucleolar disruption after impairment of 40S ribosome biogenesis reveals an

rpL11-translation-dependent mechanism of p53 induction. *Nature Cell Biology*, *11*(4), 501–508. https://doi.org/10.1038/ncb1858

Galluzzi, L., Vitale, I., Michels, J., Brenner, C., Szabadkai, G., Harel-Bellan, A., Castedo, M., & Kroemer, G. (2014). Systems biology of cisplatin resistance: Past, present and future. In *Cell Death and Disease* (Vol. 5). Nature Publishing Group. https://doi.org/10.1038/cddis.2013.428

Gambardella, V., Gimeno-Valiente, F., Tarazona, N., Ciarpaglini, C. M., Roda, D., Fleitas, T., Tolosa, P., Cejalvo, J. M., Huerta, M., Roselló, S., Castillo, J., & Cervantes, A. (2019). NRF2 through RPS6 Activation Is Related to Anti-HER2 Drug Resistance in HER2-Amplified Gastric Cancer. *Clinical Cancer Research*, *25*(5), 1639–1649. https://doi.org/10.1158/1078-0432.CCR-18-2421

González, A., Hall, M. N., Lin, S. C., & Hardie, D. G. (2020). AMPK and TOR: The Yin and Yang of Cellular Nutrient Sensing and Growth Control. *Cell Metabolism*, *31*(3), 472–492. https://doi.org/10.1016/J.CMET.2020.01.015

Guha, S., Coffey, E. E., Lu, W., Lim, J. C., Beckel, J. M., Laties, A. M., Boesze-Battaglia, K., & Mitchell, C. H. (2014). Approaches for detecting lysosomal alkalinization and impaired degradation in fresh and cultured RPE cells: evidence for a role in retinal degenerations. *Experimental Eye Research*, *126*, 68–76. https://doi.org/10.1016/j.exer.2014.05.013

Guo, B., Li, D., Du, L., & Zhu, X. (2020). piRNAs: biogenesis and their potential roles in cancer. *Cancer and Metastasis Reviews*, *39*(2), 567–575. https://doi.org/10.1007/s10555-020-09863-0

Guo, B., Tam, A., Santi, S. A., & Parissenti, A. M. (2016). Role of autophagy and lysosomal drug sequestration in acquired resistance to doxorubicin in MCF-7 cells. *BMC Cancer*, *16*(1). https://doi.org/10.1186/s12885-016-2790-3

Guo, Y., Pan, W., Liu, S., Shen, Z., Xu, Y., & Hu, L. (2020). ERK/MAPK signalling pathway and tumorigenesis (Review). *Experimental and Therapeutic Medicine*. https://doi.org/10.3892/etm.2020.8454

Hanahan, D., & Weinberg, R. A. (2011). Hallmarks of cancer: The next generation. In *Cell* (Vol. 144, Issue 5, pp. 646–674). https://doi.org/10.1016/j.cell.2011.02.013

Harisha Rajanala, S., Ringquist, R., & Cryns, V. L. (2019). Methionine restriction activates the integrated stress response in triple-negative breast cancer cells by a GCN2-and PERK-independent mechanism. In *Am J Cancer Res* (Vol. 9, Issue 8). www.ajcr.us/

Hernandez, G. A., & Perera, R. M. (2022). Autophagy in cancer cell remodeling and quality control. In *Molecular Cell* (Vol. 82, Issue 8, pp. 1514–1527). Cell Press. https://doi.org/10.1016/j.molcel.2022.03.023

Hraběta, J., Belhajová, M., Šubrtová, H., Rodrigo, M. A. M., Heger, Z., & Eckschlager, T. (2020). Drug sequestration in lysosomes as one of the mechanisms of chemoresistance of cancer cells and the possibilities of its inhibition. In *International Journal of Molecular Sciences* (Vol. 21, Issue 12, pp. 1–18). MDPI AG. https://doi.org/10.3390/ijms21124392

Hsieh, A. C., Liu, Y., Edlind, M. P., Ingolia, N. T., Janes, M. R., Sher, A., Shi, E. Y., Stumpf, C. R., Christensen, C., Bonham, M. J., Wang, S., Ren, P., Martin, M., Jessen, K., Feldman, M. E., Weissman, J. S., Shokat, K. M., Rommel, C., & Ruggero, D. (2012). The translational landscape of mTOR signalling steers cancer initiation and metastasis. *Nature*, *485*(7396), 55–61. https://doi.org/10.1038/nature10912

Hu, Y. L., Yin, Y., Liu, H. Y., Feng, Y. Y., Bian, Z. H., Zhou, L. Y., Zhang, J. W., Fei, B. J., Wang, Y. G., & Huang, Z. H. (2016). Glucose deprivation induces chemoresistance in colorectal cancer cells by increasing ATF4 expression. *World Journal of Gastroenterology*, *22*(27), 6235–6245. https://doi.org/10.3748/wjg.v22.i27.6235

Inoki, K., Kim, J., & Guan, K.-L. (2012). AMPK and mTOR in Cellular Energy Homeostasis and Drug Targets. *Annual Review of Pharmacology and Toxicology*, *52*(1), 381–400. https://doi.org/10.1146/annurev-pharmtox-010611-134537

Jeon, Y.-J., Kim, I. K., Hong, S.-H., Nan, H., Kim, H.-J., Lee, H.-J., Masuda, E. S., Meyuhas, O., Oh, B.-H., & Jung, Y.-K. (2008). Ribosomal protein S6 is a selective mediator of TRAIL-apoptotic signaling. *Oncogene*, *27*(31), 4344–4352. https://doi.org/10.1038/onc.2008.73

Johnson, D. E., Ostrowski, P., Jaumouillé, V., & Grinstein, S. (2016). The position of lysosomes within the cell determines their luminal pH. *Journal of Cell Biology*, *212*(6), 677–692. https://doi.org/10.1083/jcb.201507112

Juhász, G. (2012). Interpretation of bafilomycin, pH neutralizing or protease inhibitor treatments in autophagic flux experiments: Novel considerations. In *Autophagy* (Vol. 8, Issue 12, pp. 1875–1876). Taylor and Francis Inc. https://doi.org/10.4161/auto.21544

Kanarek, N., Petrova, B., & Sabatini, D. M. (2020). Dietary modifications for enhanced cancer therapy. *Nature*, *579*(7800), 507–517. https://doi.org/10.1038/s41586-020-2124-0

Kang, R., Zeh, H. J., Lotze, M. T., & Tang, D. (2011). The Beclin 1 network regulates autophagy and apoptosis. In *Cell Death and Differentiation* (Vol. 18, Issue 4, pp. 571–580). https://doi.org/10.1038/cdd.2010.191

Kazemi, S., Mounir, Z., Baltzis, D., Raven, J. F., Wang, S., Krishnamoorthy, J.-L., Pluquet, O., Pelletier, J., & Koromilas, A. E. (2007). A novel function of eIF2alpha kinases as inducers of the phosphoinositide-3 kinase signaling pathway. *Molecular Biology of the Cell*, *18*(9), 3635–3644. https://doi.org/10.1091/mbc.e07-01-0053

Khalaileh, A., Dreazen, A., Khatib, A., Apel, R., Swisa, A., Kidess-Bassir, N., Maitra, A., Meyuhas, O., Dor, Y., & Zamir, G. (2013). Phosphorylation of Ribosomal Protein S6 Attenuates DNA Damage and Tumor Suppression during Development of Pancreatic Cancer. *Cancer Research*, *73*(6), 1811–1820. https://doi.org/10.1158/0008-5472.CAN-12-2014

Kim, J., & Guan, K.-L. (2019). mTOR as a central hub of nutrient signalling and cell growth. *Nature Cell Biology*, *21*(1), 63–71. https://doi.org/10.1038/s41556-018-0205-1

Kim, J., Kundu, M., Viollet, B., & Guan, K. L. (2011). AMPK and mTOR regulate autophagy through direct phosphorylation of Ulk1. *Nature Cell Biology*, *13*(2), 132–141. https://doi.org/10.1038/ncb2152

Kim, J., Yang, G., Kim, Y., Kim, J., & Ha, J. (2016). AMPK activators: mechanisms of action and physiological activities. *Experimental & Molecular Medicine*, *48*(4). https://doi.org/10.1038/EMM.2016.16

Klionsky, D. J., Abdelmohsen, K., Abe, A., Abedin, M. J., Abeliovich, H., Acevedo Arozena, A., Adachi, H., Adams, C. M., Adams, P. D., Adeli, K., Adhihetty, P. J., Adler, S. G., Agam, G., Agarwal, R., Aghi, M. K., Agnello, M., Agostinis, P., Aguilar, P. v, Aguirre-Ghiso, J., … Zughaier, S. M. (2016). Guidelines for the use and interpretation of assays for monitoring autophagy (3rd edition). *Autophagy*, *12*(1), 1–222. https://doi.org/10.1080/15548627.2015.1100356

Kocaturk, N. M., Akkoc, Y., Kig, C., Bayraktar, O., Gozuacik, D., & Kutlu, O. (2019). Autophagy as a molecular target for cancer treatment. *European Journal of Pharmaceutical Sciences*, *134*, 116–137. https://doi.org/https://doi.org/10.1016/j.ejps.2019.04.011

Korennykh, A., & Walter, P. (2012). Structural Basis of the Unfolded Protein Response. *Annual Review of Cell and Developmental Biology*, *28*(1), 251–277. https://doi.org/10.1146/annurev-cellbio-101011-155826

Langan, T. J., Rodgers, K. R., & Chou, R. C. (2016). Synchronization of mammalian cell cultures by serum deprivation. In *Methods in Molecular Biology* (Vol. 1524, pp. 97–105). Humana Press Inc. https://doi.org/10.1007/978-1-4939-6603-5_6

Lee, S.-H., Jung, Y.-S., Chung, J.-Y., Oh, A. Y., Lee, S.-J., Choi, D. H., Jang, S. M., Jang, K.-S., Paik, S. S., Ha, N.-C., & Park, B.-J. (2011). Novel tumor suppressive function of Smad4 in serum starvation-induced cell death through PAK1–PUMA

pathway. *Cell Death & Disease*, *2*(12), e235–e235. https://doi.org/10.1038/cddis.2011.116

Levine, B., & Kroemer, G. (2019). Biological Functions of Autophagy Genes: A Disease Perspective. *Cell*, *176*(1–2), 11–42. https://doi.org/10.1016/J.CELL.2018.09.048

Levy, J. M. M., Towers, C. G., & Thorburn, A. (2017). Targeting autophagy in cancer. *Nature Reviews. Cancer*, *17*(9), 528–542. https://doi.org/10.1038/NRC.2017.53

Li, S., Tian, J., Zhang, H., Zhou, S., Wang, X., Zhang, L., Yang, J., Zhang, Z., & Ji, Z. (2018). Down-regulating IL-6/GP130 targets improved the anti-tumor effects of 5-fluorouracil in colon cancer. *Apoptosis*, *23*(5), 356–374. https://doi.org/10.1007/s10495-018-1460-0

Lin, J. F., Lin, Y. C., Tsai, T. F., Chen, H. E., Chou, K. Y., & Hwang, T. I. S. (2017). Cisplatin induces protective autophagy through activation of BECN1 in human bladder cancer cells. *Drug Design, Development and Therapy*, *11*, 1517–1533. https://doi.org/10.2147/DDDT.S126464

Liu, E. Y., & Ryan, K. M. (n.d.). Autophagy and cancer-issues we need to digest. *Journal of Cell Science*, *125*, 1–10. https://doi.org/10.1242/jcs.093708

Liu, E. Y., & Ryan, K. M. (2012). Autophagy and cancer – issues we need to digest. *Journal of Cell Science*, *125*(10), 2349–2358. https://doi.org/10.1242/jcs.093708

Liu, T., Zhang, J., Li, K., Deng, L., & Wang, H. (2020). Combination of an Autophagy Inducer and an Autophagy Inhibitor: A Smarter Strategy Emerging in Cancer Therapy. In *Frontiers in Pharmacology* (Vol. 11). Frontiers Media S.A. https://doi.org/10.3389/fphar.2020.00408

Lőrincz, P., & Juhász, G. (2020). Autophagosome-Lysosome Fusion. In *Journal of Molecular Biology* (Vol. 432, Issue 8, pp. 2462–2482). Academic Press. https://doi.org/10.1016/j.jmb.2019.10.028

Lu, T., Zhu, Z., Wu, J., She, H., Han, R., Xu, H., & Qin, Z.-H. (2019). DRAM1 regulates autophagy and cell proliferation via inhibition of the phosphoinositide 3-kinase-Akt-mTOR-ribosomal protein S6 pathway. *Cell Communication and Signaling : CCS*, *17*(1), 28. https://doi.org/10.1186/s12964-019-0341-7

Lu, Z., Shi, X., Gong, F., Li, S., Wang, Y., Ren, Y., Zhang, M., Yu, B., Li, Y., Zhao, W., Zhang, J., & Hou, G. (2020). RICTOR/mTORC2 affects tumorigenesis and therapeutic efficacy of mTOR inhibitors in esophageal squamous cell carcinoma. *Acta Pharmaceutica Sinica B*, *10*(6), 1004–1019. https://doi.org/10.1016/j.apsb.2020.01.010

Lunt, S. Y., & vander Heiden, M. G. (2011). Aerobic glycolysis: Meeting the metabolic requirements of cell proliferation. *Annual Review of Cell and Developmental Biology*, *27*, 441–464. https://doi.org/10.1146/annurev-cellbio-092910-154237

Ma, J., Zeng, S., Zhang, Y., Deng, G., Qu, Y., Guo, C., Yin, L., Han, Y., Cai, C., Li, Y., Wang, G., Bonkovsky, H. L., & Shen, H. (2017). BMP4 promotes oxaliplatin resistance by an induction of epithelial-mesenchymal transition via MEK1/ERK/ELK1 signaling in hepatocellular carcinoma. *Cancer Letters*, *411*, 117–129. https://doi.org/https://doi.org/10.1016/j.canlet.2017.09.041

Ma, L., Chen, Z., Erdjument-Bromage, H., Tempst, P., & Pandolfi, P. P. (2005). Phosphorylation and Functional Inactivation of TSC2 by Erk: Implications for Tuberous Sclerosisand Cancer Pathogenesis. *Cell*, *121*(2), 179–193. https://doi.org/10.1016/J.CELL.2005.02.031

Maiuri, M. C., Zalckvar, E., Kimchi, A., & Kroemer, G. (2007). Self-eating and self-killing: crosstalk between autophagy and apoptosis. *Nature Reviews Molecular Cell Biology*, *8*(9), 741–752. https://doi.org/10.1038/nrm2239

Mani, J., Vallo, S., Rakel, S., Antonietti, P., Gessler, F., Blaheta, R., Bartsch, G., Michaelis, M., Cinatl, J., Haferkamp, A., & Kögel, D. (2015). Chemoresistance is associated with increased cytoprotective autophagy and diminished apoptosis in

bladder cancer cells treated with the BH3 mimetic (-)-Gossypol (AT-101). *BMC Cancer*, *15*, 224. https://doi.org/10.1186/s12885-015-1239-4

Martina, J. A., Chen, Y., Gucek, M., & Puertollano, R. (2012). MTORC1 functions as a transcriptional regulator of autophagy by preventing nuclear transport of TFEB. *Autophagy*, *8*(6), 903–914. https://doi.org/10.4161/auto.19653

Mauvezin, C., Nagy, P., Juhász, G., & Neufeld, T. P. (2015). Autophagosome-lysosome fusion is independent of V-ATPase-mediated acidification. *Nature Communications*, *6*. https://doi.org/10.1038/ncomms8007

McConkey, D. J. (2017). The integrated stress response and proteotoxicity in cancer therapy. *Biochemical and Biophysical Research Communications*, *482*(3), 450–453. https://doi.org/10.1016/j.bbrc.2016.11.047

McCubrey, J. A., Steelman, L. S., Chappell, W. H., Abrams, S. L., Wong, E. W. T., Chang, F., Lehmann, B., Terrian, D. M., Milella, M., Tafuri, A., Stivala, F., Libra, M., Basecke, J., Evangelisti, C., Martelli, A. M., & Franklin, R. A. (2007). Roles of the Raf/MEK/ERK pathway in cell growth, malignant transformation and drug resistance. In *Biochimica et Biophysica Acta - Molecular Cell Research* (Vol. 1773, Issue 8, pp. 1263–1284). https://doi.org/10.1016/j.bbamcr.2006.10.001

Miyazaki, M., & Takemasa, T. (2017). TSC2/Rheb signaling mediates ERK-dependent regulation of mTORC1 activity in C2C12 myoblasts. *FEBS Open Bio*, *7*(3), 424–433. https://doi.org/10.1002/2211-5463.12195

Miyo, M., Konno, M., Nishida, N., Sueda, T., Noguchi, K., Matsui, H., Colvin, H., Kawamoto, K., Koseki, J., Haraguchi, N., Nishimura, J., Hata, T., Gotoh, N., Matsuda, F., Satoh, T., Mizushima, T., Shimizu, H., Doki, Y., Mori, M., & Ishii, H. (2016). Metabolic Adaptation to Nutritional Stress in Human Colorectal Cancer. *Scientific Reports*, *6*. https://doi.org/10.1038/srep38415

Mok, K. W., Mruk, D. D., & Cheng, C. Y. (2013). Regulation of Blood–Testis Barrier (BTB) Dynamics during Spermatogenesis via the “Yin” and “Yang” Effects of Mammalian Target of Rapamycin Complex 1 (mTORC1) and mTORC2.

International Review of Cell and Molecular Biology, *301*, 291–358. https://doi.org/10.1016/B978-0-12-407704-1.00006-3

Mossmann, D., Park, S., & Hall, M. N. (2018). mTOR signalling and cellular metabolism are mutual determinants in cancer. *Nature Reviews Cancer*, *18*(12), 744–757. https://doi.org/10.1038/s41568-018-0074-8

Muir, A., & vander Heiden, M. G. (2018). The nutrient environment affects therapy. *Science*, *360*(6392), 962–963. https://doi.org/10.1126/science.aar5986

Mukhopadhyay, N. K., Price, D. J., Kyriakis, J. M., Pelech, S., Sanghera, J., & Avruch, J. (1992). An array of insulin-activated, proline-directed serine/threonine protein kinases phosphorylate the p70 S6 kinase. *Journal of Biological Chemistry*, *267*(5), 3325–3335. https://doi.org/10.1016/s0021-9258(19)50735-9

Mutvei, A. P., Nagiec, M. J., Hamann, J. C., Kim, S. G., Vincent, C. T., & Blenis, J. (2020). Rap1-GTPases control mTORC1 activity by coordinating lysosome organization with amino acid availability. *Nature Communications*, *11*(1). https://doi.org/10.1038/s41467-020-15156-5

Nakashima, A., & Tamanoi, F. (2010). Conservation of the Tsc/Rheb/TORC1/S6K/S6 Signaling in Fission Yeast. *Enzymes*, *28*(C), 167–187. https://doi.org/10.1016/S1874-6047(10)28008-3

Napolitano, G., di Malta, C., & Ballabio, A. (2022). Non-canonical mTORC1 signaling at the lysosome. In *Trends in Cell Biology* (Vol. 32, Issue 11, pp. 920–931). Elsevier Ltd. https://doi.org/10.1016/j.tcb.2022.04.012

Napolitano, G., Esposito, A., Choi, H., Matarese, M., Benedetti, V., di Malta, C., Monfregola, J., Medina, D. L., Lippincott-Schwartz, J., & Ballabio, A. (2018a). mTOR-dependent phosphorylation controls TFEB nuclear export. *Nature Communications*, *9*(1), 3312. https://doi.org/10.1038/s41467-018-05862-6

Napolitano, G., Esposito, A., Choi, H., Matarese, M., Benedetti, V., di Malta, C., Monfregola, J., Medina, D. L., Lippincott-Schwartz, J., & Ballabio, A. (2018b).

mTOR-dependent phosphorylation controls TFEB nuclear export. *Nature Communications*, *9*(1). https://doi.org/10.1038/s41467-018-05862-6

Naveed, S., Aslam, M., & Ahmad, A. (2014). Starvation based differential chemotherapy: A novel approach for cancer treatment. *Oman Medical Journal*, *29*(6), 391–398. https://doi.org/10.5001/OMJ.2014.107

Newton, P. T., Vuppalapati, K. K., Bouderlique, T., & Chagin, A. S. (2015). Pharmacological inhibition of lysosomes activates the MTORC1 signaling pathway in chondrocytes in an autophagy-independent manner. *Autophagy*, *11*(9), 1594–1607. https://doi.org/10.1080/15548627.2015.1068489

Nguyen, T. L., & Durán, R. v. (2018). Glutamine metabolism in cancer therapy. In *Cancer Drug Resistance* (Vol. 1, Issue 3, pp. 126–138). OAE Publishing Inc. https://doi.org/10.20517/cdr.2018.08

Ohshima, K., & Morii, E. (2021). Metabolic Reprogramming of Cancer Cells during Tumor Progression and Metastasis. *Metabolites*, *11*(1), 1–23. https://doi.org/10.3390/METABO11010028

Ojha, R., Bhattacharyya, S., & Singh, S. K. (2015). Autophagy in Cancer Stem Cells: A Potential Link Between Chemoresistance, Recurrence, and Metastasis. *BioResearch Open Access*, *4*(1), 97–108. https://doi.org/10.1089/biores.2014.0035

Pakos-Zebrucka, K., Koryga, I., Mnich, K., Ljujic, M., Samali, A., & Gorman, A. M. (2016). The integrated stress response. *EMBO Reports*, *17*(10), 1374–1395. https://doi.org/10.15252/embr.201642195

Palam, L. R., Gore, J., Craven, K. E., Wilson, J. L., & Korc, M. (2015). Integrated stress response is critical for gemcitabine resistance in pancreatic ductal adenocarcinoma. *Cell Death & Disease*, *6*(10), e1913–e1913. https://doi.org/10.1038/cddis.2015.264

Palm, W., & Thompson, C. B. (2017). Nutrient acquisition strategies of mammalian cells. *Nature*, *546*(7657), 234–242. https://doi.org/10.1038/nature22379

Palmieri, M., Impey, S., Kang, H., di Ronza, A., Pelz, C., Sardiello, M., & Ballabio, A. (2011). Characterization of the CLEAR network reveals an integrated control of cellular clearance pathways. *Human Molecular Genetics*, *20*(19), 3852–3866. https://doi.org/10.1093/hmg/ddr306

Panić, L., Tamarut, S., Sticker-Jantscheff, M., Barkić, M., Solter, D., Uzelac, M., Grabušić, K., & Volarević, S. (2006). Ribosomal Protein S6 Gene Haploinsufficiency Is Associated with Activation of a p53-Dependent Checkpoint during Gastrulation . *Molecular and Cellular Biology*, *26*(23), 8880–8891. https://doi.org/10.1128/MCB.00751-06/SUPPL_FILE/TABLES_S1_S2.ZIP

Park, Y., Reyna-Neyra, A., Philippe, L., & Thoreen, C. C. (2017). mTORC1 Balances Cellular Amino Acid Supply with Demand for Protein Synthesis through Post-transcriptional Control of ATF4. *Cell Reports*, *19*(6), 1083–1090. https://doi.org/10.1016/j.celrep.2017.04.042

Pattingre, S., Tassa, A., Qu, X., Garuti, R., Xiao, H. L., Mizushima, N., Packer, M., Schneider, M. D., & Levine, B. (2005). Bcl-2 antiapoptotic proteins inhibit Beclin 1-dependent autophagy. *Cell*, *122*(6), 927–939. https://doi.org/10.1016/J.CELL.2005.07.002

Pavitt, G. D. (2013). Less translational control, more memory. *ELife*, *2013*(2). https://doi.org/10.7554/eLife.00895

Pavlova, N. N., & Thompson, C. B. (2016). The Emerging Hallmarks of Cancer Metabolism. In *Cell Metabolism* (Vol. 23, Issue 1, pp. 27–47). Cell Press. https://doi.org/10.1016/j.cmet.2015.12.006

Pedersen, A. K., Mendes Lopes de Melo, J., Mørup, N., Tritsaris, K., & Pedersen, S. F. (2017). Tumor microenvironment conditions alter Akt and Na(+)/H(+) exchanger NHE1 expression in endothelial cells more than hypoxia alone: implications for endothelial cell function in cancer. *BMC Cancer*, *17*(1), 542. https://doi.org/10.1186/s12885-017-3532-x

Penning, T. M. (2017). Aldo-Keto Reductase Regulation by the Nrf2 System: Implications for Stress Response, Chemotherapy Drug Resistance, and Carcinogenesis. *Chemical Research in Toxicology*, *30*(1), 162–176. https://doi.org/10.1021/acs.chemrestox.6b00319

Polyak, K., Lee, M. H., Erdjument-Bromage, H., Koff, A., Roberts, J. M., Tempst, P., & Massagué, J. (1994). Cloning of p27Kip1, a cyclin-dependent kinase inhibitor and a potential mediator of extracellular antimitogenic signals. *Cell*, *78*(1), 59–66. https://doi.org/10.1016/0092-8674(94)90572-X

Porporato, P. E., Domenicotti, C., Chiarugi, P., Cirri, P., Comito, G., & Ippolito, L. (2020). Nutritional Exchanges Within Tumor Microenvironment: Impact for Cancer Aggressiveness. *Frontiers in Oncology | Www.Frontiersin.Org*, *1*, 396. https://doi.org/10.3389/fonc.2020.00396

Poüs, C., & Codogno, P. (2011). Lysosome positioning coordinates mTORC1 activity and autophagy. *Nature Cell Biology*, *13*(4), 342–344. https://doi.org/10.1038/ncb0411-342

Proud, C. G., & Xie, J. (2021). Regulation: mTOR and its substrates. *Encyclopedia of Biological Chemistry: Third Edition*, *1*, 614–630. https://doi.org/10.1016/B978-0-12-819460-7.00001-3

Puertollano, R. (2014). mTOR and lysosome regulation. *F1000Prime Reports*, *6*. https://doi.org/10.12703/P6-52

Puertollano, R., Ferguson, S. M., Brugarolas, J., & Ballabio, A. (2018). The complex relationship between TFEB transcription factor phosphorylation and subcellular localization . *The EMBO Journal*, *37*(11). https://doi.org/10.15252/embj.201798804

Puissant, A., Robert, G., Fenouille, N., Luciano, F., Cassuto, J.-P., Raynaud, S., & Auberger, P. (2010). Resveratrol Promotes Autophagic Cell Death in Chronic Myelogenous Leukemia Cells via JNK-Mediated p62/SQSTM1 Expression and

AMPK Activation. *Cancer Research*, *70*(3), 1042–1052. https://doi.org/10.1158/0008-5472.CAN-09-3537

Qin, X., Jiang, B., & Zhang, Y. (2016). 4E-BP1, a multifactor regulated multifunctional protein. In *Cell Cycle* (Vol. 15, Issue 6, pp. 781–786). Taylor and Francis Inc. https://doi.org/10.1080/15384101.2016.1151581

Raben, N., & Puertollano, R. (2016). TFEB and TFE3: Linking Lysosomes to Cellular Adaptation to Stress. *Annual Review of Cell and Developmental Biology*, *32*, 255–278. https://doi.org/10.1146/annurev-cellbio-111315-125407

Rabouw, H. H., Langereis, M. A., Anand, A. A., Visser, L. J., de Groot, R. J., Walter, P., & van Kuppeveld, F. J. M. (2019). Small molecule ISRIB suppresses the integrated stress response within a defined window of activation. *Proceedings of the National Academy of Sciences of the United States of America*, *116*(6), 2097–2102. https://doi.org/10.1073/pnas.1815767116

Ravanan, P., Srikumar, I. F., & Talwar, P. (2017). Autophagy: The spotlight for cellular stress responses. *Life Sciences*, *188*, 53–67. https://doi.org/10.1016/J.LFS.2017.08.029

Roberts, P. J., & Der, C. J. (2007). Targeting the Raf-MEK-ERK mitogen-activated protein kinase cascade for the treatment of cancer. In *Oncogene* (Vol. 26, Issue 22, pp. 3291–3310). https://doi.org/10.1038/sj.onc.1210422

Robles-Flores, M., Moreno-Londoño, A. P., & Castañeda-Patlán, M. C. (2021). Signaling Pathways Involved in Nutrient Sensing Control in Cancer Stem Cells: An Overview. In *Frontiers in Endocrinology* (Vol. 12). Frontiers Media S.A. https://doi.org/10.3389/fendo.2021.627745

Roux, P. P., Shahbazian, D., Vu, H., Holz, M. K., Cohen, M. S., Taunton, J., Sonenberg, N., & Blenis, J. (2007). RAS/ERK signaling promotes site-specific ribosomal protein S6 phosphorylation via RSK and stimulates cap-dependent translation. *Journal of Biological Chemistry*, *282*(19), 14056–14064. https://doi.org/10.1074/jbc.M700906200

Salaroglio, I. C., Mungo, E., Gazzano, E., Kopecka, J., & Riganti, C. (2019). ERK is a pivotal player of chemo-immune-resistance in cancer. In *International Journal of Molecular Sciences* (Vol. 20, Issue 10). MDPI AG. https://doi.org/10.3390/ijms20102505

Sambuy, Y., Angelis, I. de, Ranaldi, G., Scarino, M. L., Stammati, A., & Zucco, F. (2005). The Caco-2 cell line as a model of the intestinal barrier: in£uence of cell and culture-related factors on Caco-2 cell functional characteristics. *Cell Biology and Toxicology*, *21*.

Sato, K., Tsuchihara, K., Fujii, S., Sugiyama, M., Goya, T., Atomi, Y., Ueno, T., Ochiai, A., & Esumi, H. (2007). Autophagy Is Activated in Colorectal Cancer Cells and Contributes to the Tolerance to Nutrient Deprivation. *Cancer Research*, *67*(20), 9677–9684. https://doi.org/10.1158/0008-5472.CAN-07-1462

Sela, Y., Li, J., Maheswaran, S., Norgard, R., Yuan, S., Hubbi, M., Doepner, M., Xu, J. P., Ho, E. S., Mesaros, C., Sheehan, C., Croley, G., Muir, A., Blair, I. A., Shalem, O., Dang, C. v., & Stanger, B. Z. (2022). Bcl-xL Enforces a Slow-Cycling State Necessary for Survival in the Nutrient-Deprived Microenvironment of Pancreatic Cancer. *Cancer Research*, *82*(10), 1890–1908. https://doi.org/10.1158/0008-5472.CAN-22-0431

Settembre, C., di Malta, C., Polito, V. A., Arencibia, M. G., Vetrini, F., Erdin, S., Erdin, S. U., Huynh, T., Medina, D., Colella, P., Sardiello, M., Rubinsztein, D. C., & Ballabio, A. (2011). TFEB links autophagy to lysosomal biogenesis. *Science*, *332*(6036), 1429–1433. https://doi.org/10.1126/science.1204592

Shackelford, D. B., & Shaw, R. J. (2009). The LKB1-AMPK pathway: metabolism and growth control in tumor suppression. *Nature Reviews. Cancer*, *9*(8), 563. https://doi.org/10.1038/NRC2676

Shi, H., Chen, S., Jin, H., Xu, C., Dong, G., Zhao, Q., Wang, W., Zhang, H., Lin, W., Zhang, J., Davidovic, L., Yao, L., & Fan, D. (2009). Downregulation of MSP58 inhibits growth of human colorectal cancer cells via regulation of the cyclin D1–

cyclin-dependent kinase 4–p21 pathway. *Cancer Science*, *100*(9), 1585–1590. https://doi.org/https://doi.org/10.1111/j.1349-7006.2009.01223.x

Shi, Y., Felley-Bosco, E., Marti, T. M., Orlowski, K., Pruschy, M., & Stahel, R. A. (2012). Starvation-induced activation of ATM/Chk2/p53 signaling sensitizes cancer cells to cisplatin. *BMC Cancer*, *12*(1), 571. https://doi.org/10.1186/1471-2407-12-571

Shi, Y., Hu, Y., Wang, Y., Ma, X., Tang, L., Tao, M., Qiu, A., Zhuang, S., & Liu, N. (2021). Blockade of Autophagy Prevents the Development and Progression of Peritoneal Fibrosis. *Frontiers in Pharmacology*, *12*. https://doi.org/10.3389/fphar.2021.724141

Simcox, J., & Lamming, D. W. (2022). The central moTOR of metabolism. *Developmental Cell*, *57*(6), 691–706. https://doi.org/10.1016/J.DEVCEL.2022.02.024

Stone, K. P., Ghosh, S., Kovalik, J. P., Orgeron, M., Wanders, D., Sims, L. C., & Gettys, T. W. (2021). The acute transcriptional responses to dietary methionine restriction are triggered by inhibition of ternary complex formation and linked to Erk1/2, mTOR, and ATF4. *Scientific Reports*, *11*(1). https://doi.org/10.1038/s41598-021-83380-0

Su, J., Liu, F., Xia, M., Xu, Y., Li, X., Kang, J., Li, Y., & Sun, L. (2015). p62 participates in the inhibition of NF-κB signaling and apoptosis induced by sulfasalazine in human glioma U251 cells. *Oncology Reports*, *34*(1), 235–243. https://doi.org/10.3892/or.2015.3944

Sulic, S., Panic, L., Barkic, M., Mercep, M., Uzelac, M., & Volarevic, S. (2005). Inactivation of S6 ribosomal protein gene in T lymphocytes activates a p53-dependent checkpoint response. *Genes & Development*, *19*(24), 3070–3082. https://doi.org/10.1101/gad.359305

Tameire, F., Verginadis, I. I., Leli, N. M., Polte, C., Conn, C. S., Ojha, R., Salas Salinas, C., Chinga, F., Monroy, Alexandra. M., Fu, W., Wang, P., Kossenkov, A., Ye, J.,

Amaravadi, R. K., Ignatova, Z., Fuchs, S. Y., Diehl, J. A., Ruggero, D., & Koumenis, C. (2019). ATF4 couples MYC-dependent translational activity to bioenergetic demands during tumour progression. *Nature Cell Biology*, *21*(7), 889–899. https://doi.org/10.1038/s41556-019-0347-9

Tang, Q., Gao, P., Arzberger, T., Höllerhage, M., Herms, J., Höglinger, G., & Koeglsperger, T. (2021). Alpha-Synuclein defects autophagy by impairing SNAP29-mediated autophagosome-lysosome fusion. *Cell Death and Disease*, *12*(10). https://doi.org/10.1038/s41419-021-04138-0

Thomas, M., Davis, T., Nell, T., Sishi, B., & Engelbrecht, A. M. (2020). Amino Acid Starvation Sensitizes Resistant Breast Cancer to Doxorubicin-Induced Cell Death. *Frontiers in Cell and Developmental Biology*, *8*, 1071. https://doi.org/10.3389/FCELL.2020.565915/BIBTEX

Tian, X., Zhang, S., Zhou, L., Seyhan, A. A., Hernandez Borrero, L., Zhang, Y., & El-Deiry, W. S. (2021). Targeting the Integrated Stress Response in Cancer Therapy. *Frontiers in Pharmacology*, *12*, 747837. https://doi.org/10.3389/fphar.2021.747837

Tong, J. H. M., Lung, R. W. M., Sin, F. M. C., Law, P. P. Y., Kang, W., Chan, A. W. H., Ma, B. B. Y., Mak, T. W. C., Ng, S. S. M., & To, K. F. (2014). Characterization of rare transforming KRAS mutations in sporadic colorectal cancer. *Cancer Biology and Therapy*, *15*(6), 768–776. https://doi.org/10.4161/cbt.28550

Torrence, M. E., Macarthur, M. R., Hosios, A. M., Valvezan, A. J., Asara, J. M., Mitchell, J. R., & Manning, B. D. (2021). The mtorc1-mediated activation of atf4 promotes protein and glutathione synthesis downstream of growth signals. *ELife*, *10*. https://doi.org/10.7554/eLife.63326

Vaziri-Gohar, A., Cassel, J., Mohammed, F. S., Zarei, M., Hue, J. J., Hajihassani, O., Graor, H. J., Srikanth, Y. V. v, Karim, S. A., Abbas, A., Prendergast, E., Chen, V., Katayama, E. S., Dukleska, K., Khokhar, I., Andren, A., Zhang, L., Wu, C., Erokwu, B., … Winter, J. M. (2022). Limited nutrient availability in the tumor

microenvironment renders pancreatic tumors sensitive to allosteric IDH1 inhibitors. *Nature Cancer*, *3*(7), 852–865. https://doi.org/10.1038/s43018-022-00393-y

Vinette, V., Placet, M., Arguin, G., & Gendron, F.-P. (2015). Multidrug Resistance-Associated Protein 2 Expression Is Upregulated by Adenosine 5'-Triphosphate in Colorectal Cancer Cells and Enhances Their Survival to Chemotherapeutic Drugs. *PloS One*, *10*(8), e0136080–e0136080. https://doi.org/10.1371/journal.pone.0136080

Wang, J., & Wu, G. S. (2014). Role of autophagy in cisplatin resistance in ovarian cancer cells. *Journal of Biological Chemistry*, *289*(24), 17163–17173. https://doi.org/10.1074/jbc.M114.558288

Wang, R., Wang, J., Hassan, A., Lee, C. H., Xie, X. S., & Li, X. (2021). Molecular basis of V-ATPase inhibition by bafilomycin A1. *Nature Communications*, *12*(1). https://doi.org/10.1038/s41467-021-22111-5

Wang, Y.-P., & Lei, Q.-Y. (2018). Metabolite sensing and signaling in cell metabolism. *Signal Transduction and Targeted Therapy*, *3*(1), 30. https://doi.org/10.1038/s41392-018-0024-7

White, E. Z., Pennant, N. M., Carter, J. R., Hawsawi, O., Odero-Marah, V., & Hinton, C. v. (2020). Serum deprivation initiates adaptation and survival to oxidative stress in prostate cancer cells. *Scientific Reports*, *10*(1), 12505. https://doi.org/10.1038/s41598-020-68668-x

Wortel, I. M. N., van der Meer, L. T., Kilberg, M. S., & van Leeuwen, F. N. (2017). Surviving Stress: Modulation of ATF4-Mediated Stress Responses in Normal and Malignant Cells. *Trends in Endocrinology and Metabolism: TEM*, *28*(11), 794–806. https://doi.org/10.1016/j.tem.2017.07.003

Wu, Y. C., Wu, W. K. K., Li, Y., Yu, L., Li, Z. J., Wong, C. C. M., Li, H. T., Sung, J. J. Y., & Cho, C. H. (2009). Inhibition of macroautophagy by bafilomycin A1 lowers proliferation and induces apoptosis in colon cancer cells. *Biochemical and*

Biophysical Research Communications, *382*(2), 451–456. https://doi.org/10.1016/j.bbrc.2009.03.051

Xie, Z., Xie, Y., Xu, Y., Zhou, H., Xu, W., & Dong, Q. (2014). Bafilomycin A1 inhibits autophagy and induces apoptosis in MG63 osteosarcoma cells. *Molecular Medicine Reports*, *10*(2), 1103–1107. https://doi.org/10.3892/mmr.2014.2281

Xu, M., Chen, S., Yang, W., Cheng, X., Ye, Y., Mao, J., Wu, X., Huang, L., & Ji, J. (2018). FGFR4 Links Glucose Metabolism and Chemotherapy Resistance in Breast Cancer. *Cellular Physiology and Biochemistry*, *47*(1), 151–160. https://doi.org/10.1159/000489759

Yakisich, J. S., Venkatadri, R., Azad, N., & Iyer, A. K. v. (2017). Chemoresistance of Lung and Breast Cancer Cells Growing Under Prolonged Periods of Serum Starvation. *Journal of Cellular Physiology*, *232*(8), 2033–2043. https://doi.org/10.1002/JCP.25514

Ye, J., Palm, W., Peng, M., King, B., Lindsten, T., Li, M. O., Koumenis, C., & Thompson, C. B. (2015). GCN2 sustains mTORC1 suppression upon amino acid deprivation by inducing Sestrin2. *Genes & Development*, *29*(22), 2331–2336. https://doi.org/10.1101/gad.269324.115

Yi, Y. W., You, K. S., Park, J. S., Lee, S. G., & Seong, Y. S. (2022). Ribosomal protein S6: A potential therapeutic target against cancer? In *International Journal of Molecular Sciences* (Vol. 23, Issue 1). MDPI. https://doi.org/10.3390/ijms23010048

Young, L., Sung, J., Stacey, G., & Masters, J. R. (2010). Detection of Mycoplasma in cell cultures. *Nature Protocols*, *5*(5), 929–934. https://doi.org/10.1038/nprot.2010.43

Yu, L., McPhee, C. K., Zheng, L., Mardones, G. A., Rong, Y., Peng, J., Mi, N., Zhao, Y., Liu, Z., Wan, F., Hailey, D. W., Oorschot, V., Klumperman, J., Baehrecke, E. H., & Lenardo, M. J. (2010). Termination of autophagy and reformation of

lysosomes regulated by mTOR. *Nature*, *465*(7300), 942–946. https://doi.org/10.1038/nature09076

Zaffagnini, G., & Martens, S. (2016). Mechanisms of Selective Autophagy. *Journal of Molecular Biology*, *428*(9Part A), 1714. https://doi.org/10.1016/J.JMB.2016.02.004

Zhang, M., Peng, R., Haizhou, W., Yang, Z., Zhang, H., Zhang, Y., Wang, M., Wang, H., Lin, J., Zhao, Q., & Liu, J. (2022). Nanog mediated by FAO/ACLY signaling induces cellular dormancy in colorectal cancer cells. *Cell Death & Disease*, *13*, 159. https://doi.org/10.1038/s41419-022-04606-1

Zhang, Q., Cao, S., Qiu, F., & Kang, N. (2022). Incomplete autophagy: Trouble is a friend. In *Medicinal Research Reviews* (Vol. 42, Issue 4, pp. 1545–1587). John Wiley and Sons Inc. https://doi.org/10.1002/med.21884

Zhang, Y., Jia, Q. A., Kadel, D., Zhang, X. F., & Zhang, Q. B. (2018). Targeting mTORC1/2 complexes inhibit tumorigenesis and enhance sensitivity to 5-flourouracil (5-FU) in hepatocellular carcinoma: A preclinical study of mTORC1/2-targeted therapy in hepatocellular carcinoma (HCC). *Medical Science Monitor*, *24*, 2735–2743. https://doi.org/10.12659/MSM.907514

Zheng, H.-C. (2017). *The molecular mechanisms of chemoresistance in cancers* (Vol. 8, Issue 35). www.impactjournals.com/oncotarget

Zhu, J., & Thompson, C. B. (2019). Metabolic regulation of cell growth and proliferation. *Nature Reviews Molecular Cell Biology*, *20*(7), 436–450. https://doi.org/10.1038/s41580-019-0123-5

Zhuge, J., & Cederbaum, A. I. (2006). Serum deprivation-induced HepG2 cell death is potentiated by CYP2E1. *Free Radical Biology and Medicine*, *40*(1), 63–74. https://doi.org/https://doi.org/10.1016/j.freeradbiomed.2005.08.012

Zoncu, R., Bar-Peled, L., Efeyan, A., Wang, S., Sancak, Y., & Sabatini, D. M. (2011). mTORC1 senses lysosomal amino acids through an inside-out mechanism that

requires the vacuolar H+-ATPase. *Science*, *334*(6056), 678–683. https://doi.org/10.1126/science.1207056

APPENDICES

A. Full Blot Image of Figure 3.5

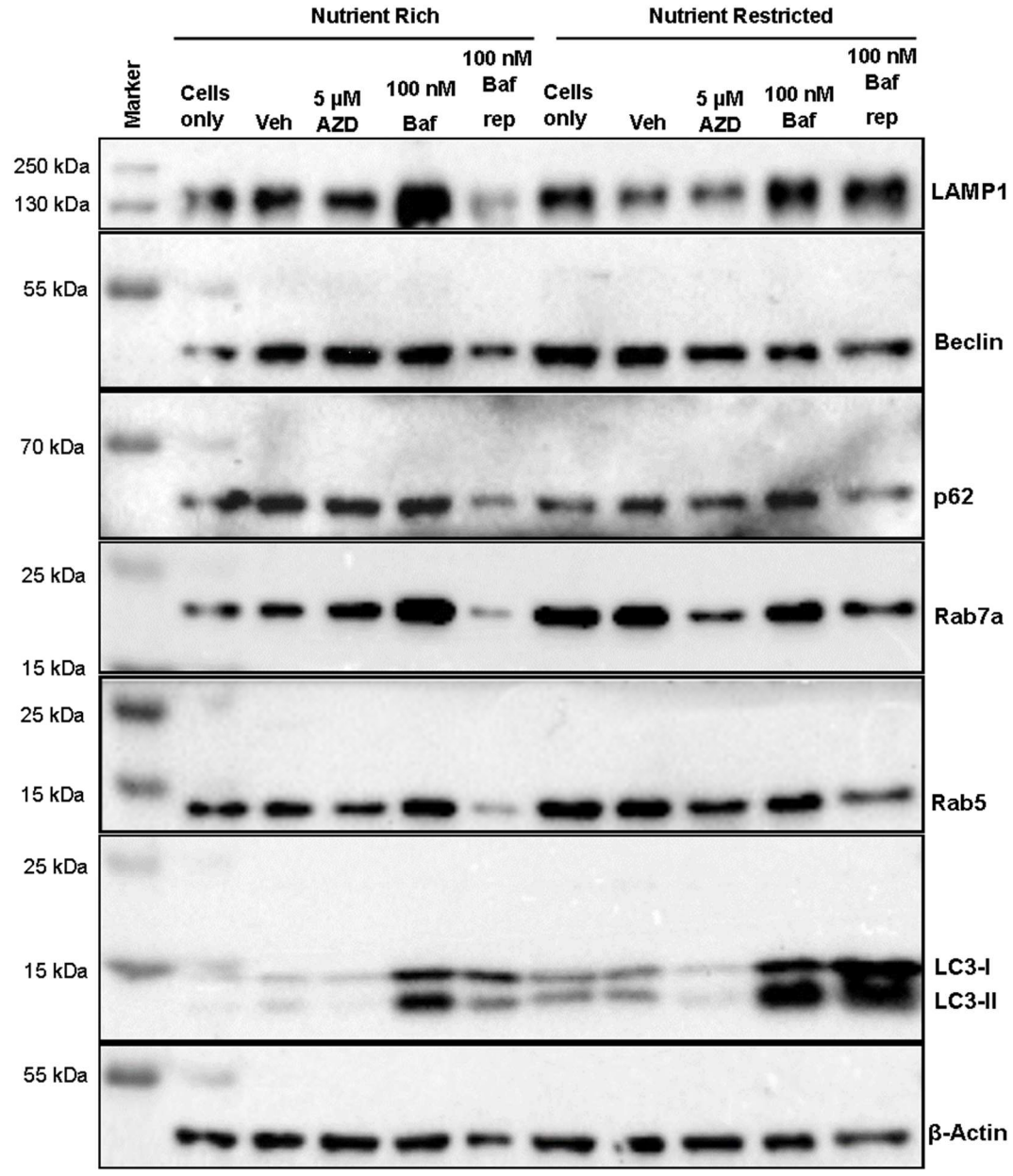

Supp. Figure 1 Determination of Autophagic Flux in Nutrient-rich and Nutrient-restricted LoVo Cells

B. Role of MAPK Signaling Pathway to ATF4 Upon Nutrient Restriction

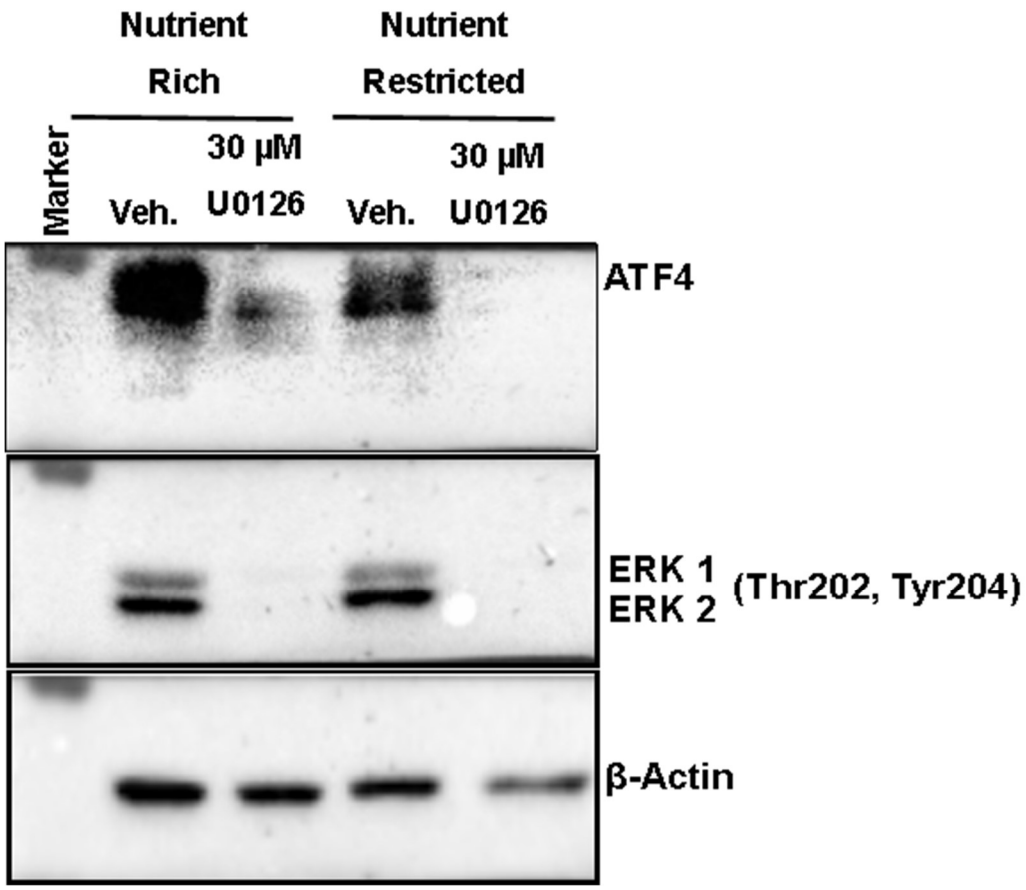

Supp. Figure 2 Possible Link Between ATF4 and ERK Signaling

C. Buffer Contents Used is This Study

CYTOPLASMIC AND NUCLEAR PROTEIN ISOLATION BUFFERS

- HYPOTONIC BUFFER

  10 mM HEPES, pH 7
  4 mM sodium fluoride
  10 μM sodium molybdate
  0.1 mM EDTA
  1X protease and phosphatase inhibitors

- NUCLEAR EXTRACTION BUFFER

  10 mM HEPES, pH 7.9
  1.5 mM MgCl2
  420 mM NaCl
  0.1 mM EDTA
  1X protease and phosphatase inhibitors
  10% glycerol

4% SDS-PAGE STACKING GEL

3.1 mL dH2O
1.25 mL Stacking Buffer (10% SDS, 1.5M Tris, pH 6.8)
650 μL Acrylamide/Bis Solution (SERVA, Germany)
50 μL 10% APS
5 μL TEMED

12% SDS-PAGE SEPARATING GEL

3.4 mL dH2O
2.5 mL 4X Separating Buffer (10% SDS, 1.5M Tris, pH 8.8)
4 mL Acrylamide/Bis Solution (SERVA, Germany)

100 µL 10% APS

10 µL TEMED

6X SDS-PAGE SAMPLE LOADING DYE

12% SDS

30% β-mercaptoethanol

30% Glycerol

0.012% Bromophenol Blue

0.375 M Tris-HCl pH 6.8

10X SDS-PAGE RUNNING BUFFER

25 mM Tris

192 mM Glycine

0.1% SDS

1X SDS-PAGE RUNNING BUFFER

100 mL 10X Running Buffer

900 mL dH2O

10X TRANSFER BUFFER

0.25 M Tris

1.92 M Glycine

pH 8.3 in 1 L dH2O

1X TRANSFER BUFFER

200 mL Methanol

100 mL 10X Blotting Buffer

700 mL dH2O

0.1% SDS

20X TBS

50 mM Tris

300 mM NaCl

4mM KCl

pH 7.4 in 1 L dH2O

1X TBS-T

50 mL 20X TBS

950 mL dH2O

1 mL Tween 20

MILD STRIPPING BUFFER

15 g Glycine

1 g SDS

10 mL Tween-20

pH 2.2 in 1L dH2O